University of Mississippi

eGrove

Electronic Theses and Dissertations | Graduate School

2017

Lipid Based Frameworks And Topical Ocular Inserts For The Delivery Of Small Molecule Therapeutics To The Posterior Segment Of The Eye

Sai Prachetan Balguri
University of Mississippi

Follow this and additional works at: https://egrove.olemiss.edu/etd

Part of the Pharmacy and Pharmaceutical Sciences Commons

Recommended Citation

Balguri, Sai Prachetan, "Lipid Based Frameworks And Topical Ocular Inserts For The Delivery Of Small Molecule Therapeutics To The Posterior Segment Of The Eye" (2017). *Electronic Theses and Dissertations*. 729.
https://egrove.olemiss.edu/etd/729

This Dissertation is brought to you for free and open access by the Graduate School at eGrove. It has been accepted for inclusion in Electronic Theses and Dissertations by an authorized administrator of eGrove. For more information, please contact egrove@olemiss.edu.

LIPID BASED FRAMEWORKS AND TOPICAL OCULAR INSERTS FOR THE DELIVERY OF SMALL MOLECULE THERAPEUTICS TO THE POSTERIOR SEGMENT OF THE EYE

A Dissertation
presented in partial fulfillment of requirements
for the degree of Doctor of Philosophy
in Pharmaceutical Sciences with an emphasis in Pharmaceutics and Drug Delivery
The University of Mississippi

By

SAI PRACHETAN BALGURI

August 2017

Copyright® Sai Prachetan Balguri 2017

ALL RIGHTS RESERVED

ABSTRACT

Lipid based systems and topical ocular inserts of various drugs were developed for the intervention/treatment of posterior segment ocular complications. Indomethacin (IN) was developed into solid lipid nanoparticles (SLNs) and Nanostructured lipid carriers (NLCs). Effect of surface functionalization using chitosan (CS) on lipid nanocarriers was tested to evaluate corneal penetration. Surface modification of SLNs with CS increased ocular penetration of IN. NLCs maintained significantly higher IN concentrations in all ocular tissues tested, compared to the other formulations evaluated *in vivo.*

Effect of surface poly (ethylene) glycol (PEG) functionalization of the NLCs on ocular disposition was studied using Ciprofloxacin (CIP) as a model drug. Transcorneal penetration of CIP from NLCs was optimum with PEG molecular weight in between 2K to 10K. *In vivo* ocular tissue CIP concentrations attained from the various formulations was consistent with the *in vitro* data obtained.

Feasibility of melt-cast, topical, ocular inserts for delivery of drugs, with different physicochemical properties, to the posterior segment of the eye was studied. The model drugs tested include indomethacin (IN), ciprofloxacin hydrochloride (CIP) and prednisolone sodium phosphate (PSP). Transmembrane flux of IN, PSP and CIP were enhanced by ~3.5-folds, ~3.6-folds and ~2.9-folds, respectively, from the polymeric inserts when compared to the control formulations, post 3 h. Moreover, ocular inserts generated significantly higher drug levels in all the ocular tissues, including the retina-choroid, when compared to their control formulations.

Cationic lipid nanoparticles of Natamycin (NT) were also evaluated. NT SLNs were compared with NT marketed formulation – 5% w/v ophthalmic suspension - in terms of transcorneal permeation and *in vivo* ocular tissue distribution. Compared to Natacyn® control, transcorneal permeability of NT was enhanced ~ 3-folds with the CLBN formulation. *In vivo* studies demonstrated that CLBN, at a 50-fold lower dose, was as effective as the control formulation in terms of NT delivery to the retinal tissues.

Resveratrol (RES), a multi-faceted candidate was formulated into SLNs. Transcorneal flux of RES was increased ~ 1.5-folds with the SLN formulation, when compared to control formulation. The results from the all the above studies demonstrated that lipid based systems and melt-cast topical ocular inserts serve as viable platforms in the niche of ocular delivery.

DEDICATION

This dissertation is dedicated to my parents Padma Balguri and Rajeshwar Rao Balguri. I would not have reached this milestone without their love, support, encouragement and patience. This dissertation is also dedicated to my brothers Sai Dushyanth Balguri and Sai Nitish Balguri for being my moral support.

LIST OF ABBREVIATIONS

IN - Indomethacin

CIP - Ciprofloxacin

PSP - Prednisolone Sodium Phosphate

NSAIDs - Nonsteroidal anti-inflammatory drugs

NT- Natamycin

RES - Resveratrol

GMS - Glyceryl monostereate

DSPE- 1, 2-distearoyl-sn-glycero phosphoethanolamine

DSPE-mPEG-2000 - (N-Carbonyl-methoxypolyethylene glycol-2000)-1,2 di-stearoyl-sn glycero phosphoethanolamine

DSPE-mPEG-1000 - (N-Carbonyl-methoxypolyethylene glycol-1000)-1,2 di-stearoyl-sn glycero phosphoethanolamine

DSPE-mPEG-5000 - (N-Carbonyl-methoxypolyethylene glycol-5000)-1,2 di-stearoyl-sn glycero-phosphoethanolamine

DSPE-mPEG-10000 - (N-Carbonyl-methoxypolyethylene glycol-10000)-1,2 di-stearoyl-sn glycero phosphoethanolamine

DSPE-mPEG-20000 - (N-Carbonyl-methoxypolyethylene glycol-10000)-1,2 di-stearoyl-sn-glycero-phosphoethanolamine

DMPE- 1,2- dimyristoyl-sn-glycero phosphoethanolamine

DMPE-mPEG-2000 – (N-Carbonyl-methoxypolyethylene glycol-10000)-1,2 di-myristoyl-sn glycero phosphoethanolamine

DPPE-1,2- dipalmitoyl-sn-glycero phosphoethanolamine

DPPE-mPEG-2000 – (N-Carbonyl-methoxypolyethylene glycol-10000)-1,2 di-palmitoyl sn glycero phosphoethanolamine

ChCl - Chitosan Chloride

PEO N10 - Polyethylene oxide N10

βCD - Beta cyclodextrin

HPβCD - Hydroxy propyl beta cyclodextrin

RMβCD - Randomly methylated beta cyclodextrin

SLN's - Solid lipid nanoparticles

NLC's - Nano structured lipid carriers

DR - Diabetic retinopathy

RPE - Retinal pigmented epithelium

COX - Cyclooxygenase

EE - Entrapment efficiency

IPBS - Isotonic phosphate buffered saline

DSC - Differential scanning calorimetry

FTIR - Fourier transform infrared spectroscopy

HPLC-UV - High performance liquid chromatography- Ultra violet

mM - Millimolar

μg- Microgram

DMSO - Dimethyl sulfoxide

ACN - Acetonitrile

AH - Aqueous humor

VH - Vitreous humor

IC - Iris ciliary bodies

RC - Retina-choroid

ACKNOWLEDGMENTS

Ph.D. degree would be a dream for me without my advisor Dr. Soumyajit Majumdar. His constant support, expertise, and guidance helped me a lot to reach this level. I am indebted for his encouragement, patience, understanding and support throughout my graduate studies. He was very kind and supportive during my tough times. Words fall short if I start expressing my gratitude for him. I am truly grateful and admire his help and attention towards my academic growth. Thank you so very much for being my advisor!

I express my heartfelt gratitude to my dissertation committee members Dr. Michael A. Repka, Dr. Samir A. Ross, and Dr. Seong Bong Jo for their valuable time, guidance, suggestions and help during the evaluation of this dissertation. I extend my thanks to Dr. Bonnie A. Avery, Dr. Narasimha Murthy and Dr. Christy M. Wyandt for making the experience at Ole Miss worthwhile, Ms. Deborah King for her help, patience and affection. I also thank the support extended by Ms. Penni Bolton during animal experiments.

I thank all graduate students at Department of Pharmaceutics and Drug delivery for their support and for making my stay at Ole Miss memorable. I profusely thank my colleagues and friends, especially Goutham Adelli, Prashanth Manda and Abhishek Juluri for being such a great support and fun to hang out with. I owe goutham a lot for his help during experimental work and during my stay at Ole Miss. I had spent good time with Pranjal Taskar, Akshaya Tatke, and karthik, they have made my grad school very joyful and memorable.

I specially fall short of words to thank my brothers Nithish and Dushyanth. They are my inspiration, strength and moral support. Without their support, encouragement and sacrifices I

would not have attended Ole Miss. All these years I was away from my parents and Nithish was the one taking care of everything at home. Thank you for everything!

Most importantly I thank my mother for her patience, moral support and guidance. Her sacrifices and mad love for me can’t be expressed in words. I miss u a lot …

Thank you, Mom, for everything!

DISSERTATION COMMITTEE

Research Advisor: Dr. Soumyajit Majumdar (Dept. of Pharmaceutics and Drug Delivery)

Committee Members: Dr. Michael A. Repka (Dept. of Pharmaceutics and Drug Delivery)

Dr. Seongbong Jo (Dept. of Pharmaceutics and Drug Delivery)

Dr. Samir A. Ross (Dept. of BioMolecular Sciences)

CONTENTS

DISSERTATION TITLE…… i
ABSTRACT……..…….. ii
DEDICATION…….....……..iv
LIST OF ABBREVIATIONS……..v
ACKNOWLEDGEMENTS…….……..viii
DISSERTATION COMMITTEE…….……x
LIST OF TABLES……xiv
LIST OF FIGURES……... xv

1. CHAPTER 1. **……..…… 1**
INTRODUCTION …….……... 2
SPECIFIC OBJECTIVES ……..... 8
SPECIFIC AIMS ……..... 8

2. CHAPTER 2. TOPICAL OPHTHALMIC LIPID NANOPARTICLE FORMULATIONS (SLN, NLC) OF INDOMETHACIN FOR DELIVERY TO THE POSTERIOR SEGMENT OCULAR TISSUES **……...…….……...… 9**
INTRODUCTION …….……..…. 10
METHODS ……...….... 11
RESULTS …….……. …..… 20
DISCUSSION …….….…….…... 30
CONCLUSION…….....…. 34

3. CHAPTER 3. OCULAR DISPOSITION OF CIPROFLOXACIN FROM TOPICAL NANOSTRUCTURED LIPID CARRIERS: EFFECT OF SURFACE DENSITY AND TYPE OF POLYETHYLENE GLYCOL**…….…….…….... 36**
INTRODUCTION …….….……...37

METHODS …….….…...…. 39
RESULTS …….…… 48
DISCUSSION……...……. 63
CONCLUSION ……...…....……. 67

4. CHAPTER 4. MELT-CAST NONINVASIVE OCULAR INSERTS FOR POSTERIOR SEGMENT DRUG DELIVERY**…….……68**
INTRODUCTION …….……...…..……...69
METHODS ……...…...…. 71
RESULTS ……..……...…… 77
DISCUSSION …….…….……. 84
CONCLUSION…….……..……87

5. CHAPTER 5. NON-INVASIVE CATIONIC COLLOIDAL NANOCARRIERS FOR OCULAR DELIVERY OF NATAMYCIN: PREPARATION AND EVALUATION**…….……89**
INTRODUCTION …….…….……...90
METHODS …….…….……...…...92
RESULTS …….…… 96
DISCUSSION……...…….98
CONCLUSION……100

6. CHAPTER 6. OCULAR DELIVERY OF RESVERATROL FOR THE TREATMENT OF DIABETIC RETINOPATHY**……....102**
INTRODUCTION ……103
METHODS……..…….…….....…...104
RESULTS….…….……..…….….…107
DISCUSSION……..……...…….…..110

CONCLUSION……..……112

7. BIBLIOGRAPHY **…….….....… 113**

8. APPENDIX **……...……..……..126**

9. APPENDIX A**……..……..127**

10. APPENDIX B**……129**

11. VITA**……..131**

LIST OF TABLES

2.1: Quantitative composition of IN formulations……..20

2.2: Physico-chemical characteristics of IN-NLC formulations…….21

3.1: Quantitative composition of CIP NLC and PEGylated CIP NLC formulations……..49

3.2: Physicochemical characteristics of CIP-NLCs and PEGylated CIP-NLC formulation…...50

3.3: Effect of autoclaving on the physicochemical attributes of CIP-NLCs and PEG-CIP-NLCs (pre and post sterilization)……...50

3.4: Effect of autoclaving on the physicochemical characteristics of PEG-CIP-NLC formulations prepared with higher molecular weight PEG's pre and post sterilization……..54

3.5: Physical stability of placebo NLC formulations (n=2) prepared with different lipids (solid and / or liquid) post autoclave sterilization……..…….…..54

3.6: Effect of PEGylated to unPEGylated phospholipid ratio and PEG molecular weight on physical stability of placebo PEG-NLC post autoclave sterilization……..…...56

6.1: Physico-chemical characteristics of RES loaded SLN formulations……..108

LIST OF FIGURES

1.1: Ocular anatomy showing different barriers……. 2

1.2: Schematic representation of ocular pathways and the underlying barriers encountered in topical delivery to the back-of-the eye……7

2.1: pH-dependent saturation solubility of IN in various solvents……..22

2.2: Particle size characteristics of various IN formulations following storage at 4°C, 25°C/60% RH, and 40°C/75% RH…….23

2.3 a): Entrapment efficiency (% EE) of various IN formulations following storage at 4°C, 25°C/60% RH, and 40°C/75% RH……..…….23

2.3 b) Zeta potential of various IN formulations following storage at 4°C, 25°C/60% RH, and 40°C/75% RH…….…..24

2.3 c) Polydispersity indices of various IN formulations following storage at 4°C, 25°C/60% RH, and 40°C/75% RH…….……24

2.4: Physico-chemical characteristics of the IN SLN and NLC formulations pre (Fig 2.4A) and post-sterilization (2.4B)…….25

2.5: FTIR spectral images of the IN + Compritol physical mixture, Compritol, IN, IN-SLN, IN-CS-SLN and IN-NLC F-1 formulations……..…….25

2.6: *In vitro* release of IN from various formulations across Spectra/Por® membranes at 34°C..26

2.7: Transcorneal flux across isolated rabbit cornea from various IN topical formulations …....26

2.8: Trans-SCR permeability of IN from various topical ocular formulations at 34ºC……..…27

2.9: IN ocular tissue concentrations (ng/g of tissue) obtained from the IN-SOL, IN-HPβCD, and IN-SLN formulations 2 hrs post-topical administration in the anesthetized rabbit model. The data represent the mean ± S.D. (n=3). AH: Aqueous humor; VH: Vitreous humor; IC: Iris-Ciliary; RC: Retina-Choroid (N.D. not detected)…….…….29

2.10: IN ocular tissue concentrations (ng/gm of tissue) obtained from the IN-CS-SOL, IN-SLN, IN-CS-SLN (n=6) and IN-NLC formulations 2 hrs post-topical administration in the conscious rabbit model…….…….29

3.1: STEM images of CIP loaded NLCs. A) CIP NLCs. B) PEG(2K)-CIP-NLCs…….……...52

3.2: *In vitro r*elease of CIP obtained across Spectra/Por® membrane (MWCO: 3.5 KDa) from CIP loaded PEGylated NLCs (PEG(2K)-CIP-NLCs), 0.3% w/v CIP ophthalmic Solution, and CIP-NLCs (DSPE-CIP-NLCs) obtained using Valia-Chien cells at 34°C. (Dose: 500 µL; 1500 µg)……..57

3.3: Transcorneal flux of CIP obtained from CIP ophthalmic Solution, DSPE-CIP-NLCs, PEG(2K)-CIP-NLCs and Chitosan Chloride coated DSPE-CIP-NLCs (CIP-ChCl-NLCs) using Valia-Chien cells (Dose: 500 µL; 1500 µg; n=4)……..58

3.4: Transcorneal flux of CIP obtained from various topical NLC formulations tested with different molecular weights of PEG grafted, DSPE phospholipid (PEG-1K (PEG(1K)-CIP-NLCs / 2K (PEG(2K)-CIP-NLCs / 5K (PEG(5K)-CIP-NLCs) and varied chain lengths of PEG-2000 conjugated phospholipids (DMPE(2K)-CIP-NLCs, DPPE(DPPE(2K)-CIP-NLCs) using side-by-side diffusion cells (PermeGear, Inc) at 34°C (Dose: 3 mL; 0.3% w/v) (n=4)……..…..59

3.5: Transcorneal flux of CIP obtained from NLC systems with higher molecular weights of PEG's grafted to DSPE phospholipid (2K / 5K / 10K (PEG (10K)-CIP-NLCs / 20K (PEG (20K)-CIP-NLCs), using side-by-side cells at 34° C (Dose: 3 mL; 0.3% w/v; n=4 …….……..…….….60

3.6: Ocular tissue concentrations of CIP obtained from CIP Ophthalmic Solution, DSPE-CIP-NLCs with and without Chitosan Chloride (ChCl) and CIP loaded PEGylated NLCs with different molecular weights of PEGs (DSPE-PEG-2K, DSPE-PEG-5K, DSPE-10K, DSPE-20K) 2 h post topical application (Dose: 300 µg; 100 µL at -30 and 0 min) in a conscious rabbit model……..……...62

4.1: DSC thermograms of IN Insert, IN physical Mixture, pure IN, PEO Insert and pure PEO..78

4.2: DSC thermograms of CIP Insert, CIP physical Mixture, pure CIP, PEO Insert and pure PEO……..…….79

4.3: FT-IR spectra of IN Insert, IN Physical Mixture, pure IN, PEO Insert and pure PEO N10……79

4.4: FT-IR spectra of PSP Physical Mixture, PSP Insert, pure PSP, PEO Insert and pure PEO N10……...….80

4.5: FT-IR spectra of CIP Physical Mixture, CIP Insert, PEO N10 Insert, pure CIP and PEO N10……...…….80

4.6: *In vitro* transcorneal flux obtained from different topical formulations at equivalent doses using valia-chien cells at 34°C……..…81

4.7: *In vivo* IN concentrations (µg/gm of tissue) obtained from 0.1% w/v IN-CS-SOL, and 10% w/w IN Insert (Dose: 0.1 mg, 0.8 mg & 0.8 mg respectively), 2 h post topical application in conscious rabbit model…….……82

4.8: *In vivo* PSP concentrations (µg/gm of tissue) obtained from 10% w/w PSP Insert and PSP control solution (1% w/v) (Dose: 0.8 mg, 1 mg respectively), 2 h post application in conscious rabbit model……..83

4.9: *In vivo* ocular tissue concentrations of CIP obtained from 0.3% w/v CIP control solution (Dose: 100 µL; 350 µg), 10% w/w CIP Insert (Dose: 0.8 mg) in conscious rabbit model following 2 h post topical application……..84

5.1: Chemical structure of Natamycin……..91

5.2: Transcorneal permeation characteristics of NT from CLBN (1 mg/mL) and Natacyn® (17 mg/mL) suspension across isolated rabbit cornea at 34° C (n=3)……97

5.3: Ocular tissue concentrations of NT obtained from marketed control suspension and NT CLBN 1 & 2 h post topical application in a conscious rabbit model……98

6.1: Saturation solubility of RES (µg/mL) obtained from various surfactants (1% w/v)…..109

6.2: *In vitro* release of RES from the topical ocular formulations and diffusion across Spectra/Por® membrane (MWCO 3.5k Da) at 34°C obtained using Valia-chien cells…..…110

6.3: *In vitro* transcorneal permeability of RES from the topical ocular formulations obtained using Valia-chien cells at 34°C……..……..110

CHAPTER 1
INTRODUCTION

1.1. Introduction

The eye is an extremely complex, secluded, and sensitive organ of the human body. Owing to its unique anatomical, physiological, metabolic, dynamic and efflux barrier functionalities, delivery of drugs / development of novel therapies targeting the posterior segment ocular tissues (retina & vitreous humor) remains a significant challenge. The human

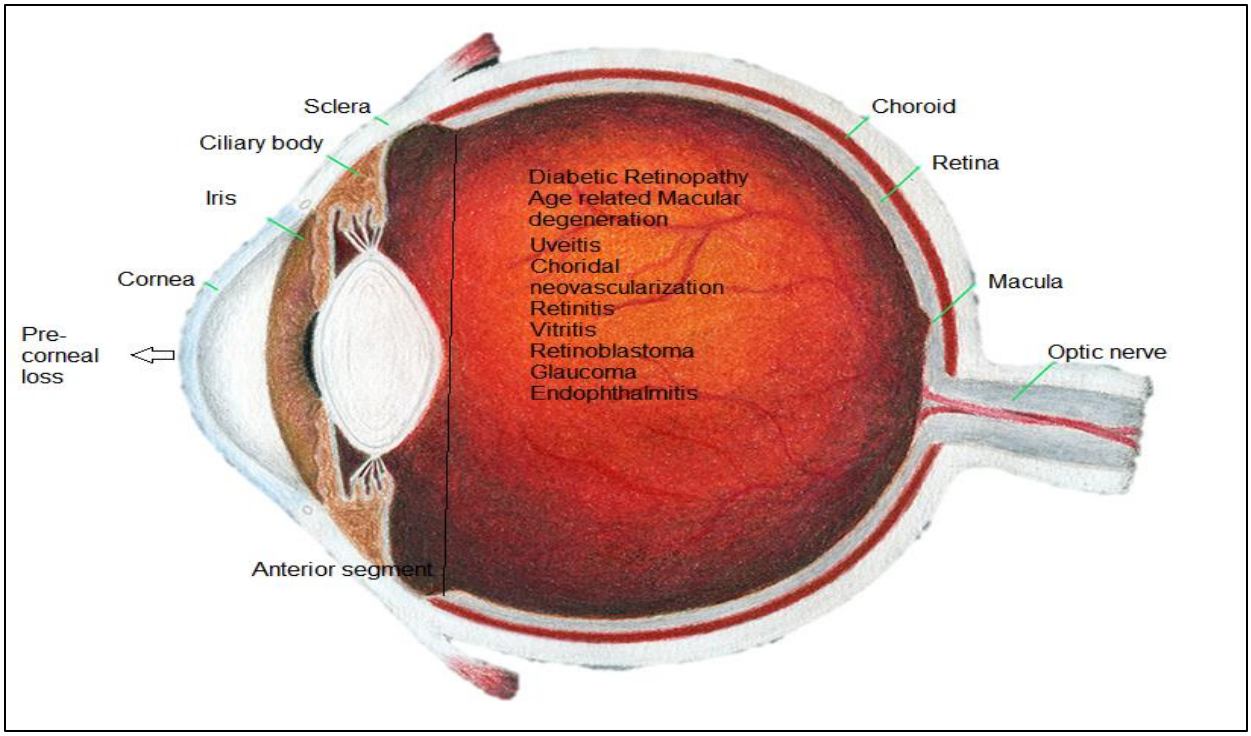

Figure 1.1: Ocular anatomy showing different barriers

ocular structure and the penetration pathways involved in topical delivery are shown in figure 1.1. The anterior and posterior segment of eye is demarcated by the transparent crystalline lens. Cornea, iris-ciliary (IC), lens, aqueous humor (AH), trabecular meshwork and Schlemm's canal constitute anterior segment. The anterior segment occupies approximately one-third portion of the eye. The posterior segment consists of sclera, choroid, retina, vitreous humor and optic nerve (1).

1.1.1. Ocular anatomy and physiology

In humans, tear fluid often serves to clean and lubricate the eyes in response to irritation. Lacrimal gland located at the upper lateral region of each orbit secretes the tear fluid which continuously bathes the eye surface. Tear fluid forms tear film or pre-corneal film which consists

of three layers. The outermost lipid layer retards evaporation of water. The middle aqueous layer which contains mainly water and small amounts of proteins. The innermost layer consists of mucin and mainly water (95%). Mucins are typically large glycoproteins with molecular weight between 0.5 to 20 MDa. Following ocular instillation, topical eye drops will be diluted with the tear fluid and get dispersed over the ocular surface with peak drug concentrations usually attained after 20 to 30 minutes. Eye drops are eliminated from the precorneal area within 90 seconds and undergo systemic absorption. It is reported that precorneal half-life of topically applied drugs is between 1-3 min (2-4).

The cornea is major and primary structural component of the eye. The cornea is continuous with white sclera and semi-transparent conjunctival tissue. The cornea is divided into three major functional layers namely epithelium, stroma and endothelium. The corneal epithelium is lipophilic and consists of three to six layers of tightly adherent cells which contribute to about 90% of the barrier towards hydrophilic drugs. The stroma is hydrophilic constituting 90% of the corneal thickness and acts as rate limiting barrier for lipophilic drugs. The endothelium is a one cell layer thick lipophilic membrane with large intracellular junctions which does not restrict hydrophilic drugs but may offer some resistance towards lipophilic drugs. The pore size of cornea is approximately 1 nm (permeable for drugs with molecular weight (MW) less than about 700 Da) while some studies indicate that some pores could be up to 5 nm in diameter. Pore density and intercellular pore size in the cornea are much smaller than in the conjunctiva (5-7). The space between the iris and the cornea is filled by fluid called aqueous humor, which maintains the intraocular pressure in the eye. The amount of aqueous humor in the human and rabbit eye varies between 200 and 300 µL. Reports indicated the entire fluid will be replaced in nearly 100 min (8).

Lipophilic drugs are cleared by aqueous humor at a turnover rate of approximately 3 μL per minute (9, 10).

The sclera is composed primarily of collagen fibers with mean thickness of 0.53 mm and the mean total area of 16.3 cm^2. The passive diffusion is primary route of drug penetration through sclera. The permeability of sclera is largely dependent on the hydrodynamic radius of the permeating drug molecule. Sclera is poorly vascularized and transport of large molecule may occur through perivascular spaces or as diffusion between scleral fibrils (11, 12).

The conjunctival membrane is a vascularized tissue that covers ∼80% of the ocular surface and secretes mucus. Hydrophilic drugs traverse through tight junctions of epithelium by paracellular transport whereas lipophilic species penetrate through the transcellular route. The conjunctiva–scleral route is alternative to major corneal absorption pathway for the topically applied drugs to reach intraocular tissues. Propranolol, with logP of 3.21, is absorbed through cornea and conjunctiva up to ten-fold greater than sotalol, a hydrophilic drug with a log P of −0.62. However, efflux pumps (P-gp) localized on the apical side of conjunctiva restrict permeation of lipophilic drugs. The conjunctiva is approximately 15 to 25 times more permeable than cornea (13-15).

The blood ocular barriers comprise blood-aqueous barrier and the blood-retinal barrier protecting the eye from xenobiotics. The blood-aqueous barrier is formed by the non-pigmented epithelium of the ciliary body and the endothelium of the iris vessels. The blood-retinal barrier consists of the retinal pigment epithelium and the endothelial membrane of the retinal vessels. The two functional barriers restrict movement of drugs from oral or systemic administration into intraocular tissues. However, the tight junctions of ciliary epithelium in rabbit eye are not effective when compared to tight junctions of retina. Thus, blood-retinal barrier is superior to blood aqueous

barrier in terms of limiting molecular diffusion (16). Lipophilic compounds are eliminated by uveal blood flow at about 20 to 30 µL per minute (17-19). The choroid is a highly vascularized layer between retina and sclera. It is composed of layers of blood vessels that nourish the back of the eye of tissues. The choroidal vasculature serves as permeation barrier promoting clearance and thus decreasing the bioavailability of drugs in the posterior segment from the topically applied drugs. The vitreous humor is a clear aqueous gel consisting of mainly collagen and hyaluronan. Long terms posterior complications require totally invasive intravitreal administration (20-22).

1.1.2. Posterior ocular segment complications

Diseases such as age-related macular degeneration (AMD), diabetic retinopathy (DR), Glaucoma, uveitis, choroidal neovascularization (CNV), retinitis pigmentosa and retinoblastoma account for most cases of irreversible blindness worldwide. However, statistical evidence suggests that DR and AMD are the leading causes for irreversible blindness in the United States. DR is the main cause of blindness in adults aged between 20 and 65 years, with incidence rates of 29% and 56% for proliferative and non-proliferative DR, respectively. Macular edema (ME) occurs in approximately 10% of the diabetic population. AMD is the major cause of irreversible blindness in adults older than 65 years. The prevalence of all forms of AMD in the 65 to 74 year age group is 20%, and it is closer to 35% in older people (23).

Inflammation and oxidative stress are the underlying principal factors involved in the etiology of most posterior segment ocular disorders. The relationship between hyperglycemia and oxidative stress, which leads to the initiation and progression of several sight threatening ocular diseases such as DR, AMD and cataract formation, is well established. The retina is highly susceptible to oxidative damage due to the peroxidation of fatty acids present in its lipid bilayer. Also, reports demonstrate that the total antioxidant capacity of the vitreous humor and aqueous

humor is lowered in DR, accompanying generation of increased reactive oxygen species. Numerous studies substantiate the prominent and critical role of inflammatory and angiogenic pathways in the pathogenesis of DR. Thus, oxidative, inflammatory and angiogenic mechanisms are involved in DR (24, 25). The multifactorial etiology of DR could be manifested in other posterior diseases, hence there is increasing need for the development of multi-faceted candidates and robust formulation platforms for the effective treatment of chorio-retinal complications.

DR can be broadly categorized into three stages; background DR, pre-proliferative DR and proliferative DR (PDR). In background DR, hyperglycemia is considered to induce death in endothelial cells of retinal blood vessels. Micro aneurysms and vascular leakage follow, and blockage of retinal capillaries take place. In pre-proliferative DR, increasing retinal hypoxia and multiple hemorrhages occurs in some areas. The angiogenic factors will be produced leading to the proliferation of vessels, which is a typical feature of PDR. The newly formed blood vessels by themselves do not lead to vision loss, but leakage of blood through their weak walls can result in visual impairment and can ultimately lead to complete loss of sight (26-28).

Age-related macular degeneration (AMD) can be categorized into dry and wet AMD. Progression of AMD is linked to the activation of inflammatory and immunological pathways. Presence of excess ROS and decreased antioxidant capacity in the ocular tissues is also considered to play a significant role in the initiation and progression of AMD. Oxidative stress induced damage to the lens fibers is well documented in the case of cataracts. It is thought that these free radicals accelerate and aggravate cataract development (29-32).

1.1.3. Challenges encountered in topical drug delivery

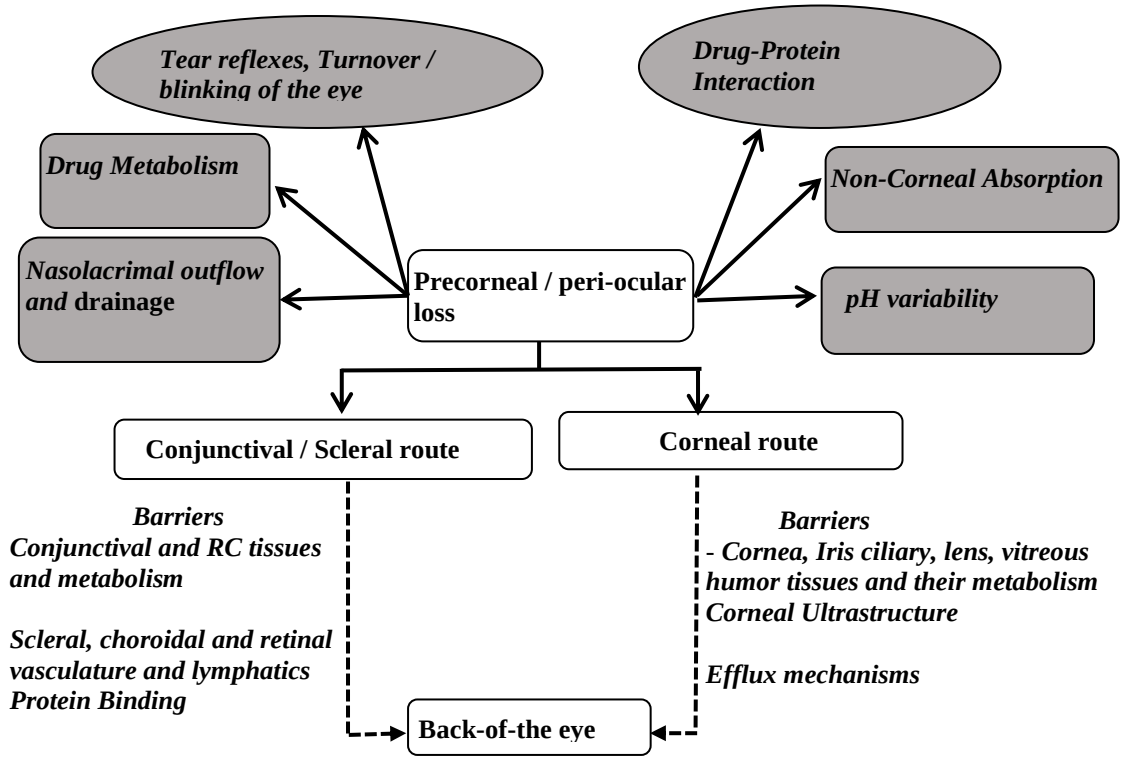

Figure 1.2: Schematic representation of ocular pathways and the underlying barriers encountered in topical delivery to the BACK-OF-THE EYE.

Topical delivery of drugs to the posterior segment ocular tissues is an extremely challenging task. Topical administration is the most favored route of administration, like other localized modes, due to minimum non-specific systemic exposure, safety and patient compliance. Conventional formulations such as eye drops, most favorably adopt the corneal route for delivery of drugs. However, only 5-10% of the applied drug dose will be able to penetrate the inner ocular tissues, following topical instillation, due to the pre-corneal factors. Moreover, efflux protein pumps namely P-gp, multi-drug resistance protein (MRP) and breast cancer resistance protein (BCRP) expression on the various ocular tissues play a critical role in lowering ocular bioavailability of drug molecules. Drugs administered through alternative oral and

systemic routes need to overcome the blood ocular barriers and may require higher doses, resulting systemic toxicity (33).

1.2. Specific Objectives:

The goal of the present project is to develop topical lipid nanoparticulate and ocular insert formulations with wide classes of drugs with anti-bacterial, anti-inflammatory, anti-fungal properties. Model drugs tested include Indomethacin (IN), Ciprofloxacin (CIP), Prednisolone sodium phosphate (PSP) and Natamycin. These drugs can be used especially in the treatment of ocular inflammation/infections either alone or as a multi-drug combination therapy. The model drugs chosen were formulated and evaluated *in vitro* / *in vivo* to demonstrate the feasibility of lipid based systems and topical melt cast inserts for the back-of-the eye drug delivery.

1.3. Specific Aims

1. To evaluate the ocular penetration and distribution characteristics of IN loaded solid lipid nanoparticles (IN-SLNs), IN loaded nanostructured lipid carriers (IN-NLCs) and IN loaded chitosan coated SLNs (IN-CS-SLNs).
2. To demonstrate the effect of PEGylation in improving the penetration and sterilization-stabilization properties of CIP loaded NLCs.
3. To investigate the feasibility of melt cast ocular inserts to deliver drugs with wide range of physico-chemical properties into the back-of-the eye.
4. To assess the ocular permeability and disposition of Natamycin from lipid nanoparticles in comparison to marketed ophthalmic suspension.
5. To investigate the corneal penetration of Resveratrol from solid lipid nanoparticle formulations.

CHAPTER 2

TOPICAL OPHTHALMIC LIPID NANOPARTICLE FORMULATIONS (SLN, NLC) OF INDOMETHACIN FOR DELIVERY TO THE POSTERIOR SEGMENT OCULAR TISSUES

2. Introduction

Indomethacin (IN), 2-{1-[(4-chlorophenyl) carbonyl] -5-methoxy-2-methyl-1*H*-indol-3-yl} acetic acid, a topical non-steroidal anti-inflammatory drug (NSAID) is used in the treatment of the ocular inflammatory disorders such as conjunctivitis, uveitis, cystoid macular edema, and anterior segment inflammation, including post-operative pain following cataract surgery (34-36). The compound elicits its anti-inflammatory action through the inhibition of COX-2 enzymes, which are essential for prostaglandin biosynthesis, and thus possesses analgesic and anti-pyretic properties (37). The potential effects of prostaglandins include elevation of intraocular pressure, vasodilatation, disruption of blood ocular barriers, and leukocyte migration; hence, potent inhibition of COX-2 enzymes may provide therapeutic effects (38). NSAIDs are employed in the treatment of diabetic retinopathy and age-related macular degeneration (39). Formulating IN as a topical ophthalmic solution is challenging due to its poor solubility and stability (40). Indosol, which is an aqueous solution of IN complexed in TRIS-sodium salt (tromethamine), has been widely used in ophthalmic research to treat inflammation of the anterior segment and the uvea (41). Currently, topical ophthalmic formulations of IN are not marketed in the United States. Indocollyre® (hydro-poly(ethylene glycol) (PEG) ophthalmic) 0.1% w/v eye drops, which are commercially available in Europe, are associated with poor ocular bioavailability (42).

Approaches for improving the pre-corneal residence time and transcorneal permeability characteristics could enhance intraocular bioavailability (1, 43). In recent years, colloidal nanoparticulate systems have gained popularity as a promising ocular drug delivery platform (44). Solid lipid nanoparticles (SLNs) and nanostructured lipid carriers (NLCs) are colloidal nanoparticulate systems designed and developed to deliver lipophilic drugs. These particulates are composed of biocompatible and biodegradable materials and are in the nanometer size range. All

excipients used in these formulations are generally regarded as safe, and process scale-up is feasible. Several studies have demonstrated superior ocular bioavailability of therapeutic agents from these colloidal nanoparticulate systems, possibly because of improved retention and phagocytosis by epithelial cells. Furthermore, adsorption of polymers, such as chitosan, on the surface of SLNs may further improve the retention of the nanoparticles on the epithelial surface and increase cellular uptake of the nanoparticles (45, 46). Chitosan possesses favorable biological characteristics, such as biodegradability, biocompatibility and mucoadhesive properties (47, 48). The ability of chitosan and its derivatives in ophthalmic solutions to modulate characteristics of the epithelial barrier through the transient opening of the tight junctions, which results in enhanced transmembrane absorption, has been widely reported in the literature (49-51). In this study, chitosan was used to modify the surface characteristics of SLNs (chitosan adsorbed onto the SLN surface), and the ocular penetration of IN from the chitosan-coated SLNs was evaluated.

NLCs, however, appear to be a viable alternative to SLNs in terms of drug loading efficiency and are prepared by incorporating liquid lipids within the solid lipid structure. Depending on the ratio and concentration of the solid and liquid lipids, NLCs with different structural matrices can be obtained (52, 53).

The objective of the current study was to develop and characterize various formulations, such as SLNs, CS-SLNs and NLCs, and to evaluate the ocular delivery and disposition of IN from these topically administered formulations.

2.1. Methods

2.1.1. Saturation solubility studies

Saturation solubility, as a function of pH, was studied by adding excess amount of IN to screw-capped glass vials containing 200 mM phosphate buffer at different pH values, namely 5.5,

6.0, 6.5, 7.0, and 7.4, and phosphate buffer with various solubilizers, such as HPβCD, RMβCD, poloxamer 188, and Tween® 80. To achieve uniform mixing, samples were stirred at 100 rpm for 24 hrs at 25°C in a reciprocating water bath (Fisher Scientific). After 24 hrs, the samples were centrifuged (AccuSpin 17R), and the supernatant was analyzed for drug content.

2.1.2. Chromatography system for *in vitro* sample analysis

Samples were analyzed for IN content using an high performance liquid chromatography (HPLC) -UV method. A Phenomenex Luna® C_{18} 4.6 mm x 250 mm column was used for the analysis. The mobile phase used was methanol, water, and orthophosphoric acid (70:29.05:0.05). The detection wavelength λ_{max} for IN was 270 nm. The flow rate was set to 1 mL/min during the analysis.

2.1.3. Formulations

IN-TSOL, IN-SOL and IN-CS-SOL formulations

IN-TSOL was prepared by dissolving 0.1% w/v IN in 1% w/v Tween® 80 solution, which was used to investigate the release characteristics compared to the test formulations and to evaluate barrier resistance. Additionally, IN-SOL was prepared by dissolving IN (0.1% w/v final concentration) in an aqueous solution containing Tween®80 (1% w/v) and propylene glycol (29.3% w/v). Sodium hydroxide (1N) was added in small increments to adjust the pH. IN-CS-SOL was prepared by adding chitosan chloride (CS; 0.1% w/v final concentration) to IN-SOL. The pH of the final formulations was maintained at 6.8 because Indocollyre®, a formulation marketed in Europe, is at this pH.

IN-HPβCD and IN-CS- HPβCD solution formulations

IN-HPβCD formulation was prepared by dissolving IN (0.1% w/v) in 2.5% w/v HPβCD solution prepared in isotonic phosphate-buffered saline (IPBS; pH 6.8). IN-CS-HPβCD was

prepared by the addition of 0.1% w/v CS to the IN-HPβCD formulation. The final pH of the formulations was adjusted to 6.8.

Indomethacin solid lipid nanoparticles (IN-SLN) and IN-SLN-HPβCD formulations

The solubility of IN in a wide variety of lipids was visually evaluated to select suitable lipid excipients for formulating the SLNs/NLCs. Solid lipid, namely Compritol® 888 ATO, was melted, and IN (5% w/w with respect to the lipid) was dissolved therein to obtain a clear lipid phase. Simultaneously, an aqueous phase prepared using the surfactants poloxamer 188 (0.25% w/v) and Tween® 80 (0.75% w/v) and glycerin (2.25% w/v) in bidistilled water, was heated. The hot aqueous phase was added to the melted lipid phase while stirring, and the premix was then subjected to emulsification at 16,000 rpm for 6 min using a T 25 digital Ultra-Turrax. The pre-emulsion obtained was homogenized under high pressure, using previously optimized process parameters (15-20 K psi; 6 cycles; 6 min), using a thermostated Emulsiflex C5 (Avestin) resulting in the formation of a hot emulsion dispersion (42). The hot emulsion obtained was slowly cooled to room temperature to form the IN-SLNs. The final concentrations of Compritol® 888 ATO and IN in the formulation were kept constant at 2% w/v and 0.1% w/v, respectively.

Additionally, a variation of the IN-SLN formulation was prepared wherein 2.5% w/v HPβCD (final concentration) was added to the aqueous phase described above prior to the preparation of the SLNs. The pH of the resulting formulations was adjusted to 6.8 using NaOH (1N).

Indomethacin nanostructured lipid carriers (IN-NLCs)

The NLCs contained both solid (Compritol 888® ATO) and liquid lipids (Miglyol® 812 or 829), unlike the SLNs, which contained only solid lipids. The total amount of lipid employed in the NLCs was 4 and 8% w/v, of which Compritol 888® ATO constituted 60% and Miglyol® 812

or 829 made up the remaining 40% of the lipids. The concentration of surfactants (Tween 80® and poloxamer 188) and propylene glycol in the NLC formulations were maintained identical to that in the SLNs. Drug loading in all NLC formulations was kept constant at 0.8% w/v.

Chitosan-coated IN solid lipid nanoparticles (IN-CS-SLNs)

CS (mol. wt. < 200 kDa) was used for surface modification of the SLNs. CS (0.1% w/v) was incorporated into the aqueous phase prior to preparation of the SLNs, as described above (*in vitro* studies). CS at a concentration of 0.25% w/v was used in the SLNs for the *in vivo* experiments. Surface modification of the CS-coated formulations was confirmed through zeta potential measurements.

2.1.4. Particle size, polydispersity index (PDI) and zeta potential measurements

The hydrodynamic radius and the PDI of the SLN dispersion, the IN-CS-SLNs and the IN-NLCs were determined by photon correlation spectroscopy using a Zetasizer Nano ZS Zen3600 (Malvern Instruments, Inc.) at 25°C and with 173° backscatter detection in disposable folded capillary clear cells. Zeta potentials were measured at 25°C in folded capillary cells using the same instrument. To measure the particle size distribution and zeta potential, the SLN samples were diluted (1:500) with bidistilled and 0.2 μ filtered water.

2.1.5. Assay and entrapment efficiency (EE)

The lipid in the IN-SLN dispersion, the IN-CS-SLNs and the IN-NLCs was precipitated using 190-proof alcohol ("over proof''), or 95% alcohol by volume ("ABV"), and the drug content in the supernatant after centrifugation (13,000 rpm for 20 min), as such or after further dilution with 190-proof alcohol, was measured using an HPLC system.

The percentages of IN entrapped (% EE) in the IN-SLNs and IN-NLCs were determined by measuring the concentration of free drug in the aqueous phase of an undiluted formulation. The

EE was evaluated by an ultrafiltration technique with a 100-kDa centrifugal filter device that included a regenerated cellulose membrane (Amicon Ultra). A 500-µL aliquot of the corresponding formulation was added to the sample reservoir and centrifuged at 5,000 rpm for 10 min. The filtrate was then further diluted with 190-proof alcohol and analyzed for drug content using HPLC-UV (Section 2.1). The % EE was calculated using Eq. (1).

$$\% \text{ EE} = \left[\frac{\text{Wi}-\text{Wf}}{\text{Wi}}\right] \times 100 \qquad (1)$$

Where W_i is the total drug content, and W_f is the amount of free drug in the aqueous phase.

2.1.6. Terminal moist-heat sterilization and stability assessment of IN formulations

Two batches each of the optimized IN lipid-based formulations, namely the IN-SLNs, the IN-CS-SLNs and the IN-NLCs, were prepared and subjected to moist-heat sterilization (121°C for 15 min at 15 psi) in appropriately labelled glass vials using a thermo-controlled autoclave (AMSCO® Scientific Model SI-120). Following autoclaving, the sterilized samples were evaluated in terms of their physical appearance, color, particle size and physicochemical characteristics compared to un-sterilized reference formulations that were maintained at room temperature.

Additionally, three batches of IN-SLNs, IN-CS-SLNs and IN-NLCs were evaluated for their physical and chemical stability upon storage for a period of 3 months at 40°C/60% RH, 25°C/75% RH and 4°C. The particle size, PDI, zeta potential, EE and drug content were evaluated, as described in Sections 2.1.4 and 2.1.5.

2.1.7. Fourier transform infrared spectroscopy (FTIR)

The infrared spectra (IR) of the SLN and NLC formulations were obtained using Cary 660 series FTIR (Agilent Technologies) and MIRacle ATR (attenuated total reflectance) systems. The ratios of drug and lipids used in this set of studies were similar to the weight ratios in the IN lipid formulations.

2.1.8. *In vitro* release studies

In vitro release profiles of IN from the respective formulations, such as the IN-Tween® 80 solution (IN-TSOL), the IN-SLNs and the IN-NLCs (F-1 and F-2), were evaluated using Valia-Chien cells (PermeGear, Inc.). Spectra/por® dialysis membranes (3.5K MWCO) were mounted on diffusion cell chambers and securely fastened with air tight clamps between the donor and receptor chambers through which the transport or release kinetics were being studied. The temperature of the cells was maintained at 34°C using a circulating water bath. Five milliliters of isotonic phosphate buffer (IPBS) (pH 7.4) containing 2.5% w/v RMβCD was used as the receptor media during the course of the study (6 hrs). Five hundred microliters of formulation was added to the donor chamber. The, 600-µL aliquots were withdrawn from the receiver chamber at predetermined time points and replaced with an equal volume of the 2.5% w/v RMβCD in IPBS (pH 7.4) solution. The donor concentration was maintained at 0.1% w/v in all the formulations. The samples taken were analyzed using a HPLC-UV system, as described in Section 2.1.2.

2.1.9. *In vitro* corneal permeation studies

Corneas excised from whole eyes, obtained from Pel-Freez Biologicals, were used for the determination of *in vitro* transcorneal permeability. The whole eyes were shipped overnight in Hanks' balanced salt solution over wet ice and were used immediately upon receipt. The corneas were excised with some scleral portion adhering to help secure the membrane between the diffusion half-cells during the course of the transport study. After excision, the corneas were washed with the IPBS (pH 7.4) and mounted on side-by-side diffusion half-cells (Perme Gear, Inc®) with the epithelial side facing the donor chamber. The temperature of the half-cells was maintained at 34°C via a circulating water bath. The IN contents in the IN-SLN, IN-CS-SLN and IN-NLC formulations were 0.1% w/v, 0.1% w/v and 0.8% w/v, respectively. Three milliliters of

the optimized IN-SLNs, IN-CS-SLNs or IN-NLCs was added to the donor chamber after adjusting the pH to 6.8. The donor IN concentration was maintained at 0.1% w/v in the SLN formulation and 0.8% w/v in the NLC formulation. The receiver chamber medium consisted of 3.2 mL RMβCD (2.5% w/v) in IPBS solution for all the transport studies. The contents of both chambers were stirred continuously with a magnetic stirrer. Aliquots (600 μL) were withdrawn from the receiver chamber at predetermined time points up to 3 hrs and replaced with an equal volume of 2.5% w/v RMβCD in IPBS. The samples were stored at −80°C until further analysis of IN using the chromatography system described in Section 2.1.2. Additionally, the transcorneal permeabilities of IN from the IN-SOL formulation (control) and IN-HPβCD in the presence of CS as a penetration enhancer were also determined.

2.1.10. Trans-SCR permeability studies of IN formulations

The scleral tissue with the retinal pigmental epithelium and choroid layers excised from whole eyes, obtained from Pel-Freez Biologicals, were used to determine the *in vitro* trans-SCR (sclera-choroidal RPE) permeability of IN from the formulations. After excision, the scleral membranes were washed with IPBS (pH 7.4) and mounted on Valia-Chien cells (Perme Gear, Inc®). The scleral tissues were mounted as an inverted cup onto diffusion cells between the donor and receptor chamber and fastened securely with air tight clamps such that the scleral membrane was exposed to the donor compartment (episcleral side) and the RPE-choroidal tissues were in contact with the receptor compartment (vitreous body side). Five milliliters of 2.5% w/v RMβCD solution prepared in IPBS (pH 7.4) was used as the media in the receiver chamber during the course of the study for 2.5 hrs. Five hundred microliters of IN-SOL, IN-HPβCD, IN-SLNs (pH 6.8 and 7.4), and IN-SLNs+HPβCD were added to the donor chambers, and the concentration was maintained at 0.1% w/v. Aliquots (600 μL) were withdrawn from the receiver chamber at

predetermined time points (15, 30, 45, 60, 90, 120 and 150 min) and replaced with an equal volume of receiver medium. The samples taken were analyzed using the HPLC-UV system as discussed in Section 2.1.2.

2.1.11. *In vivo* bioavailability studies

In vivo bioavailability of IN was determined in Male New Zealand White albino Rabbits, weighing between 2-2.5 kg, procured from Harlan Labs. All the animal studies conformed to the tenets of the Association for Research in Vision and Ophthalmology statement on the use of animals in ophthalmic vision and research and the University of Mississippi Institutional Animal Care and Use Committee approved protocols. Rabbits were anesthetized using a combination of ketamine (35 mg/kg) and xylazine (3.5 mg/kg) injected intramuscularly and were maintained under anesthesia throughout the experiment. The IN formulations, namely the IN-SOL, IN-HPβCD, and IN-SLNs, were evaluated *in vivo.* All the above IN topical formulations (100 µL) were given as two doses (50 µL), 30 min apart, (T-30 min and 0 min) to reduce precorneal loss. Additionally, the IN-CS-SOL, IN-SLNs, IN-CS-SLNs (n=6) and IN-NLCs were administered to conscious rabbits to delineate the effects of anesthesia on the ocular bioavailability of IN. CS was used at a concentration of 0.25% w/v (*in vivo).* Two hours post-topical application, the rabbits were euthanized with an overdose of pentobarbital injected through a marginal ear vein. The eyes were washed thoroughly with ice-cold IPBS and were immediately enucleated. All the intraocular tissues were separated and stored at -80°C, and further analysis was carried out using the HPLC-UV system (Section 2.1.2.). All experiments were performed in triplicate.

2.1.12. Biosample preparation for the determination of IN content in ocular tissue homogenates

The *in vitro* analytical HPLC-UV method described above was employed for sample analysis following method validation. A protein precipitation technique was employed to determine the amount of IN in the ocular tissue homogenates. Briefly, tissues including the cornea, sclera, iris-ciliary (IC), and retina-choroid (RC) were cut into small pieces, and a mixture of ice-cold acetonitrile and 0.1% v/v formic acid was added (1 mL) to precipitate proteins from each individual tissue. The supernatant was then collected via centrifugation for 1 hr at 13000 rpm prior to the analysis. The aqueous humor (AH) (200 µL) and vitreous humor (VH) (500 µL) were precipitated by adding an ice-cold mixture of acetonitrile and formic acid, 200 µL of each for the AH and 500 µL of each for the VH corresponding to a ratio of 1:1. Quantification of IN was performed using standard calibration curves constructed from various ocular tissues, such as the cornea (20-500 ng), the sclera (20-500 ng), the AH (10-200 ng), the VH (10-200 ng), the IC (10-200 ng), and the RPE (10-200 ng). All the standard curves had a coefficient of determination $r^2 \geq 0.96$. The recovery of IN was evaluated by spiking the drug in pure AH and VH and comparing the expected IN concentration with the standard concentration. Recovery values were determined for AH (93.1) and VH (91.5). Interference was not observed from co-eluted protein residues with respect to IN peaks in any of the tissues. The limit of detection (LOD) for various ocular tissues was determined and corresponded to 10 ng for AH, 10 ng or VH, 5 ng for the cornea, 5 ng for the sclera, 10 ng for the RPE, and 10 ng for the IC.

2.3. Data analysis

The steady-state flux (SSF) for transcorneal and trans-SCR experiments was calculated by dividing the rate of transport by the surface area. The slope of the cumulative amount of IN transported versus time plot was used to obtain the rate of IN transport across the excised rabbit cornea. The flux was calculated using the Eq. (2).

$$\text{Flux(J)} = (\text{dM/dt})/\text{A} \quad (2)$$

where M is the cumulative amount of drug transported, and A is the surface area of the corneal membrane (0.636 cm^2) exposed to the permeant (drug).

The transcorneal permeability was determined by normalizing the SSF to the donor concentration, C_d, according to Eq. (3).

$$\text{Permeability(Papp)} = \text{Flux/Cd} \quad (3)$$

2.3.1. Statistical analysis

One-way-ANOVA coupled with a post hoc test was employed to analyze the differences between groups (*in vivo*). The difference in data obtained were considered statistically significant at level of $p<0.05$.

2.4. Results

2.4.1. Morphometrical and physico-chemical characteristics

The particle size, zeta potential, PDI and EE of IN-SLN, the IN-CS-SLNs and the IN-NLCs were observed to be 226 ± 5, 265 ± 8, and 227 ± 11 nm; -22 ± 0.8, 27 ± 1.2, and -12.2 ± 2.3 mV; 0.17, 0.30, and 0.23; and 81 ± 0.9, 91.5 ± 3.2 and 99.8 ± 0.2%, respectively. The quantitative compositions of the various IN formulations are presented in **Table 2.1**. The particle size of the IN-NLCs increased as the total lipid content increased, and IN-NLC-F1 appears to be a promising formulation, exhibiting a lower hydrodynamic radius and better physico-chemical characteristics compared to the other formulations **(Table 2.2).**

Table 2.1: Composition of IN formulations with individual components represented by weight (mg).

Formulation composition	IN formulations							
	IN-TSOL	IN-SOL	IN-CS-SOL	IN-HPBCD	IN-SLN-HPβCD	IN-SLN	IN-CS-SLN	F-1 IN-NLC
IN (mg)	10	10	10	10	10	10	10	80

Compritol (mg)	-	-	-	-	200	200	200	260
Miglyol® 812	-	-	-	-	-	-	-	140
Poloxamer 188 (mg)	-	-	-	-	25	25	25	25
Tween® 80 (mg)	100	100	100	-	75	75	75	75
Glycerin (mg)	-	-	-	-	225	225	225	225
Propylene glycol (mg)	-	2930	2930	-	-	-	-	-
CS (mg)	-	-	10	-	-	-	25	-
HPβCD (mg)	-	-	-	250	250	-	-	-
Water (mL)	10	10	10	10	10	10	10	10

Table 2.2: Composition of lipid mixtures used in the NLC formulations. The particle size characteristics, PDI, zeta potential, entrapment efficiency and assay values for each formulation are presented below.

IN-NLC formulations	F-1	F-2	F-3	F-4	F-5	F-6
IN (0.8% w/v)	80	80	80	80	80	80
Compritol (60%)	240	240	240	240	240	240
Miglyol 812 (40%)	160	-	320	640	-	-
Miglyol 829 (40%)	-	160	-	-	320	640
Total lipid (%; mg)	4%; 400	4%; 400	8%; 800	16%; 1600	8%; 800	16%; 1600
particle size (nm)	227	279.1	304.1	519.2	385.1	629.1
Polydispersity index (PDI)	0.235	0.259	0.433	0.58	0.456	0.381
Zeta potential (mV)	-12.2	-5.57	-0.92	0.027	-2.58	-0.304
Entrapment efficiency (%) EE	99.8	99.74	100	100	100	99.9
Assay (%)	96.8	97.8	97.4	91.3	96.2	92.5

2.4.2. Solubility of IN in the presence of cyclodextrins and surfactants

Cyclodextrins and surfactants are frequently employed as solubilizers in topical ophthalmic formulations. The solubilities of IN in 0.25 and 0.5% w/v poloxamer 188 at pH 7.4 were measured as 251.8 ± 78 and 657 ± 127 µg. The solubility of IN in 0.5% w/v Tween® 80 at pH 7.4 was determined to be 1055 ± 106 µg. The solubility profiles of IN in 5% w/v HPβCD and RMβCD were found to be similar. However, the solubility of IN is highly pH-dependent and tends to be predominantly solubilized at high pH **(Figure 2.1)**.

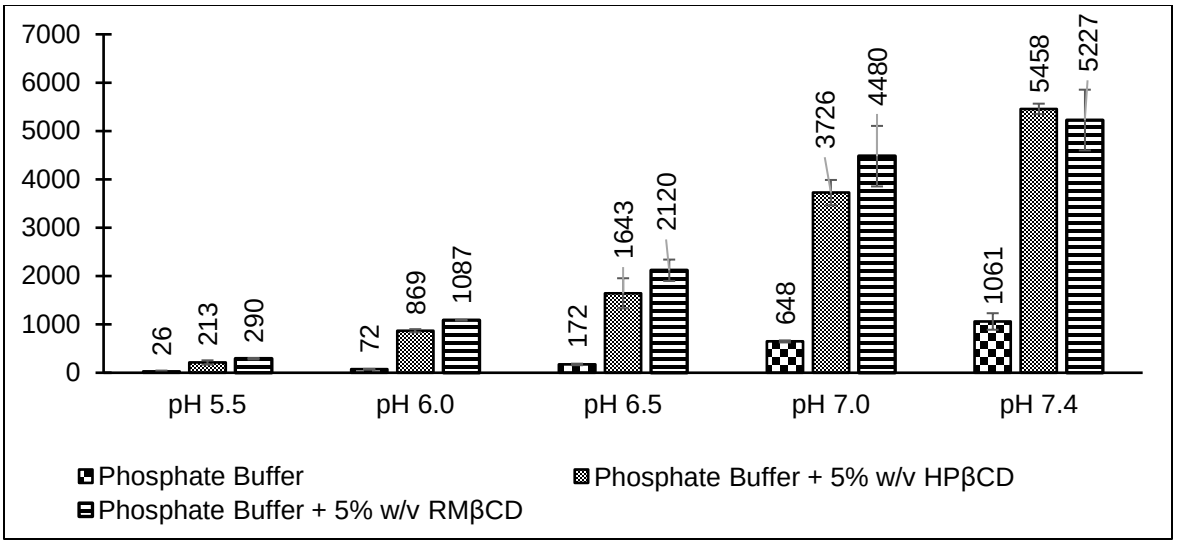

Figure 2.1: pH-dependent saturation solubility of IN in phosphate buffer, 5% w/v HPβCD in phosphate buffer, and 5% w/v RMβCD in phosphate buffer (µg/mL). The results are depicted as the mean ± SD (n=3).

2.4.3. Stability, moist-heat sterilization and FTIR studies

IN-CS-SLNs and IN-NLCs exhibited good stability when compared to the IN-SLN formulation. The particle size of the IN-SLN formulation after storage for 90 days at 40°C was increased by 65%, whereas the IN-CS-SLNs and IN-NLCs displayed a 15-20% increase in particle size (**Figure 2.2**). Additionally, the EE of the SLN formulations decreased by 12% compared to the IN-CS-SLNs (6%) and IN-NLCs (5%) (**Figure 2.3a**). The zeta potential and PDI of the IN formulations were not changed significantly under the storage conditions tested here (**Figure 2.3b and 2.3c**). **Figure 2.4** shows the effect of sterilization on the physicochemical characteristics of the IN lipid-based formulations. No significant differences were observed post-sterilization. The particle size of the IN-CS-SLNs and IN-NLC formulations slightly increased compared to the IN-SLNs following autoclaving. Additionally, the FTIR spectra revealed a slight drug-excipient interaction in the lipid formulations **(Figure 2.5)**.

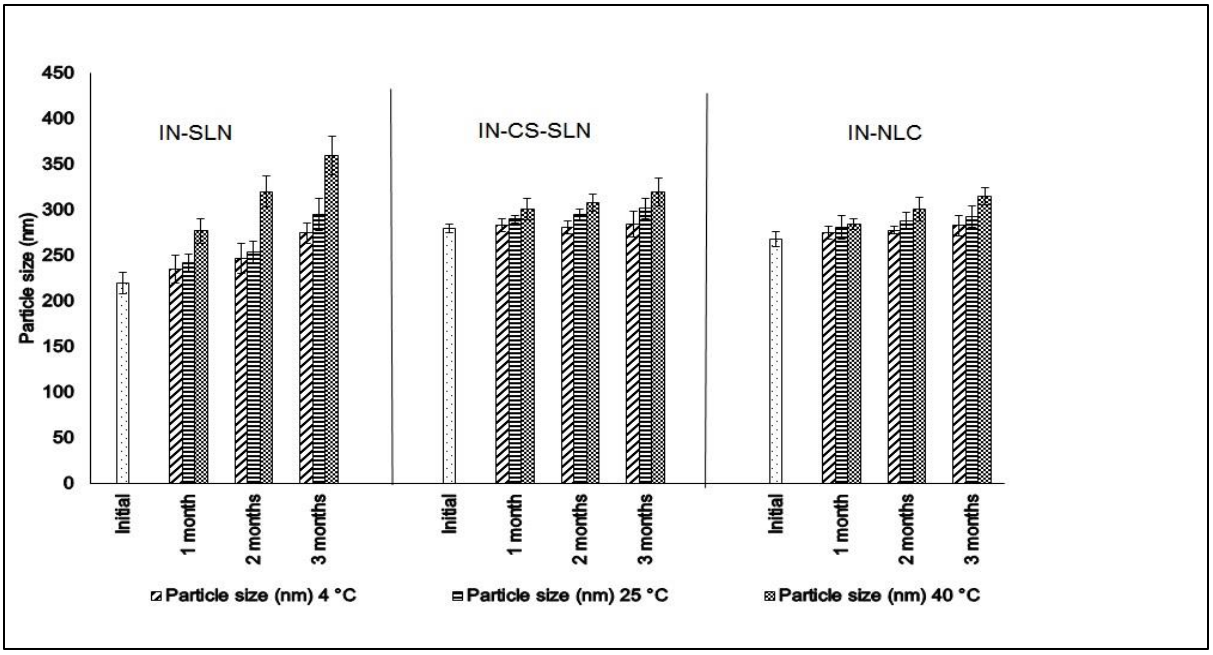

Figure 2.2: Particle size characteristics of various IN formulations following storage at 4°C, 25°C/60% RH, and 40°C/75% RH. The data represent the mean ± S.D (n=3).

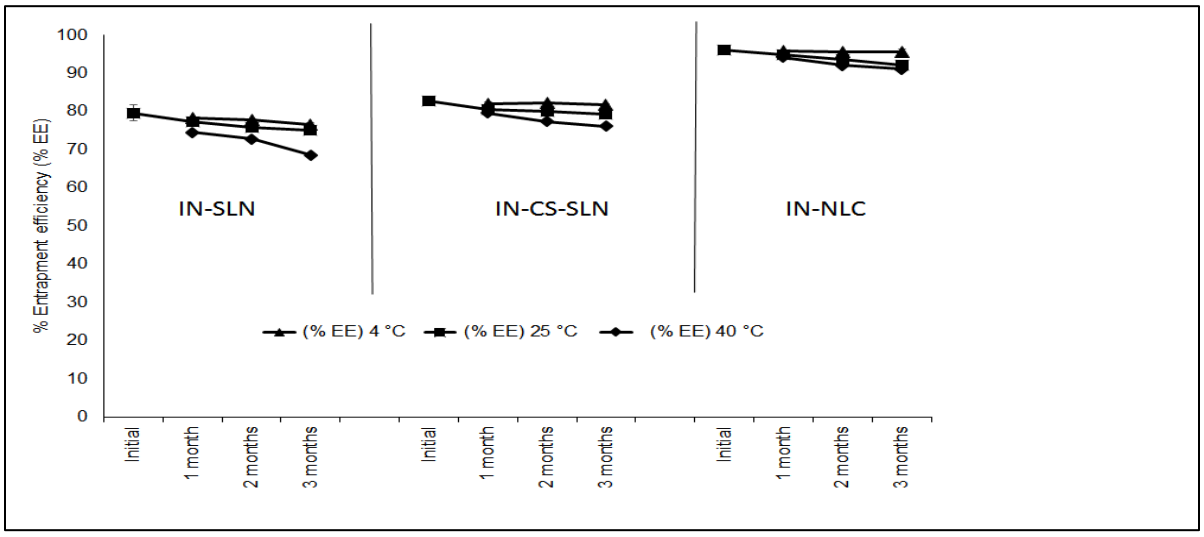

Figure 2.3a: Entrapment efficiency (% EE) of various IN formulations following storage at 4°C, 25°C/60% RH, and 40°C/75% RH. The data represent the mean ± S.D (n=3).

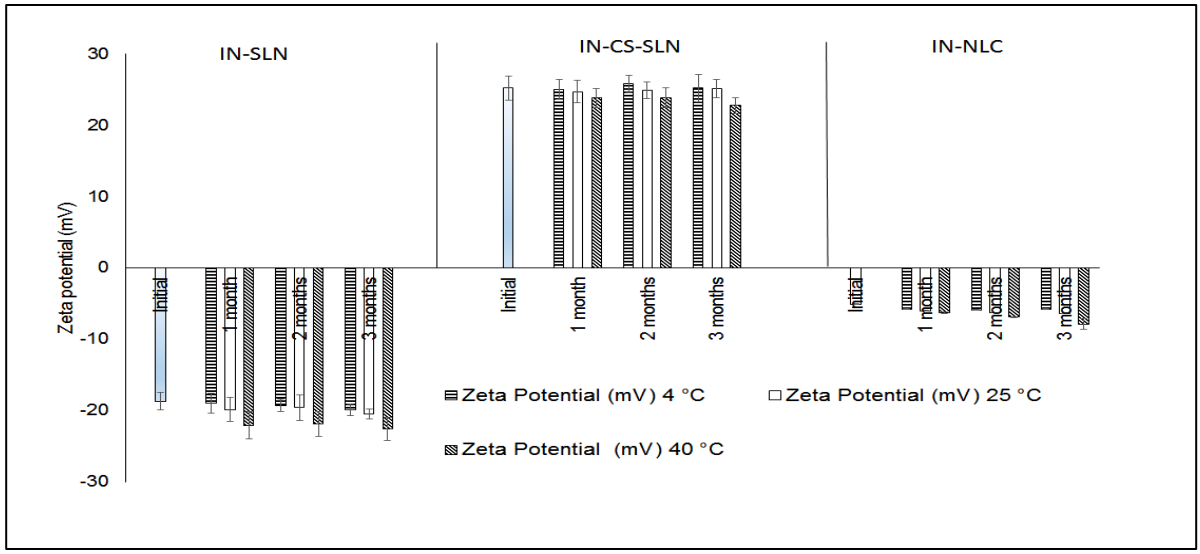

Figure 2.3b: Zeta potential of various IN formulations following storage at 4°C, 25°C/60% RH, and 40°C/75% RH. The data represent the mean ± S.D (n=3).

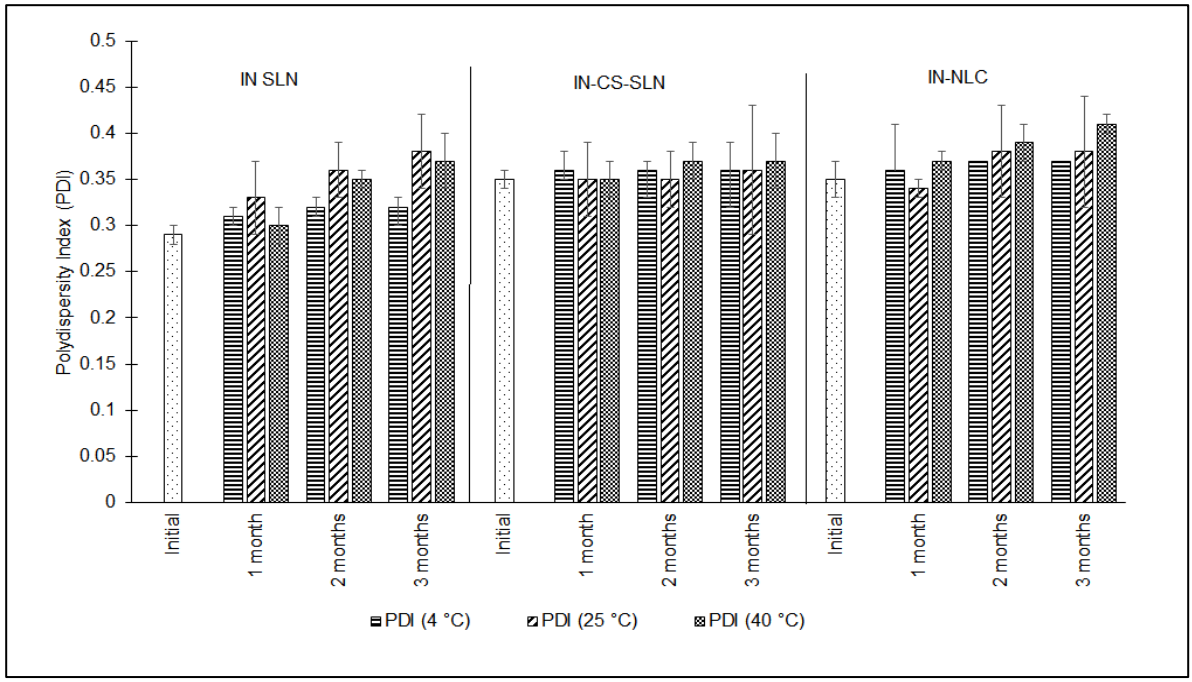

Figure 2.3c: Polydispersity indices (PDI) of various IN formulations following storage at 4°C, 25°C/60% RH, and 40°C/75% RH. The data represent the mean ± S.D (n=3).

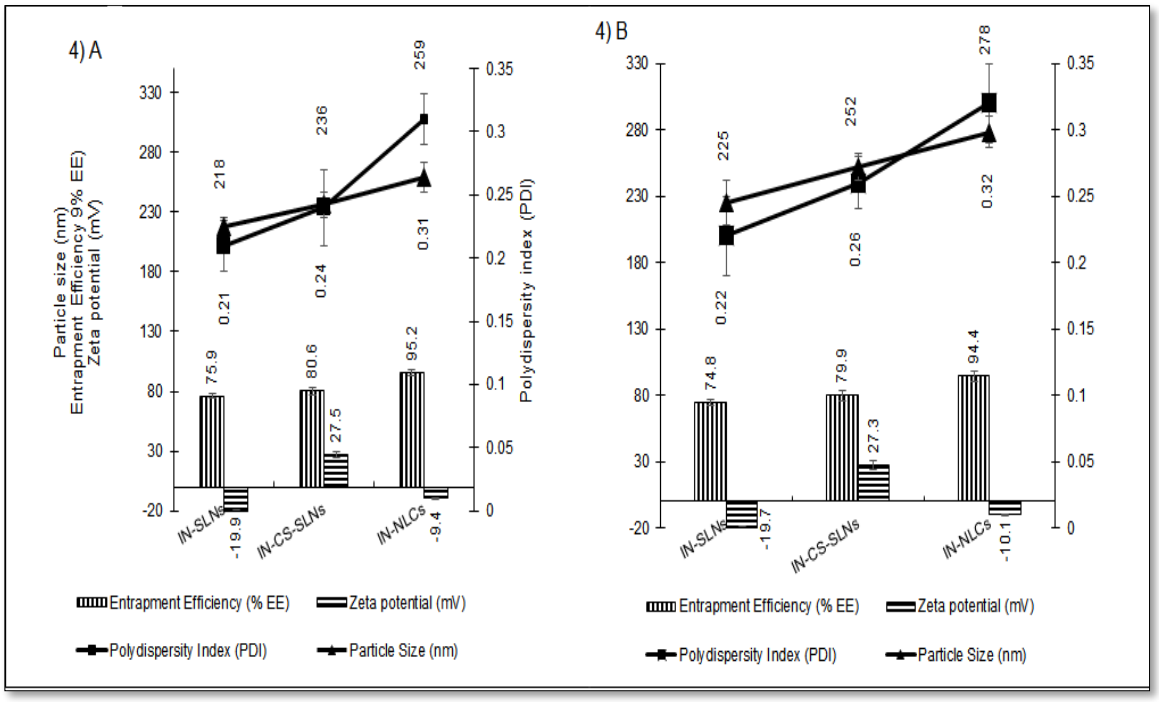

Figure 2.4: Physico-chemical characteristics of the IN SLN and NLC formulations pre (Fig 2.4A) and post-sterilization (2.4B). The data represent the mean ± S.D (n=3).

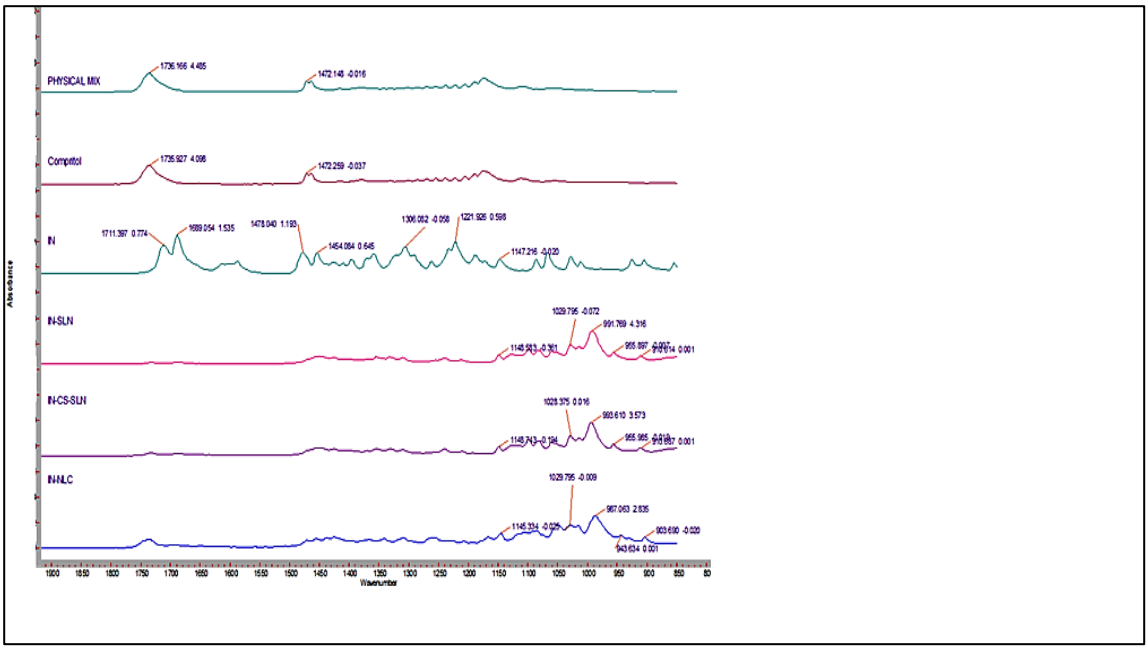

Figure 2.5: FTIR spectral images of the IN + Compritol physical mixture, Compritol, IN, IN-SLN, IN-CS-SLN and IN-NLC F-1 formulations.

2.4.4. *In vitro* release studies

Based on the solubility profile of IN in different solubilizing agents, RMβCD in IPBS at pH 7.4 was chosen as the receptor media for the *in vitro* release and transcorneal permeability experiments. The *in vitro* releases of IN from the IN-TSOL, the IN-SLNs, the F-1IN-NLCs, and the F-2 IN-NLCs were observed to be 81.6 ± 2.1 µg, 18.7 ± 0.9 µg, 31.8 ± 3.9 µg, and 23.3 ± 3.1 µg within the time period tested (6 hrs). The *in vitro* release of IN from these formulations is depicted in **Figure 2.6**.

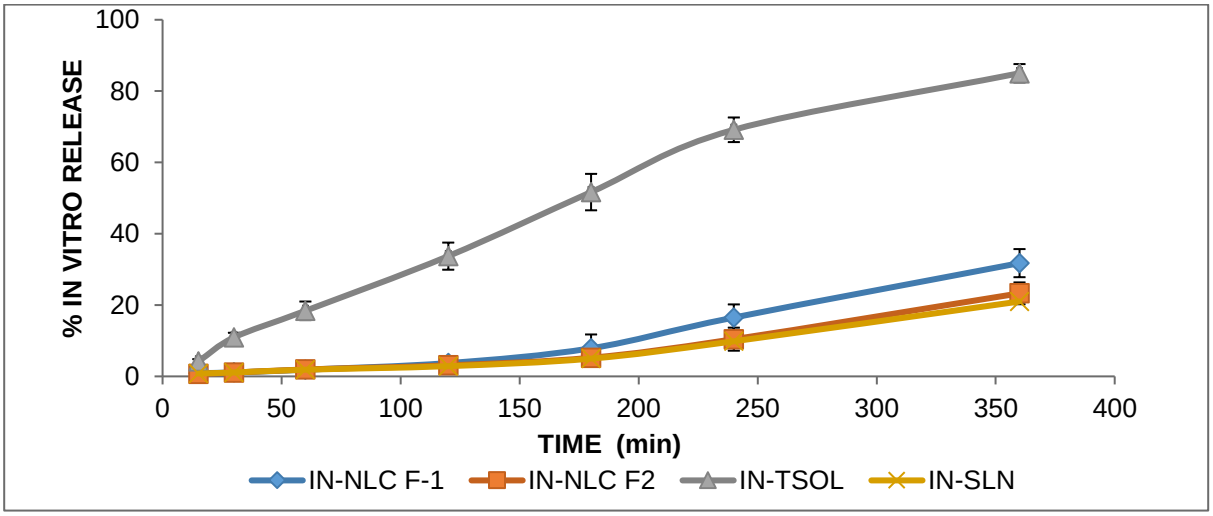

Figure 2.6: *In vitro* release of IN from various formulations across Spectra/Por® membranes at 34°C. Receiver solution consisted of IPBS containing 2.5% w/v RMβCD (pH 7.4). The results are depicted as the mean ± S.D (n=3).

2.4.5. Transcorneal permeability studies

The transmembrane permeabilities of IN from the IN-SLNs, the F-1IN-NLCs, and the F-2 IN-NLCs were observed to be 1.93 ± 0.17 x 10^{-5}, 1.34 ± 0.13 x 10^{-5}, and 1.2 ± 0.1 x 10^{-5} cm/s, respectively. The transcorneal flux of IN was increased by two-fold when CS was used as a permeation enhancer in the SLN formulation. Moreover, the effect of including CS as a penetration enhancer in the solution formulations, namely in IN-SOL and IN-HPβCD, was also investigated. CS significantly enhanced the transcorneal flux of IN by ~3.5 and ~2-fold for the IN-SOL and IN-HPβCD formulations, respectively **(Figure 2.7)**.

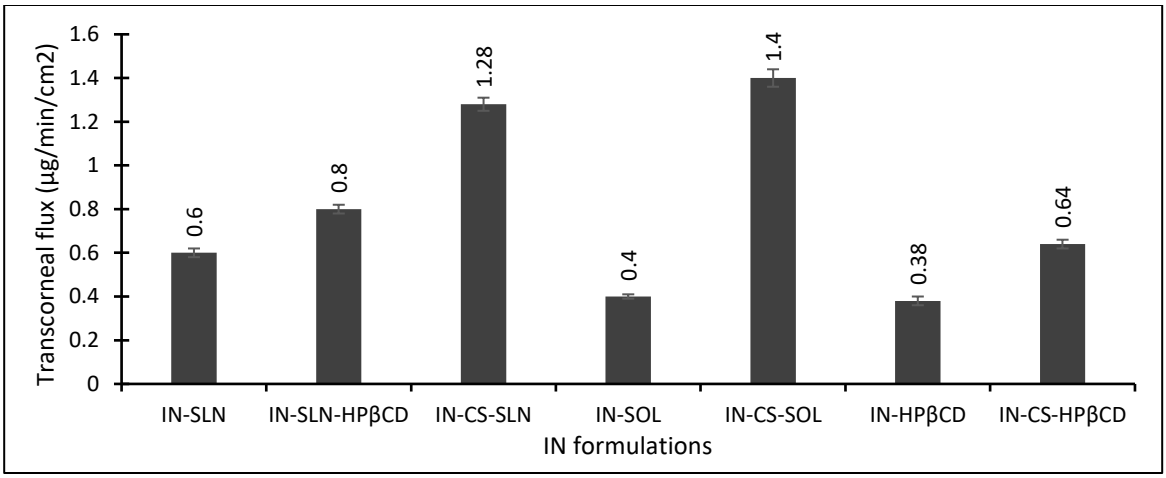

Figure 2.7: Transcorneal flux across isolated rabbit cornea from various IN topical formulations at 34ºC. The receiver solution consisted of IPBS containing 2.5% w/v RMβCD (pH 7.4). The results are depicted as the mean ± S.D (n=4).

2.4.6. Trans-sclera-choroid-RPE (SCR) permeability studies

Trans-SCR permeability experiments were carried out to assess the scleral penetration capability of IN from the formulations compared to the corneal absorption route. The trans-SCR permeability of IN-HPβCD was markedly higher compared to IN-SOL. The trans-SCR permeabilities of the SLN increased in the order of IN-SLNs (pH 6.8) < IN-SLNs (pH 7.4) < IN-SLNs + HPβCD (pH 6.8). The SLNs in combination with HPβCD demonstrated a higher trans-SCR permeability than the SLN formulation alone **(Figure 2.8)**.

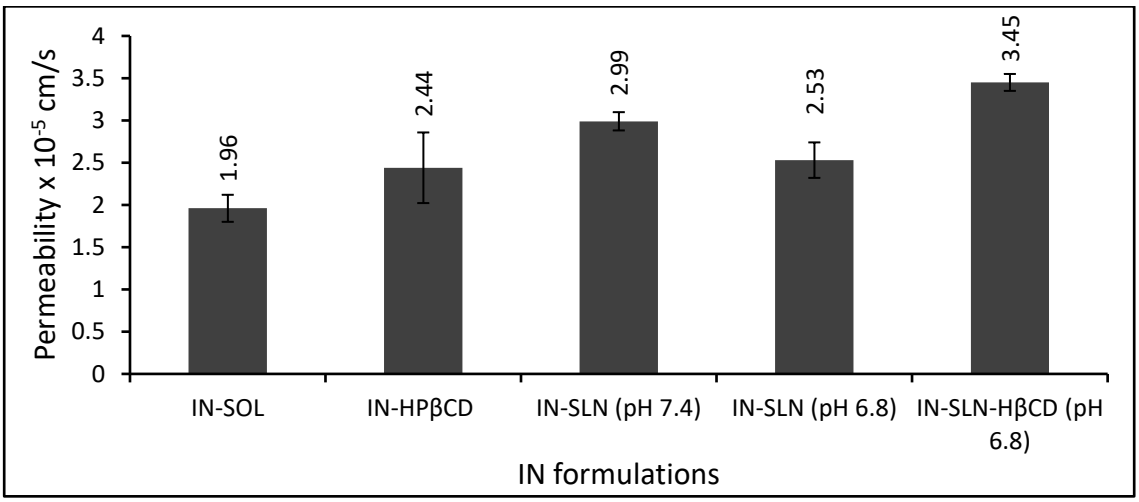

Figure 2.8: Trans-SCR permeability of IN from various topical ocular formulations at 34ºC.

The receiver solution consisted of IPBS containing 2.5% w/v RMβCD (pH 7.4). The results are depicted as the mean ± S.D (n=3).

2.4.7. *In vivo* bioavailability studies

Based on the transcorneal and trans-SCR data obtained, the IN formulations were investigated for their ocular bioavailability and disposition of IN 2 hrs post-topical administration in anesthetized and conscious rabbits. The IN-SOL formulation could not deliver the drug to the posterior ocular tissues. However, the IN-SOL formulation was able to achieve drug levels in the anterior segments of the eye, including 463.5 ± 15 ng/g in the cornea and 224 ± 8.6 ng/g in the scleral tissues. CS as a penetration enhancer further improved the ocular bioavailability of IN-SOL. Significant drug levels were attained from the IN-HPβCD formulation in most of the ocular tissues tested, namely in the cornea (3267.3 ± 1867.6 ng/g), the sclera (575.7 ± 433.5 ng/g), the AH (877.4 ± 492.5 ng/g), the RC (94.4 ± 79.9 ng/g) and the IC (1203.9 ± 547 ng/g). Significantly higher levels of IN were observed in the posterior segments of the eye for the use of the SLN formulation compared to the IN-SOL and IN-HPβCD formulations. The formulation of SLNs in combination with 0.25% w/v CS achieved higher levels of IN in conscious rabbits (n=6). The NLC formulations, however, were the most effective in terms of drug loading and ocular IN levels. The ocular tissue IN concentrations obtained from the above formulations are shown in **Figures 2.9 and 2.10**.

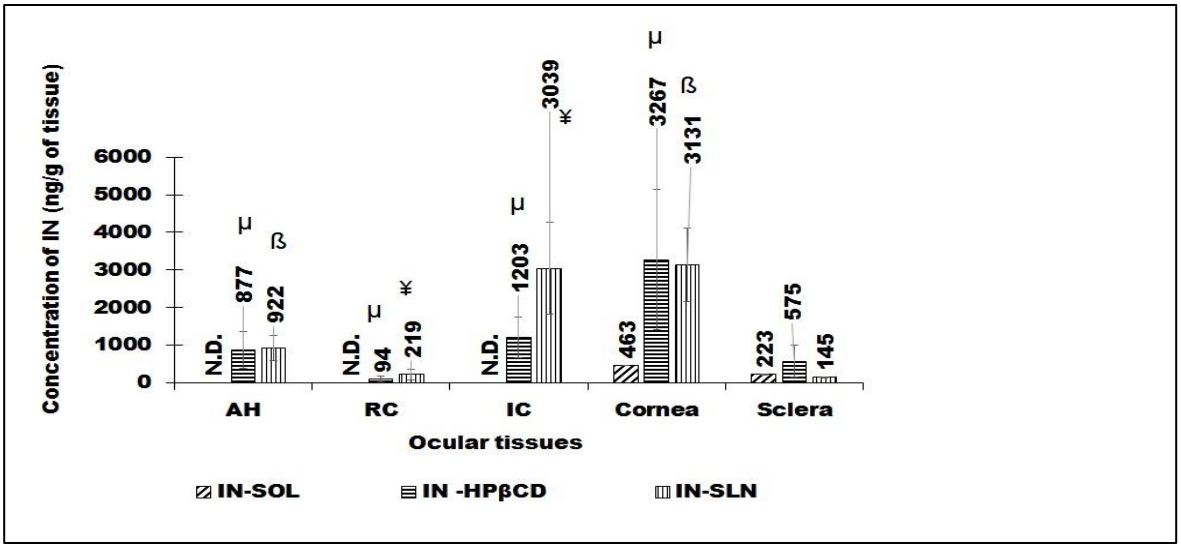

Figure 2.9: IN ocular tissue concentrations (ng/g of tissue) obtained from the IN-SOL, IN-HPβCD, and IN-SLN formulations 2 hrs post-topical administration in the anesthetized rabbit model. The data represent the mean ± S.D. (n=3). AH: Aqueous humor; VH: Vitreous humor; IC: Iris-Ciliary; RC: Retina-Choroid. (N.D., not detected). Different symbols, such as μ and β, indicate significant differences ($p<0.05$) of the IN-HPβCD and IN-SLN formulations compared to IN-SOL. ¥ represents a significant difference in the ocular tissue concentrations of IN for use of the IN-SLNs compared to all other formulations.

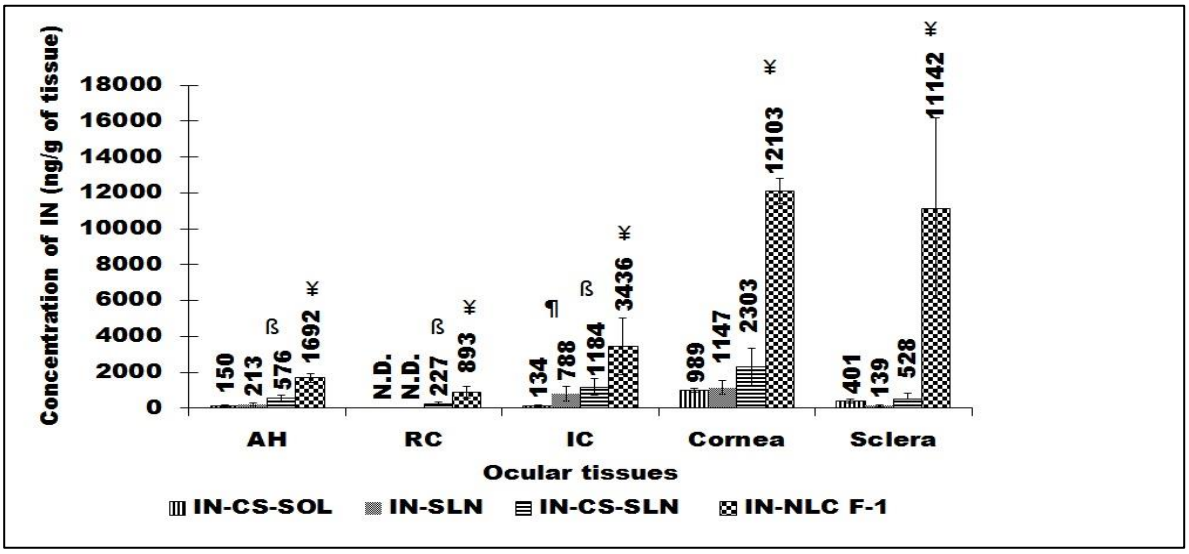

Figure 2.10: IN ocular tissue concentrations (ng/gm of tissue) obtained from the IN-CS-SOL, IN-SLN, IN-CS-SLN (n=6) and IN-NLC formulations 2 hrs post-topical administration in the conscious rabbit model. The data represent the mean ± S.D. All the experiments were performed in triplicate if not indicated otherwise. Different symbols, such as ¶ and β, indicate significant differences ($p<0.05$) of the IN-SLN and IN-CS-SLN formulations compared to IN-CS-SOL. ¥ represents a significant difference in the ocular tissue concentrations of IN for use of the IN-NLCs compared to all other formulations.

2.5. Discussion

The objective of the current work was to develop IN-loaded lipid-based nanoparticles and to investigate the *in vitro* corneal permeation and *in vivo* ocular disposition of IN from these formulations. Most NSAIDs are inherently weak acidic drugs with poor corneal penetration due to their ionization at lacrimal pH. Lowering the pH of these formulations increases corneal penetration but also increases potential irritation. Additionally, it has been reported that due to the anionic nature of NSAIDs, they are incompatible with preservatives such as benzalkonium chloride and could form insoluble complexes (54-56). IN (pKa of 4.5) exhibits pH-dependent solubility, which increases as a function of higher pH (acidic to neutral/alkaline: 1.5 µg/mL at pH 1.2 and 105.2 µg/mL at pH 7.4). IN displayed a solubility of 0.64 ± 0.02 mg/mL in phosphate buffer at pH 7.0, which is consistent with previously reported data (57, 58). Additionally, the solubility of IN was increased by ~5 and ~6-fold with 5% w/v HPβCD and RMβCD in phosphate buffer at pH 7.0.

SLNs and NLCs are colloidal nanoparticulate dispersions that can be administered topically in the form of eye drops. A major advantage of the nanoparticulate systems is their uptake by epithelial cells, which allows for greater penetration into the surface layers (59-61). Moreover, the small size, biocompatibility and mucoadhesive properties of SLNs improve their interactions and prolong the pre-ocular residence time of drugs, thus enhancing drug bioavailability (62, 63). The literature suggests that surface modification of SLNs by coating with hydrophilic agents such as poly (ethylene) glycol derivatives (PEGs) or chitosan can further improve ocular penetration, mainly due to enhancing interactions with the ocular mucosa and increasing cellular uptake and internalization (64, 65). Additionally, previous reports have demonstrated the ability of chitosan nanoparticles to produce a sharp, reversible decrease in the transepithelial electrical resistance

(TEER) and to improve the permeability of model macromolecules (66). The mechanism of mucoadhesion is possibly through the electrostatic interaction between the positively charged amino groups of chitosan and the negatively charged sialic acid residues of ocular mucosa (67).

The corneal route is a major absorption pathway for topically administered medications (68). Compared to other formulations, IN-SLNs demonstrated higher transcorneal permeability, which may be ascribed to endocytosis or transcytosis uptake mechanisms (69, 70). The *in vitro* transcorneal permeability of IN from the NLC formulations was comparatively lower than that of the SLNs, probably because of higher entrapment in the oily phase and thus lower partitioning into the membrane. Reports have suggested that chitosans with a moderate degree of deacetylation (65-80%) and a relatively high molecular weight (170-200 kDa) is required for the exertion of optimal transepithelial penetration and low toxicity (71-73). The *in vitro* transcorneal flux of IN from the IN-SOL, IN-HPβCD, and IN-SLN formulations increased by ~3.5-fold, ~2-fold and ~2-fold, respectively, in the presence of CS, which is consistent with previous reports.

Numerous reports have demonstrated that sclera is more permeable to hydrophilic than to lipophilic molecules and approximately 10 times more permeable than the cornea (74, 75). Based on trans-scleral transport studies, the higher permeability across several static layers of ocular tissues (sclera, Bruch's membrane-choroid, RPE, and neural retina) demonstrates the diffusional ability of drugs to the back of the eye through the conjunctival-scleral pathway (76, 77). To investigate drug delivery to the posterior ocular segments, scleral diffusion of IN was assessed in trans-SCR experiments. The higher observed trans-scleral permeability of IN from the SLNs compared to the IN-SOL and IN-HPβCD formulations demonstrated that lipid carriers could enhance accumulation in scleral tissue, prolonging the ocular residence time *in vivo*. The increased permeability of IN from SLNs with HPβCD in external aqueous phase could be due to the

complexation effect of cyclodextrin with the free drug. The trans-scleral permeability of SLNs at pH 7.4 (2.99 ± 0.1 x 10^{-5} cm/s) was considerably higher than that of the SLNs at pH 6.8 (2.13 ± 0.3 x 10^{-5} cm/s), which is likely due to an increase in the ionized fraction of IN at pH 7.4.

Castelli et al. (78) fabricated SLNs and NLCs of IN and characterized the formulations with respect to drug distribution and entrapment efficiencies in the lipid matrices. However, the loaded drug in the SLNs and NLCs of IN was maintained at 2 and 1.5% w/w with respect to the total lipid, whereas in the present study, drug loading of IN in the SLNs and NLCs was achieved at 5 and 20% w/w, respectively. The IN lipid formulations demonstrated higher drug loading and entrapment efficiencies at lower lipid contents compared to Castelli's formulations. Bucolo et al. (79) investigated the ocular pharmacokinetics of IN following a multiple dosing treatment regime (30 µL/eye; four times in 8 hrs) of 0.5% IN + hydroxypropylmethylcellulose, IN-HPMC and Indocollyre® eye drops in conscious rabbits. The drug levels in the AH, RC and VH obtained 2 hrs post-topical administration of IN-HPMC and Indocollyre® solution were 360 ± 40 and 100 ng/mL, 65 and 20 ng/g, and 7± 2 and 5 ± 2 ng/mL, respectively. Campos et al. (67) studied the ocular distribution of chitosan-fluorescein nanoparticles (0.25% w/v, dose: 100 µL, 250 µg) and their interaction with the corneal and conjunctival epithelia in conscious rabbits. The drug levels in the cornea and conjunctiva 2 hrs post-topical application were 760 ± 60 and 1000 ± 150 ng/g, respectively. In another study, Klang et al. (80) formulated positively charged submicron emulsions (0.1% w/v) and compared the formulation with Indocollyre®. The drug concentrations obtained in the cornea and conjunctiva 1 hr after topical instillation of 50 µL of the test formulation were nearly 40 and 30% lower, respectively, compared to the marketed formulation. The drug concentrations obtained in the AH and sclera-retina were found to be 75 ± 38 ng/mL and 800 ± 310 ng/g (submicron emulsion) vs 110 ± 50 ng/mL and 450 ± 200 ng/g (Indocollyre®),

respectively. Yamaguchi (81) et al. investigated ocular tissue IN concentrations upon use of chitosan-coated emulsion (0.1% w/v) formulations 1 hr post-topical instillation (50 µL) in both eyes of anesthetized male Japanese albino rabbits. The drug levels attained were predominantly in the cornea (3596±425 ng/g), aqueous humor (434±90 ng/mL) and conjunctiva (668 ± 188 ng/g). In another study, an IN (0.1% w/v) ophthalmic solution was prepared using Poloxamer® 407 (10% w/w) and compared with an Indocollyre® formulation in terms of AH concentration 2 hr after a multiple post-topical administration regime of 150 µL (6 x 25 µL at 90 sec intervals). The IN concentration in the AH was enhanced by ~2-fold compared to the use of Indocollyre® (40).

In comparison to all the ocular tissue levels obtained with the above-discussed formulations, the IN-CS-SLNs delivered significantly higher levels of IN to the anterior and posterior segment ocular tissues, which could be attributed to mucoadhesive and epithelial barrier-modulating properties of chitosan. Compared to IN-SOL without CS, the incorporation of CS in the IN-SOL formulation improved penetration of IN into the AH and IC bodies, but retinal tissue IN levels remained below the detection limit. The addition of viscosity modifiers, such as hydroxypropyl methylcellulose, in the IN-CS-SOL formulation may further prolong the precorneal residence and thus increase ocular drug levels. IN concentrations were reduced by ~4- to 5-fold in conscious animals compared to the anesthetized model, delineating the effects of anesthesia on ocular pharmacokinetics. In comparison, at higher doses (0.8% w/v; 8-fold dose) the IN-NLCs delivered ~4- to 5-fold higher concentrations than the IN-CS-SLNs, which could be due to higher drug loading, EE and pre-ocular retention of IN for the use of the NLC formulation. NLCs are superior to SLNs in terms of higher drug loading, higher EE, improved storage stability and less drug expulsion during storage.

The effect of storage conditions and sterilization on the morphometrical and physico-chemical characteristics of IN formulations are shown in **Figures 2.2-2.4**. There was initially no significant difference in particle size, zeta potential, or PDI between the SLNs and NLCs, but as the time progressed, the IN-NLC and IN-CS-SLN formulations were found to be more stable than the IN-SLNs. The EE of the formulations decreased slightly as the storage time increased, although the change was not statistically significant (**Figure 2.3a**). Sterilization trials suggested that the IN lipid-based formulations were autoclavable (**Figure 2.4**). A qualitative FTIR spectral analysis was employed to investigate any interactions and/or incompatibility among the lipid, drug and other excipients. The FTIR spectra of the physical mixture indicated slight molecular interactions between the drug and Compritol. The characteristic peaks of IN at 1,711 cm^{-1} (carbonyl stretching-acid group), 1,221 cm^{-1} (asymmetric aromatic O–C stretching) and 1,086 cm^{-1} (symmetric aromatic O–H stretching) are masked in the formulations possibly due to the amorphous transition and entrapment of IN in the lipid matrices. In conclusion, the results obtained here indicate that lipid-based systems can dramatically improve the transcorneal permeability and retention characteristics of IN compared to conventional formulations *in vivo*. Thus, colloidal frameworks could be exploited to enhance ocular bioavailability significantly, including back-of-the-eye ocular tissues.

2.6. Conclusion

Targeting NSAIDs to the posterior segment of the eye via a topical route is a challenging task due to formulation constraints and the anatomical, physiological and efflux barriers present in ocular tissues. IN-loaded NLC formulations displayed higher drug-loading capabilities and entrapment efficiencies, which resulted in higher IN levels in the ocular tissues. The IN-CS-SLNs demonstrated superior trans-membrane IN permeation characteristics compared to the IN SLNs, confirming the penetration-enhancing properties of chitosan. It is worth noting that the IN-CS-

SLNs, containing a tenth of the loaded drug of the IN-NLCs, induced IN concentrations in the inner ocular tissues (the AH, IC and RPE-choroid) that were 3- to 4-fold lower than those obtained for IN-NLCs. The corneal and scleral IN concentrations achieved using the IN-NLCs were significantly higher, indicating the effect of the increased drug loading in the formulation. Thus, both the IN-CS-SLNs and IN-NLCs are viable platforms for the posterior ocular delivery.

CHAPTER 3

OCULAR DISPOSITION OF CIPROFLOXACIN FROM TOPICAL, PEGYLATED NANOSTRUCTURED LIPID CARRIERS: EFFECT OF MOLECULAR WEIGHT AND DENSITY OF POLY (ETHYLENE) GLYCOL

3. Introduction

Delivery of drugs, especially to the back-of-the eye tissues comprising sclera, choroid, retina, and vitreous body, is restricted by multiple physiological processes, anatomic, static, dynamic and efflux barrier functionalities (1, 82). Efflux protein pumps expressed on ocular tissues restrict transmembrane permeability of drugs, thus lowering penetration of substrates from the systemic, topical or periocular routes (83, 84). Topical application is the most favored route because of the ease of administration, lack of associated complications and minimal non-specific systemic exposure. Only 5-10% of the topically administered dose, however, reaches the inner ocular tissues (85, 86). Although advances have been made with respect to delivery into the anterior segment ocular tissues, significant challenges still exist for very lipophilic molecules in view of the formulation restrictions placed by the sensitivity of the ocular tissues. Several formulation approaches such as inclusion of viscosity enhancers in aqueous ophthalmic solution or suspension formulations, ion-exchange resin based formulations, implants, transporter targeted systems, emulsions, films and other nanoparticle mediated drug delivery strategies have been described in the literature, and some are commercially available (87-90). Despite technological advancements in the formulation strategies, delivery of therapeutic agents efficiently into the back-of-the eye ocular tissues through the topical route remains elusive (91). Ointments have been successful to some extent but various drawbacks, including difficulty in application and problems in vision, have limited its usefulness. Success in back-of-the eye delivery mainly depends on formulation platform, candidate's physicochemical properties and absorption pathway. Penetration of drugs across alternatively polarized (lipophilic and hydrophilic) ocular layers, and through the corneal tight junctions, is highly dependent upon their physicochemical properties.

Thus, the molecules should exhibit optimum physicochemical aspects and are to be formulated in appropriate dosage forms for enhanced retinal delivery (92, 93).

Kinetics, bio-distribution and release profile of drugs could be dramatically modulated with nano particulate systems (94, 95). Nanoparticles have been observed to exhibit superior penetration characteristics into the inner ocular tissues compared to solution or suspension formulations (96). Lipid based systems such as nanostructured lipid carriers (NLCs) are potential carriers for therapeutic agents, especially hydrophobic molecules, and possess favorable properties including but not limited to biocompatibility, mucoadhesion, penetration /retention capability, lower clearance rate, controlled release, greater stability and protection of the drug candidate from chemical degradation. NLC's can be formulated from a wide variety of lipids (solid/liquid) and phospholipid combinations with varying composition, to achieve desired morphometrical, physicochemical, surface charge and release characteristics. Mixture of solid and liquid lipids used in NLC's create imperfections in the crystal lattice accommodating higher drug loads while maintaining similar penetration capabilities as the solid lipid nanoparticulates (SLNs). In addition, NLCs allow higher drug loading compared to SLNs, exhibit better encapsulation efficiency, lesser drug expulsion and higher stability (97-99). Reports suggest that PEGylated amphiphilic lipids possess the ability to transform into lipid based lyotropic crystals with thermodynamically stable self-assembled structures in aqueous environment (100, 101). In recent years, PEGylation technology (functionalization of nano carriers with PEG's and appropriate ligands) has been widely used to improve the pharmacokinetics, bioavailability and tissue distribution characteristics of a variety of nanoparticles, because the hydrophilic and inert PEG creates a steric barrier on the surface of nanoparticles and minimizes protein binding (102). The bulky and highly hydrated corona of the PEG extending from the lipid bilayer into the aqueous phase is critical for enhancing

steric stabilization of the nanoparticles (103). Also, incorporation of PEG could allow better stabilization against aggregation, on storage and on sterilization - by amorphization and inducing imperfections in crystal lipid lattices (104, 105).

Ciprofloxacin (CIP) belongs to class of fluoroquinolone antibiotics and is active against a broad spectrum of gram-positive and gram-negative bacteria. It is usually prescribed as the first line of treatment for corneal keratitis, allergic conjunctivitis and other bacterial infections of the eye. CIP is a zwitterion with pKa values of 6.0 (acidic group) and 8.8 (basic group) and an isoelectric point of 7.2 where it is least soluble (neutral species). The compound is currently marketed as an ophthalmic solution and needs frequent dosing due to its poor ocular bioavailability (106). Because of solubility issues, the formulation has to be maintained at an acidic pH. On topical application, however, because of the buffering action of the tear fluid, the pH of the instilled formulation is quickly neutralized as a result of which the solubility of CIP in that environment is significantly reduced and precipitation can take place. Consequently, penetration of CIP into the interior ocular tissues is hampered. In general, there exists a need to enhance drug penetration into the ocular tissues through the topical route. Moreover, improved delivery and penetration of ocular drugs with solubility issues, such as CIP, would be highly beneficial for intervening in complications associated with bacterial infections.

The objective of the current research is to assess the effect of type and density of surface PEGylation of CIP loaded NLCs in terms of process (including autoclave sterilization) and storage stability characteristics and ocular disposition.

3.1. Materials and Methods

CIP was obtained from Sigma Aldrich (St. Louis, MO). DSPE-mPEG-1000, DSPE-mPEG-10000, DSPE-mPEG-20000, (N-Carbonyl-methoxypolyethylene glycol-5000)-1,2 di-myristoyl-

sn-glycero phosphoethanolamine (DMPE-mPEG-5000) were received from Creative PEG Works (Winston Salem, NC). 1,2-dipalmitoyl-sn-glycero phosphoethanolamine (DPPE), DMPE-mPEG-2000, and DPPE-mPEG-2000 were obtained from NOF America Corporation (White Plains, NY). DSPE-sodium (C_{18}), DMPE- sodium (C_{14}), DPPE- sodium (C_{16}), DSPE-mPEG-2000 and DSPE-PEG-5000 were obtained from Lipoid® (Ludwigshafen Germany). Glyceryl Monostearate was obtained as a gift sample from Gattefossé (Paramus, NJ). Amicon® Ultra centrifugal filter devices with regenerated cellulose membrane (molecular weight cut off 100 kDa), Poloxamer 188, Tween®80, high performance liquid chromatography (HPLC) - grade solvents, and other chemicals (analytical grade) were obtained from Fisher Scientific (Hampton, NH). Whole eyes of male albino New Zealand rabbits were obtained from Pel-Freez Biologicals (Rogers, AR). Male albino New Zealand rabbits were procured from Harlan Labs (Indianapolis, IN).

3.1.1. Formulations

CIP-NLCs and PEGylated CIP-NLCs (PEG-CIP-NLCs)

Glyceryl monstearate (GMS), DSPE-sodium C_{18} (phospholipid) and oleic acid (liquid lipid) were used to prepare the DSPE-CIP-NLCs by ultra-sonication method. Briefly, GMS and oleic acid were melted, DSPE-sodium salt was added in small increments to form homogenous lipid mixture and then CIP was dispersed therein to obtain a lipid phase. An aqueous phase, containing surfactants (Poloxamer 188 (0.25% w/v) and Tween® 80 (0.75% w/v) and glycerin (2.25% w/v) in bi-distilled water, was heated. The hot aqueous phase was then added to the melted lipid phase under stirring to form a premix. The premix was then sonicated at 16,000 rpm for 6 min using T 25 digital Ultra-Turrax to form a hot pre-emulsion. The pre-emulsion obtained, was subjected to ultra-sonication (Vibracell™) at an amplitude of 80 for 6 min resulting in the formation of hot emulsion dispersion. The hot emulsion obtained was slowly cooled to room

temperature to form NLCs. The pH of the resulting formulation was adjusted to 5.0 using 0.1 N NaOH.

A portion of the phospholipids in the DSPE-CIP-NLC formulations were replaced with PEGylated phospholipids, N-(Carbonyl-methoxypolyethylene glycol-2000)-DSPE (DSPE-mPEG2000), to prepare the PEG-CIP-NLCs (PEG(2K)-CIP-NLC). Total amount of the lipid in the NLCs was 6% of which solid lipid constituted 50% and oleic acid made up the remaining 50%. Drug load in the formulations was maintained at 0.3% w/v.

Additional PEG-CIP-NLCs were prepared wherein the molecular weight of the PEG (1K, 2K, 5K,10K and 20K) grafted to DSPE was varied (DSPE-mPEG-1K / DSPE-mPEG-5K /DSPE-mPEG-10K / DSPE-mPEG-20K) to study the effect of the PEG molecular weight on the biopharmaceutical characteristics of the NLCs. CIP formulations were also prepared with mPEG-2K derivatized phospholipids of different chain lengths such as PEG 2000-1,2-dimyristoyl/dipalmitoyl-sn-glycero-3-phosphoethanolamine, sodium salt (DMPE C_{14} / DPPE C_{16}). These formulations, wherein the PEG molecular weight is constant (2K) but the lipid chain length is different (DPPE and DMPE), were designed to understand the role of the phospholipid chain-length on the PEG-CIP-NLC characteristics. A detailed description of the composition of all the CIP-NLC and PEG-CIP-NLC formulations tested, including the associated formulation codes used, have been presented in Table 1. All the components (lipids/surfactants) used in the formulations are represented by weight (mg).

Table 5 includes several placebo formulations (SLNs/NLCs) prepared using different lipid (solid/liquid) mixtures (combinations varying composition and/or total lipid content) tested for physical autoclave stability. The lipid excipients and surfactants used in the formulation are represented by weight (mg). Two batches (n=2) of formulations each with batch size of 10.6 g

(volume ~10 mL) were used for stability testing. NLCs that were unstable on autoclaving were reformulated by replacing 50% of the phospholipid (DSPE) with PEGylated (2K) DSPE to yield PEG(2K)-NLCs. The effect of PEG surface packing density (0-40%) and molecular weight (1K, 2K and 5K) on the autoclave stability of the PEG-NLCs was subsequently studied.

Chitosan coated NLCs (CIP-ChCl-NLCs) and CIP control solution

The DSPE-CIP-NLC formulation was coated with chitosan chloride (ChCl – 0.25% w/v) by adding ChCl solution into the final formulation (Table 1). Surface adsorption was confirmed by way of change in the zeta potential value.

CIP control formulation

Marketed CIP ophthalmic Solution 0.3% w/v was used as control formulation for the studies (Mfg. By: Hi-Tech Pharmacal; Lot # 622553).

3.1.2. Particle size, zeta potential and polydispersity Index (PDI) measurement

The hydrodynamic radius and the PDI of the NLC formulations were determined by photon correlation spectroscopy, using Zetasizer Nano ZS Zen3600 (Malvern Instruments, Inc.) at 25°C and 173° backscatter detection, in disposable clear cells. The measurements were obtained using a helium-neon laser of 633 nm, and the particle size analysis data was evaluated using volume distribution. Zeta potential measurements were carried out at 25°C in disposable cells using the same instrument. For measurement of particle size distribution and zeta potential, NLC samples were diluted (1:500) with water. Bi-distilled and 0.2 μM filtered water was used for these measurements, and were performed in triplicates.

3.1.3. Scanning transmission electron microscopy (STEM) studies

Lipid nanoparticulate formulations were characterized by scanning transmission electron microscope (Zeiss Auriga®-40 dual beam) using 1% w/v uranyl acetate as a stain. A freshly glow

discharged 200 mesh copper grid with a thin carbon was used as a base support for the sample. A small drop (10-20 µL) of sample was placed on a piece of parafilm and the grid was floated on top of the sample for 30 sec, then the grid was removed and excess sample was blotted using a piece of filter paper. Grid was then floated on a drop of distilled water for 10 sec, the water was removed and the grid with sample was floated on a drop of stain for 1 min after which excess stain was blotted again. After drying for at least 30 min, the samples were imaged in a Zeiss Libra operating at 30kV and in STEM mode.

3.1.4. Analytical method for *in vitro* sample analysis

Samples were analyzed for CIP content using an HPLC-UV method. The system comprised of Waters 717 plus Autosampler, Waters 2487 Dual λ Absorbance detector, Water 600 controller pump, and Agilent 3395 Integrator. A Phenomenex Luna® C_{18} 4.6 mm x 250 mm column was used under isocratic elution for chromatographic analysis. The mobile phase used was mixture of acetonitrile and triethanolamine buffer (150:850 v/v) with pH adjusted to 2.36 using ortho-phosphoric acid. Triethanolamine buffer is made up of water, triethanolamine and 25 mM phosphoric acid in the ratio of (996:1.6:1.57 v/v). The flow rate was set at 1 mL/min with λ_{max} (detection wavelength) of 299 nm during the analysis (107).

3.1.5. Assay and Entrapment Efficiency

The assay (total drug content) is determined in the CIP NLC formulations. The lipid in the DSPE-CIP-NLC and PEG-CIP-NLC formulations was precipitated using 50:50 binary mixture of 0.1N HCl and 190-proof alcohol and, drug content in the supernatant after centrifugation (13,000 rpm for 20 min), was measured using an HPLC system following appropriate dilution.

The percentage of CIP entrapped (% EE) in DSPECIP-NLC and PEG-CIP-NLC was determined by measuring the concentration of free drug in the aqueous phase of an undiluted

formulation. The EE was evaluated by an ultrafiltration technique with a 100 kDa centrifugal filter device (Amicon Ultra). An aliquot (500 μL) of the corresponding formulation was added to the sample reservoir and centrifuged at 5,000 rpm for 10 min. The filtrate was analyzed for drug content using HPLC. The %EE was calculated using Eq. (1) below. All the measurements were carried out in triplicates.

$$\%EE = \left[\frac{Wi - Wf}{Wi}\right] \times 100 \qquad (1)$$

Where W_i =total drug content, and W_f =amount of free drug in aqueous phase.

3.1.6. Terminal moist heat sterilization and stability assessment of CIP formulations

CIP loaded NLCs (DSPE-CIP-NLC and PEG-CIP-NLCs) and placebo formulations were prepared and put into appropriately labelled glass vials, affixed with sterilization indicator tapes, subjected to moist-heat sterilization (121°C for 15 min under 15 psi), in thermo-controlled autoclave (AMSCO® Scientific Model SI-120). Stabilizing agents and cloud point modifiers such as polyvinyl pyrrolidone (PVP K30), polyvinyl alcohol (PVA Avg Mol wt 30K -70K Da), PEG 400, PEG 1000, PEG 4000, PEG 6000 at concentrations of 0.25% and 0.5% w/v were used in the DSPE-CIP-NLCs. Following autoclaving, sterilized samples were evaluated in terms of physical appearance, color, morphometrical and physicochemical characteristics against unsterilized reference formulations kept at room temperature. Sterilization cycle was confirmed by change in the color of indicator tapes on the glass vials.

3.1.7. *In vitro* release studies

In vitro release of CIP from the respective formulations such as marketed CIP ophthalmic control solution (0.3% w/v), DSPE-CIP-NLCs and PEG (2K)-CIP-NLCs were evaluated using Valia-Chien® cells (PermeGear, Inc.). Spectra/por® membrane (3.5K MWCO) was mounted on

diffusion cells between donor / receptor chambers and fastened with clamps, through which transport kinetics were studied. The temperature of the cells was maintained at 34°C with the help of a circulating water bath. Five milliliters of isotonic phosphate buffer (IPBS - pH 7.4) containing 2.5% w/v RMβCD was used as the receptor media during the course of the experiment (6 h). Five hundred microliters of the formulations was added into the donor chamber. Aliquots (600 µL) were withdrawn from the receiver chamber and replaced with an equal volume of the 2.5% w/v RMβCD in IPBS (pH 7.4) solution at predetermined time points. Donor CIP concentration was maintained at 0.3% w/v in all the formulations. Samples taken were analyzed using high performance liquid chromatography-UV (HPLC-UV) system.

3.1.8. *In vitro* corneal permeation studies

The corneas excised from whole eyes, obtained from Pel-Freez Biologicals, were used for the determination of *in vitro* transcorneal permeability. Whole eyes were shipped overnight in Hanks balanced salt solution, over wet ice, and were used immediately upon receipt. The corneas were excised with some scleral portion to help secure the membrane onto the diffusion cells. After excision, the corneas were washed with the (IPBS; pH 7.4) and mounted on Valia-Chien cells (PermeGear, Inc®) with the epithelial side facing the donor chamber. The temperature of the cells was maintained at 34°C with the help of a circulating water bath. Five hundred microliters of CIP formulations (CIP ophthalmic control solution, DSPE-CIP-NLCs and PEG (2K)-CIP NLCs was added to the donor chamber and the CIP concentration was maintained at 0.3% w/v in formulations. The receiver chamber consisted of 5 mL of RMβCD (2.5% w/v) in IPBS (pH 7.4) solution for all the transport studies. Aliquots (600 µL) were withdrawn from the receiver chamber at predetermined time points, until 3 h, and replaced with an equal volume of receiver medium. Samples were stored at −80°C until further analysis.

Additionally, effect of carbon chain length (DMPE / DPPE / DSPE- mPEG -2000) and molecular weight of PEG's (DSPE-PEG-1K / 2K / 5K) on transcorneal permeability of CIP from PEG-CIP-NLCs was investigated using side-by-side diffusion apparatus. Three milliliter's of CIP formulations was added to the donor chamber and receiver medium consisted of 3.2 mL of RMβCD (2.5% w/v) in the IPBS (pH 7.4). A slight difference in the donor and receiver chamber volumes helped to maintain the normal corneal curvature through marginally elevated hydrostatic pressure. The contents of both chambers were stirred continuously with a magnetic stirrer. Aliquots (600 µL) were withdrawn from the receiver chamber at predetermined time points until 3 h and replaced with an equal volume of the solution.

3.1.9. Biosample preparation for determination of CIP in ocular tissue homogenates

In vivo sample analysis was carried out using the HPLC-UV method mentioned above following method validation. Mixture of ice cold acetonitrile and 0.1% formic acid (1 mL) was added to the sample to precipitate proteins and extract the drug from individual, tissues namely cornea, sclera, iris-ciliary (IC) and retina-choroid (RC), after cutting them into small pieces. The samples were centrifuged for 1 h at 13,000 rpm and the supernatant was then collected for further analysis. Aqueous humor (AH) (200 µL), vitreous humor (VH) (500 µL) tissues were precipitated by adding an ice cold mixture of acetonitrile & formic acid; 200 µL for AH and 500 µL for VH in the ratio (1:1). Standard calibration curves constructed from various ocular tissues such as cornea (20-500 ng/mL), sclera (20-500 ng/mL), AH (10-200 ng/mL), VH (10-200 ng/mL), IC (10-200 ng/mL), RC (10-200 ng/mL) were used to determine the drug concentration in the samples. All the standard curves had a coefficient of determination $r^2 \geq 0.96$. The accuracy and precision of the bio-analytical method was determined by analyzing the quality control (QC) drug samples of all ocular matrices at three different concentration levels (50,100,200 ng/mL) each prepared in

sextuplicate (*n*=6). The inter-day and intra-day variabilities in precision (% RSD) ranged between 3.97-12.6% and 4.57-9.78% in ocular tissue homogenates tested. The intra-assay and inter-assay accuracies, expressed as the percentage difference between the measured concentration and the nominal concentration ranged from -7.57% to 11.35% and -10.3% to 12.6% in ocular tissues respectively. The precision and accuracies of the QC samples obtained met the requirements set forth under bioanalytical guidance (Guidance for Industry: bioanalytical method validation in Food and Drug Administration guidelines of September 2013) (108). Recovery of CIP was evaluated by spiking drug in blank tissues and comparing the expected CIP concentration with standard concentration. Recovery values were observed in AH (90.3), VH (92.9), cornea (89.7), sclera (87.2), IC (91.5) and RC (93.3). Interference was not observed from co-eluted protein residues with respect to CIP peaks in all the tissues. Limit of Detection (LOD) in various ocular tissues was determined in AH (10 ng/mL), VH (10 ng/mL), cornea (20 ng/mL), sclera (20 ng/mL), RC and IC (10 ng/mL).

3.1.10. *In vivo* bioavailability studies

In vivo bioavailability of CIP was determined in conscious Male New Zealand albino rabbits weighing between (2-2.5 kg), procured from Harlan labs. All the animal studies conformed to University of Mississippi Institutional Animal Care and Use Committee (IACUC) and Association for research in vision and ophthalmology (ARVO) approved protocols. CIP formulations namely marketed ophthalmic control solution, DSPE-CIP-NLCs and PEG (1K / 2K / 5K / 20K)-CIP-NLCs were evaluated *in vivo*. These topical formulations (100 µL) were instilled as two doses (50 µL each dose) at two different time points, -30min and 0 min, to reduce pre-corneal loss. At the end of 2 h post application of the second drop (0 min), rabbits were euthanized with an overdose of pentobarbital, injected through a marginal ear vein. The eyes were washed

thoroughly with ice cold DPBS and were immediately enucleated. The intraocular tissues were separated and stored at -80 °C until further analysis using an HPLC-UV system. All experiments were carried out in triplicate.

3.2. Data analysis

The steady-state flux (SSF) for transcorneal experiments was calculated by dividing the rate of transport by the surface area. Flux was calculated using Eq. (2).

$$\mathrm{Flux(J)} = (\mathrm{dM/dt})/\mathrm{A} \qquad (2)$$

Where, *M* is the cumulative amount of drug transported, and *A* is the surface area of the corneal membrane (0.636cm^2) exposed to the permeant (drug).

The transcorneal permeability was determined by normalizing the SSF to the donor concentration, C_d, according to Eq. (3).

$$\mathrm{Permeability(Papp)} = \mathrm{Flux/Cd} \qquad (3)$$

3.3. Statistical analysis

One way-ANOVA coupled Post-Hoc test was employed to analyze the differences between groups. Data obtained was considered to be statistically significant at level of ($p<0.05$).

3.4. Results

3.4.1. Physicochemical characteristics of CIP containing lipid nanoparticle formulations

A detailed description of the composition of all the CIP-NLC and PEG-CIP-NLC formulations tested, including the associated formulation codes used, have been presented in Table 3.1. Physicochemical characteristics of the various NLCs are presented in Table 3.2. Hydrodynamic radii of all the NLC formulations did not vary significantly whereas the entrapment efficiency values with the PEG-CIP-NLC formulations were comparatively higher than that with

the CIP-NLCs. PEG(2K)-CIP-NLCs displayed higher entrapment efficiency – a 10% increase in entrapment in comparison to DSPE-CIP-NLCs. Zeta potential of DSPE-CIP-NLCs decreased with PEG derivatization from -12 to -2 mv, confirming surface charge neutralization by the PEG. Coating of the CIP-NLCs (DSPE-CIP-NLC) with chitosan (ChCl), on the other hand, increased the positive charge on the NLCs (Table 3.2). Physicochemical characteristics of the various NLC formulations, post terminal moist heat sterilization are presented in Table 3.3.

Table 3.1: Composition of CIP-NLCs and PEGylated CIP-NLCs (PEG-CIP-NLC) formulations. Various PEG-CIP-NLCs were prepared using PEG conjugated phospholipids of different carbon chain lengths and PEG molecular weights.

Formulations	**CIP (mg)**	**Oleic acid (liquid lipid - mg)**	**GMS (solid lipid -mg)**	**Phospholipid (mg)**	**PEGylated Phospholipid (mg)**	**Chitosan Chloride**	**Poloxamer 188 (mg)**	**Tween® 80 (mg)**	**Glycerin (mg)**	**Water (mL)**
CIP-NLCs										
DMPE-CIP-NLCs	30	300	150	**150 (DMPE)**	-	-	25	75	225	10
DPPE-CIP-NLCs	30	300	150	**150 (DPPE)**	-	-	25	75	225	10
DSPE-CIP-NLCs	30	300 mg	150	**150 (DSPE)**	-	-	25	75	225	10
PEGylated CIP-NLCs (PEG-CIP-NLCs)										
PEG(1K)-CIP-NLCs	30	300 mg	150	-	**150 (DSPE-PEG-1K)**	-	25	75	225	10
PEG(2K)-CIP-NLCs	30	300 mg	150	-	**150 (DSPE-PEG-2K)**	-	25	75	225	10
PEG(5K)-CIP-NLCs	30	300 mg	150	-	**150 (DSPE-PEG-5K)**	-	25	75	225	10
PEG(10K)-CIP-NLCs	30	300 mg	150	-	**150 (DSPE-PEG-10K)**	-	25	75	225	10
PEG(20K)-CIP-NLCs	30	300 mg	150	-	**150 (DSPE-PEG-20K)**	-	25	75	225	10
DMPE(2K)-CIP-NLCs	30	300 mg	150	-	**150 (DMPE-PEG-2K)**		25	75	225	10
DPPE(2K)-CIP-NLCs	30	300 mg	150	-	**150 (DPPE-PEG-2K)**		25	75	225	10
Chitosan coated CIP-NLCs (CIP-ChCl-NLCs)										

Formulations	CIP (mg)	Oleic acid (liquid lipid - mg)	GMS (solid lipid -mg)	Phospholipid (mg)	PEGylated Phospholipid (mg)	Chitosan Chloride	Poloxamer 188 (mg)	Tween® 80 (mg)	Glycerin (mg)	Water (mL)
CIP-ChCl-NLCs	30	300 mg	150	**150 (DSPE)**	-	25 mg	25	75	225	10

Table 3.2: Physicochemical characteristics of CIP-NLCs and PEGylated CIP-NLC Formulations.

Characteristics	CIP-NLCs	PEGylated CIP-NLCs					CIP-ChCl-NLCs
	DSPE-CIP -NLCs	PEG(1K)-CIP-NLCs	PEG(2K)-CIP-NLCs	PEG(5K)-CIP-NLCs	DMPE(2K)-CIP-NLCs	DPPE(2K)-CIP-NLCs	CIP-ChCl-NLCs
Particle size (nm)	190±15	165±12	180.6±13	217±18	176±4.8	184±3.6	220±16
Polydispersity index (PDI)	0.26±0.03	0.29±0.01	0.31±0.01	0.37±0.03	0.28±0.02	0.27±0.03	0.33±0.06
Zeta potential (mV)	-12.2±1.08	-1.0±0.02	-1.8±0.08	-2.6±0.06	-2.3±0.03	-2.1±0.06	29.2±3.9
Entrapment Efficiency (% EE)	72.5±3.9	79.6±2.4	83.6±4.7	84.2±2.3	79.8±1.9	81.2±2	73.6±3.6
Assay (%)	CIP content was 90-95% of the theoretical value in all the formulations						

Table 3.3: Effect of autoclaving on the physicochemical attributes of CIP-NLCs and PEG -CIP-NLCs (pre and post sterilization).

Formulations	Particle Size (nm)		Polydispersity index (PDI)		Assay		pH		Zeta potential (mV)	
	Sterilization Stage		Sterilization Stage		Sterilization Stage		Sterilization Stage		Sterilization Stage	
	Pre	Post	Pre	Post	Pre	Post	Pre	Post	Pre	Post

DSPE-CIP-NLCs	**CIP-NLCs**	190±15	230±7.5	0.26±0.03	0.35±0.05	90.9±4.5	87.1±2.1	5	3.6	-12.2±1.08	-14.6±1.95
PEG(1K)-CIP-NLCs	**PEGylated CIP-NLCs**	165±12	169±8	0.29±0.01	0.29±0.02	90.2±2.8	89.1±2.6	5	4.76	-1.0±0.02	-1.12±0.01
PEG(2K)-CIP-NLCs		180.6±13	192±8	0.31±0.01	0.32±0.01	90.1±3.1	88.4±3.6	5	4.8	-1.8±0.08	-1.9±0.06
PEG(5K)-CIP-NLCs		217±18	231±9.1	0.37±0.03	0.42±0.02	92.6±1.8	91.9±2.9	5	4.4	-2.6±0.06	-3.4±0.04
DMPE(2K)-CIP-NLCs		176±4.8	191±7.6	0.28±0.02	0.31±0.04	91.4±1.1	89.4±0.67	5	4.58	-2.3±0.03	-2.9±0.053
DPPE(2K)-CIP-NLCs		184±3.6	189±8.5	0.27±0.03	0.3±0.02	93.2±0.9	91.8±1.2	5	4.82	-2.1±0.06	-3.3±0.04

3.4.2. Scanning transmission electron microscopy (STEM) studies

The STEM images of the representative samples are shown in Figure 3.1. STEM images of CIP NLCs showed the presence of spherical as well as rod-shaped nanoparticles whereas PEG-CIP-NLs appeared to be spherical in shape with a well-defined periphery. Particle sizes obtained with TEM and DLS techniques may not be in agreement for the polydisperse formulations due to the respective operating principles and other contributing factors. Zeta sizer measures particle size based on intensity of scattered light whereas STEM measures it from each individual particle. Particle size agreements may hold true in monodisperse formulations (109-111).

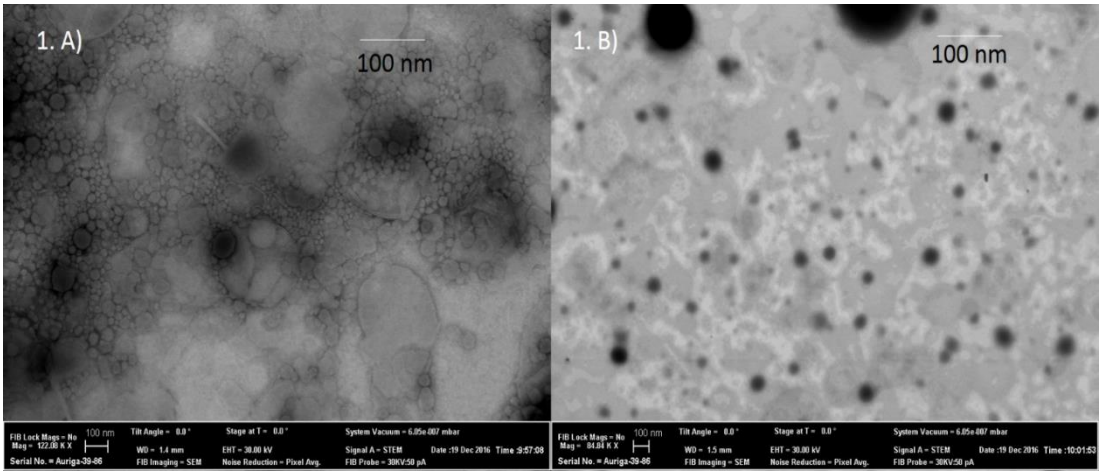

Figure 3.1. STEM images of CIP loaded NLCs. A) CIP NLCs. B) PEG(2K)-CIP-NLCs.

3.4.3. Autoclave stability of CIP formulations

Physicochemical characteristics of the various NLC formulations, post terminal moist heat sterilization are presented in Table 3.3. Following sterilization, PEGylated NLCs were able to preserve their characteristics, whereas particle size and PDI was increased in the DSPE-CIP-NLCs and was also accompanied by a 14% decrease in entrapment efficiency. Moreover, the DSPE-CIP-NLC formulation was observed to be physically unstable (color, lipid phase separation) on steam sterilization. Addition of various reported stabilizing agents and cloud point modifiers such as polyvinyl pyrrolidone (PVP K30), polyvinyl alcohol (PVA Avg Mol wt 30K -70K Da), PEG 400, PEG 1000, PEG 4000, PEG 6000 at concentrations of 0.25% and 0.5% w/v in the DSPE-CIP-NLC formulations did not stabilize the phospholipids during the sterilization process.

Particle size and PDI of PEG-CIP-NLC formulations increased and entrapment efficiencies decreased as a function of increasing molecular weights of PEG (2K to 20K) used in the formulation. Moreover, PEG (20K)-CIP-NLCs appeared to be unstable during the sterilization process, with visible supernatant oil droplets. PEGs with molecular weights of up to 10K were observed to stabilize the DSPE-CIP-NLC formulations (Table 3.4). Formulations (represented in tables 3 and 4) did not exhibit any statistically significant difference in physico-chemical

characteristics, pre and post terminal moist heat sterilization except DSPE-CIP-NLCs and PEG(20K)-CIP-NLCs, which were unstable.

Studies were then undertaken to delineate the effect of the formulation components on autoclave stability. For this purpose, placebo formulations were used. Data on the effect of autoclaving on the physical stability of different placebo formulations, prepared using different lipids/phospholipids, is summarized in Table 3.5. Non-PEGylated NLCs prepared using phospholipids (DSPE) in combination with high melting triglyceride oils such as sesame, castor and soybean oils were stable post sterilization. NLCs prepared using a combination of the phospholipid with a fatty-acid (oleic acid) or caprylic/capric triglyceride (Miglyol®829) or Transcutol P were, however, unstable. These formulations were stabilized when PEGylated phospholipid (PEG(2K)-DSPE) was used - 50% of the total DSPE used was PEGylated in these experiments.

The effect of PEG concentration (surface packing density) on autoclave stability of phospholipid containing DSPE-CIP-NLC formulations is presented in Table 3.6. In these experiments the fraction of PEGylated lipid was varied from 0 to 40%, out of the total phospholipid content in the DSPE-CIP-NLCs, using PEG grafted lipids of different molecular weights - DSPE-PEG-1K/2K/5K. It was observed that DSPE-mPEG-5K stabilized the CIP-NLCs when used at a concentration of 30% w/w of total phospholipid in the formulation. Also, DSPE-mPEG-2K had to be used at a minimum of 40% w/w of the total phospholipid in the formulation for stabilization. Thus, higher molecular weight PEGs required lower PEGylated lipid concentrations to impart stability to the CIP-NLCs composition containing phospholipid and oleic acid.

Table 3.4: Effect of autoclaving on the physicochemical characteristics of PEG-CIP-NLC formulations prepared with higher molecular weight PEG's pre and post sterilization.

Formulations (PEGylated CIP-NLCs)	Particle Size (nm)		Polydispersity Index (PDI)		Entrapment efficiency (%EE)		Zeta potential (mV)	
	Sterilization Stage		Sterilization Stage		Sterilization Stage		Sterilization Stage	
	Pre	Post	Pre	Post	Pre	Post	Pre	Post
PEG(2K)-CIP-NLCs	175.6±13	172±8	0.27±0.02	0.26±0.03	88.8±2.2	88.1±0.7	-0.4±0.03	-0.7±0.06
PEG(5K)-CIP-NLCs	207±9	209±12	0.31±0.02	0.32±0.04	80.4±6.7	76.9±2.3	-1.9±0.06	-2.1±0.03
PEG(10K)-CIP-NLCs	280±7	297±11.3	0.36±0.04	0.42±0.07	76.1±4.51	69.2±4.27	-1.4±0.07	-1.5±0.02
PEG(20K)-CIP-NLCs	320±18	cracked	0.45±0.07	cracked	73.6±.9.68	cracked	-0.2±0.03	cracked

Table 3.5: Physical stability of placebo NLC formulations (n=2) prepared with different lipids (solid and / or liquid) post autoclave sterilization.

Table 3.5						
Formulation	**Solid lipid (mg)**	**Liquid lipid (mg)**	**Poloxamer 188 (mg)**	**Tween 80 (mg)**	**Glycerin (mg)**	**Result**
F-1	GMS (400)	_	5	_	_	No change
F-2	**GMS, DSPE (1:1) 9 parts (270, 270)**	**Oleic acid 1 part (60) total 9:1 (S:L)**	**25**	**75**	**225**	**Failed**
F-3	Precirol (360) 9 parts	Oleic acid 1 part (40) total 9:1 (S:L)	_	250	_	Discoloration in one formulation
F-4	GMS (300) 3 parts	Castor oil (100) 1 part ; 3:1 (S:L)	5	_	_	No change
F-5	Compritol (200)	Castor oil (200)	25	75	225	No change
F-6	GMS (200)	Castor oil (200)	25	75	225	No change
F-7	GMS (200)	Oleic acid (200)	25	75	225	No change
F-8	GMS (300)	Soyabean oil (300)	25	75	225	No change
F-9	GMS, DSPE (150,150) (1:1)	Soyabean oil (300)	25	75	225	No change
F-10	GMS (300)	Sesame oil (300)	25	75	225	No change
F-11	GMS, DSPE (150,150) (1:1)	Sesame oil (300)	25	75	225	No change

Table 3.5						
Formulation	**Solid lipid (mg)**	**Liquid lipid (mg)**	**Poloxamer 188 (mg)**	**Tween 80 (mg)**	**Glycerin (mg)**	**Result**
F-12	GMS, DSPE (150,150) (1:1)	Castor oil (300)	25	75	225	No change
F-13	GMS (300)	Miglyol 829 (300)	25	75	225	No change
F-14	**GMS, DSPE (150,150) (1:1)**	**Miglyol 829 (300)**	**25**	**75**	**225**	**Discoloration**
F-15	GMS (300)	Capryol 90 (300)	25	75	225	No change
F-16	GMS, DSPE (150,150) (1:1)	Capryol 90 (300)	25	75	225	No change
F-17	GMS (300)	Lauroglycol (300)	25	75	225	No change
F-18	GMS, DSPE (150,150) (1:1)	Lauroglycol (300)	25	75	225	No change
F-19	GMS (300)	Lauroglycol (300)	25	75	225	No change
F-20	GMS, DSPE (150,150) (1:1)	Lauroglycol (300)	25	75	225	No change
F-21	GMS (300)	Labrafac (300)	25	75	225	No change
F-22	GMS, DSPE (150,150) (1:1)	Labrafac (300)	25	75	225	No change
F-23	GMS (300)	Isopropyl Myristate (300)	25	75	225	No change
F-24	GMS, DSPE (150,150) (1:1)	Isopropyl Myristate (300)	25	75	225	No change
F-25	GMS (300)	Labrafil (300)	25	75	225	No change
F-26	GMS, DSPE (150,150) (1:1)	Labrafil (300)	25	75	225	No change
F-27	GMS (300)	Transcutol (300)	25	75	225	No change
F-28	**GMS, DSPE (150,150) (1:1)**	**Transcutol (300)**	**25**	**75**	**225**	**Failed**

Table 3.6: Effect of PEGylated to unPEGylated phospholipid ratio and PEG molecular weight on physical stability of placebo PEG-NLC post autoclave sterilization.

% of PEG-lipid	**DSPE-PEG- 1K/2K/5K lipid (mg)**	**DSPE Phospholipid (mg)**	**Oleic acid (mg)**	**GMS (mg)**	**Result**
PEG(1K)-CIP-NLCs					
15	22.5	127.5	300	150	Cracked
30	45	105	300	150	Cracked
40	60	90	300	150	Cracked

PEG(2K)-CIP-NLCs					
0 (Control)	(0)	150	300	150	Cracked
10	15	135	300	150	Cracked
15	22.5	127.5	300	150	Cracked
25	37.5	112.5	300	150	Cracked
30	45	105	300	150	Droplets
35	52.5	97.5	300	150	Droplets
40	**60**	**90**	**300**	**150**	**No change**
PEG(5K)-CIP-NLCs					
15	22.5	127.5	300	150	Cracked
30	**45**	**105**	**300**	**150**	**No change**

3.4.4. *In vitro* release studies

These studies combined release and transmembrane diffusion – simulating ocular CIP penetration following topical application of the formulations. CIP flux from the DSPE-CIP-NLC and PEG(2K)-DSPE-CIP-NLC formulations, under the test conditions employed, were similar but the control formulation (0.3% Ophthalmic marketed control solution) showed a higher flux across the membrane – presumably because of the elimination of the release step from the process (Figure 3.2).

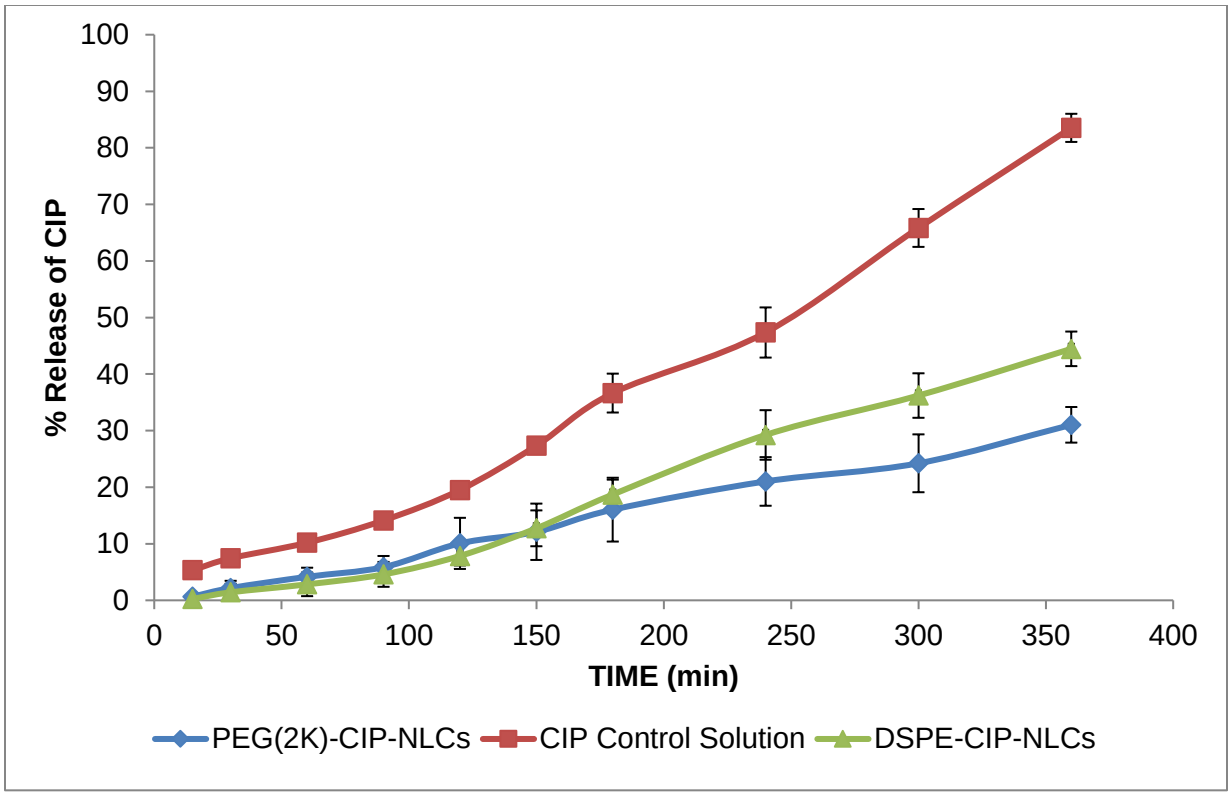

Figure 3.2: *In vitro r*elease of CIP obtained across Spectra/Por® membrane (MWCO: 3.5 KDa) from CIP loaded PEGylated NLCs (PEG(2K)-CIP-NLCs), 0.3% w/v CIP ophthalmic Solution, and CIP-NLCs (DSPE-CIP-NLCs) obtained using Valia-Chien cells at 34°C. (Dose: 500 µL; 1500 µg).

3.4.5. *In vitro* corneal permeation studies

In vitro transcorneal flux of CIP from the PEG(2K)-CIP-NLCs was almost 3-fold greater than that achieved with control solutions. CIP flux from the PEG(2K)-CIP-NLCs was about 2-fold higher compared to the DSPE-CIP-NLCs. Transcorneal flux of CIP from the chitosan coated NLCs (CIP-ChCl-NLC) was slightly better than that from the PEG(2K)-CIP-NLCs (Figure 3.3).

Carbon chain length of the phospholipid did not appear to affect transcorneal penetration of CIP from the PEG-CIP-NLCs. The molecular weight of PEG used to derivatize the phospholipid, however, had a significant effect on transcorneal flux of CIP (Figure 3.4). PEG (2K)-CIP-NLCs (DSPE-mPEG-2000) and PEG (5K)-CIP-NLCs (DSPE-mPEG-5000) enhanced transcorneal permeability of CIP by about 1.8-fold and 2.5-fold, respectively, when compared to non PEGylated CIP-NLCs (DSPE-CIP-NLCs). PEG (1K)-CIP-NLCs did not exhibit a significant

increase over the CIP-NLCs. Thus, based on the data presented in Figures 3.3 and 3.4, it can be inferred that PEG-NLCs prepared with PEG-lipids with PEG molecular weights of 2K or greater are preferred to enhance ocular penetration of CIP.

In another set of studies, comparative corneal permeability of PEG-CIP-NLCs prepared with phospholipids (DSPE) grafted with higher molecular weight PEGs namely DSPE-PEG-2K/5K/ 10K/20K was determined. Although, transcorneal penetration of CIP exhibited an increasing trend with an increase in molecular weight of PEG from 2K to 10K, the difference in flux was not significantly different (Figure 3.5).

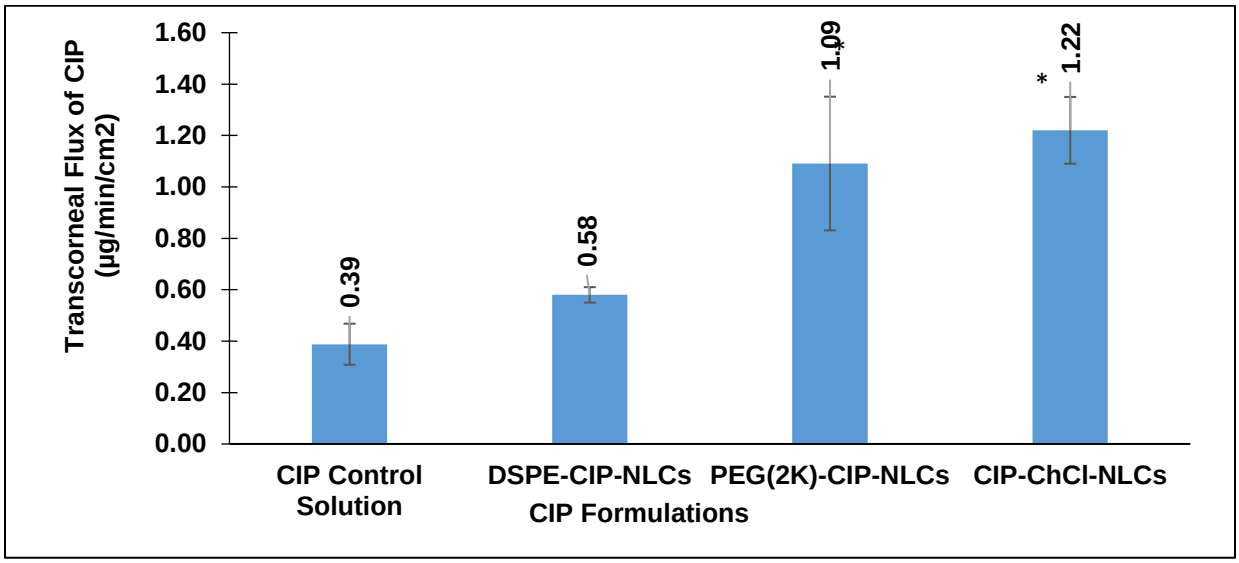

Figure 3.3: Transcorneal flux of CIP obtained from CIP ophthalmic Solution, DSPE-CIP-NLCs, PEG(2K)-CIP-NLCs and Chitosan Chloride coated DSPE-CIP-NLCs (CIP-ChCl-NLCs) using Valia-Chien cells at 34°C (Dose: 500 µL; 1500 µg; n=4). * symbol denotes statistical significance of PEG(2K)-CIP-NLCs and CIP-ChCl-NLCs when compared to control and DSPE-CIP-NLCs $p<0.05$) .

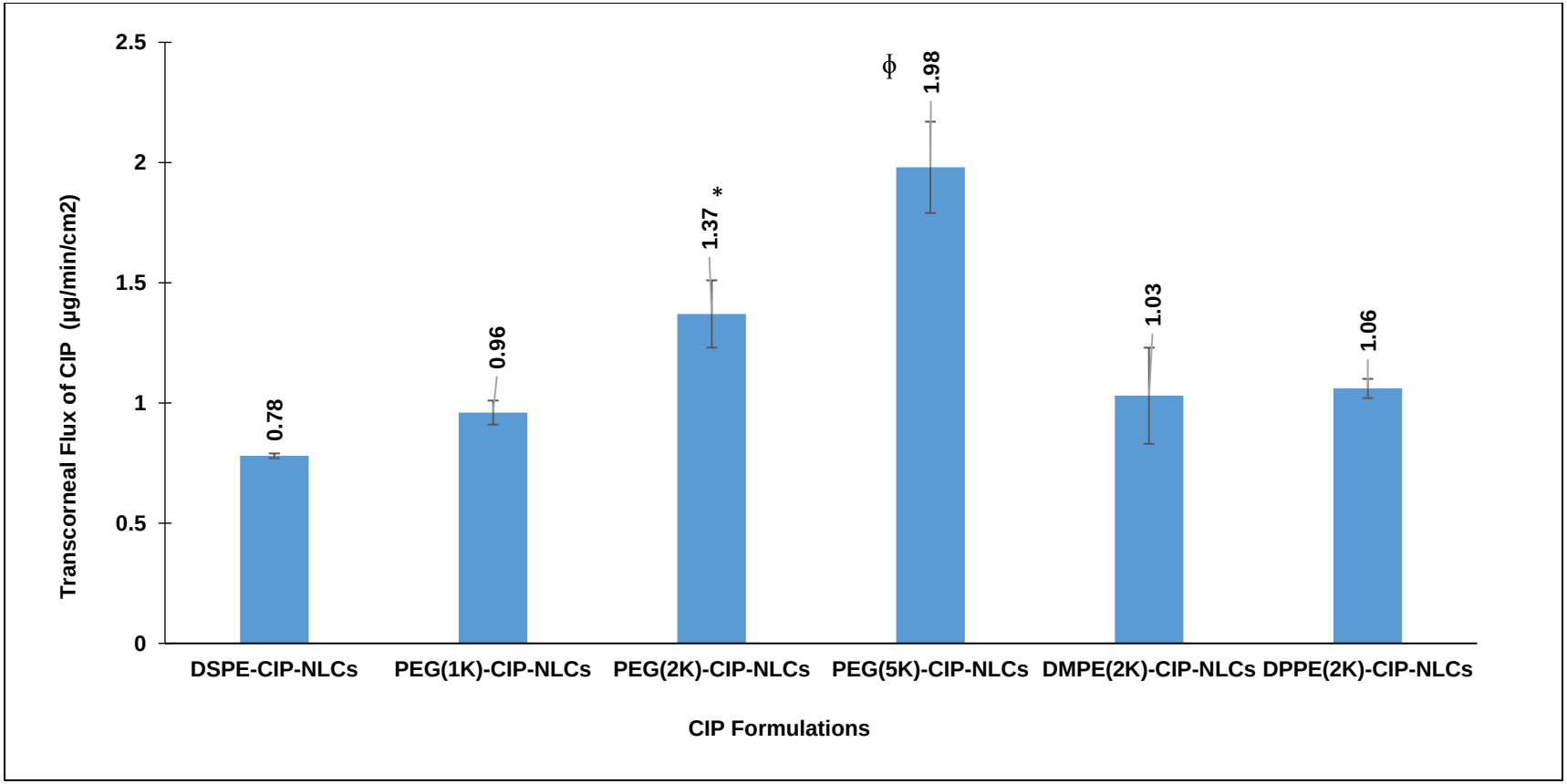

Figure 3.4: Transcorneal flux of CIP obtained from various topical NLC formulations tested with different molecular weights of PEG grafted, DSPE phospholipid (PEG-1K (PEG(1K)-CIP-NLCs / 2K (PEG(2K)-CIP-NLCs / 5K (PEG(5K)-CIP-NLCs) and varied chain lengths of PEG-2000 conjugated phospholipids (DMPE(2K)-CIP-NLCs, DPPE(DPPE(2K)-CIP-NLCs) using side-by-side diffusion cells (PermeGear, Inc) at 34°C (Dose: 3 mL; 0.3% w/v) (n=4). * symbol denotes statistically significant difference of CIP flux from PEG(2K)-CIP-NLCs when compared to DSPE-CIP-NLCs whereas ϕ symbol indicates statistically significant difference of CIP flux from PEG(5K)-CIP-NLCs in comparison to all the formulations ($p<0.05$).

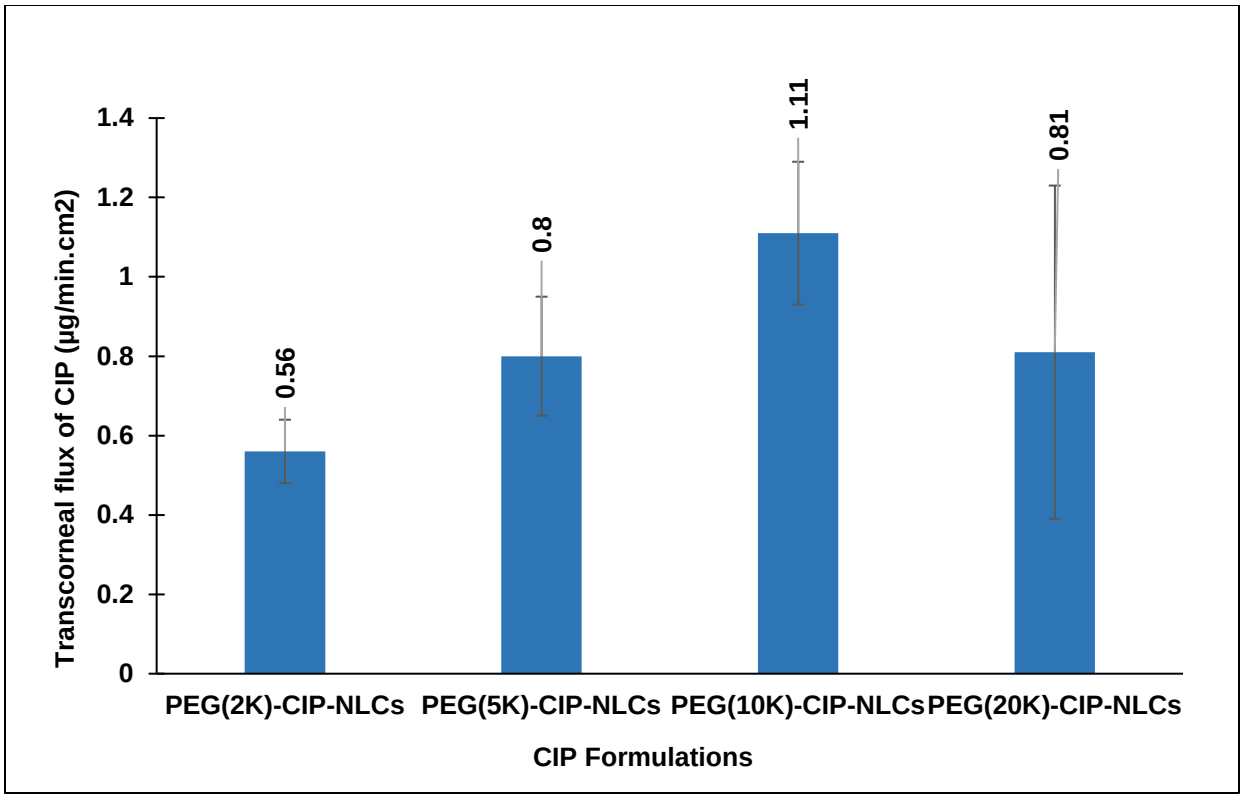

Figure 3.5: Transcorneal flux of CIP obtained from NLC systems with higher molecular weights of PEG's grafted to DSPE phospholipid (2K / 5K / 10K (PEG (10K)-CIP-NLCs / 20K (PEG (20K)-CIP-NLCs), using side-by-side cells at 34° C (Dose: 3 mL; 0.3% w/v; n=4).

3.4.6. *In vivo* bioavailability studies

Following topical application of the formulations (Table 3.1) in conscious NZW rabbits, CIP levels in all ocular tissues tested, 2 h post dosing, were observed to be nearly 2-folds higher with the PEG(2K)-CIP-NLCs compared to DSPE-CIP-NLCs (non-PEGylated CIP-NLCs). The results were consistent with the *in vitro* observations. PEG(2K)-CIP-NLCs generated higher CIP concentrations in all ocular tissues tested except for the cornea – where CIP-ChCl-NLCs were observed to be slightly better (Figure 3.6).

Retinal CIP concentrations achieved with the PEG(2K)-CIP-NLCs is significantly higher compared to all other topical formulations. PEG(5K)-CIP-NLCs was similar, if not slightly better than the PEG(2K)-CIP-NLCs with respect to CIP levels obtained in the anterior segment tissues –

AH, cornea and IC. CIP levels in the posterior segment or back-of-the eye tissues (retina-choroid) was, however, below detection levels with the PEG (5K)-CIP-NLCs. The PEG(10K)-CIP-NLCs and PEG(20K)-CIP-NLCs achieved much lower CIP concentrations in all ocular tissues tested in comparison to the PEG(2K)-CIP-NLCs (Figure 3.6). CIP concentrations in the AH and IC, achieved with the PEG(2K)-CIP-NLC and PEG(5K)-CIP-NLC formulations, were far greater than the minimum inhibitory concentration (MIC90), approximately 0.5 µg/mL (112), even 2 h post topical dosing. In contrast, commercial CIP eye drops barely maintained MIC90 levels in the AH, IC and cornea, 2 h post dosing, while CIP levels were undetectable or below MIC in the other ocular tissues tested.

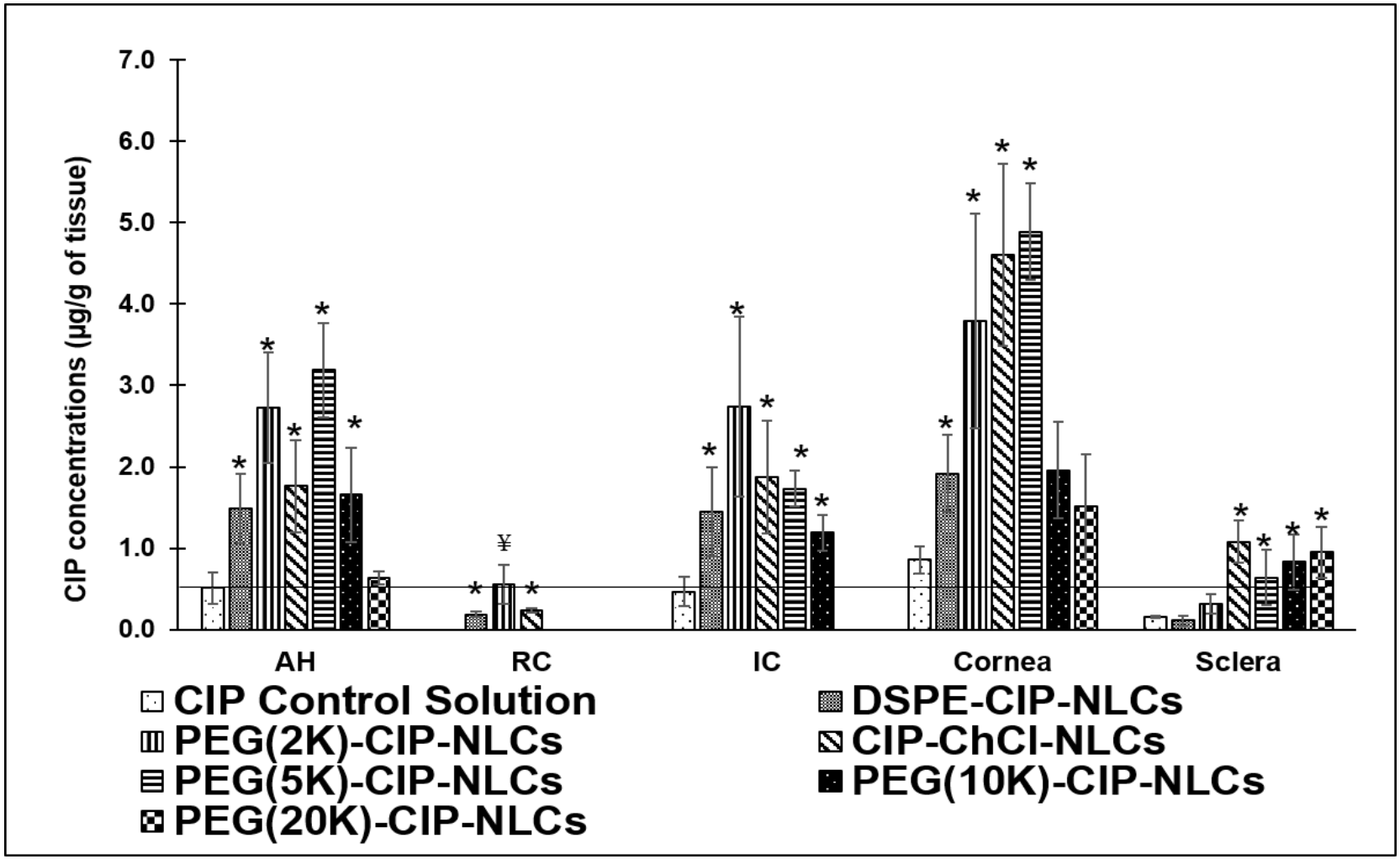
CIP concentrations (μg/g of tissue)
7.0
6.0
5.0
4.0
3.0
2.0
1.0
0.0
AH
RC
IC
Cornea
Sclera
CIP Control Solution
DSPE-CIP-NLCs
PEG(2K)-CIP-NLCs
CIP-ChCl-NLCs
PEG(5K)-CIP-NLCs
PEG(10K)-CIP-NLCs
PEG(20K)-CIP-NLCs

Figure 3.6: Ocular tissue concentrations of CIP obtained from CIP Ophthalmic Solution, DSPE-CIP-NLCs with and without Chitosan Chloride (ChCl) and CIP loaded PEGylated NLCs with different molecular weights of PEGs (DSPE-PEG-2K, DSPE-PEG-5K, DSPE-10K, DSPE-20K) 2 h post topical application (Dose: 300 µg; 100 µL at -30 and 0 min) in a conscious rabbit model. (AH- Aqueous humor, IC-Iris ciliary bodies and RC- Retina choroid). MIC90 of CIP is marked as a horizontal line in the figure. Statistical analysis by One way ANOVA with post-hoc test was performed, where symbol (*) on the ocular tissues represent statistically significant difference of CIP concentrations from different formulations in comparison to control solution. (¥) represents statistically significant difference of retinal concentrations obtained from PEG (2K)-CIP-NLCs compared to all the formulations.

3.5. Discussion

The focus of this project was to evaluate the effect of surface functionalization on ocular penetration of drugs from lipid nanocarriers and formulation stability. CIP was chosen as the model drug for preparing these formulations. Entrapment efficiency and release properties of drugs from lipid nanocarriers are highly dependent upon interfacial area, surface charge, inner structural organization, as well as nanoparticulate dimensions (113, 114). The size of the NPs plays a key role in their adhesion to and interaction with the biological cells. Smaller particles can be best internalized by receptor-mediate endocytosis uptake mechanism, while larger particles have to be taken up by phagocytosis (115-119).

In recent years, NLCs are increasingly being considered as viable carriers in drug delivery, but the present work introduces a new paradigm involving the concept of surface functionalization / modification of nanoparticles and their sterilization - stabilization characteristics. Particle size and surface properties such as charge, morphology, hydrophilicity and surface modification with targeting ligand functionalization are the major controlling factors for interactions with the biological milieu (120, 121). Reports suggest that surface modification of nanoparticles by coating with hydrophilic substances such as PEGs could further improve ocular bioavailability, mainly due to enhanced interaction with ocular mucosal epithelium and decreased phagocytic uptake (122,

123). Fresta et al formulated PEG-6000 coated polyalkyl-2-cyanoacrylate nanosphere encapsulated acyclovir formulations and reported that the higher ocular bioavailability was achieved by polyalkyl-2-cyanoacrylate colloidal carrier, but no significant difference was observed between coated and uncoated nanospheres (124). These results may have resulted from a weak interaction of PEG molecules with the surface of colloidal particles. In the present project we explored the effect of nanoparticle surface modification, by adsorption of Chitosan chloride or by firmly surface anchored PEG moieties, on ocular distribution and disposition. Also, the characteristics of the PEG's, optimal molecular weights and their relative concentrations needed to achieve improved penetration, was studied.

Drug release from the nanoparticles appears to be controlled by erosion and diffusion mechanisms through lipid matrix (125, 126). Interaction between nanoparticles and ocular epithelial cells could be attributed to endocytosis mechanism. Based on the transcorneal permeation data obtained, it could be said that penetration of CIP depends upon the molecular weight of grafted PEG's rather than it's carbon chain length (127). The permeability was not improved with PEG-1K and a decrease in the transmembrane flux was observed with PEG-20K, indicating the required range of molecular weights is between 2-10K for optimal penetration characteristics. The *in vitro* transcorneal permeability, an experimental set-up wherein the mucus layer is absent, data suggests that the PEGylation not only affects penetration across the mucus layer but also influences penetration across the corneal epithelial layers. When the PEG molecular weight went above 10K the penetration enhancing effect was lost, which could probably be because of the increased hydrophilicity and steric interference of the molecules.

PEGylation range within which the formulations exert the optimal penetration and steric stabilization characteristics was further confirmed by the *in vivo* ocular distribution of CIP from

the PEG-CIP-NLCs (Figure 3.6). PEGylated NLCs were able to deliver CIP, but penetration of CIP into posterior and anterior ocular tissues decreased as a function of increasing molecular weight of the PEG's (128, 129). These results indicate that the lipid conjugated PEGs with relatively higher molecular weights (greater than 5K) impart higher surface hydrophilicity onto the nanoparticles, which limits the penetration and partition of drugs across the surface mucus layer and epithelial membrane. The results were consistent with the *in vitro* observations. PEG-CIP-NLCs generated higher CIP concentrations in all ocular tissues except for the cornea – in which case ChCl-NLCs were observed to be slightly better (Figure 3.6). This, suggests that surface modification with chitosan favors retention of the nanoparticles at the superficial ocular layers (charge-charge interaction), whereas PEG grafting facilitates transport of the molecules across the mucus layers as well as the cornea and other ocular tissue, consistent with earlier reports (122, 130, 131).

Tai-Lee ke et al prepared two sustained release formulations of CIP using marketed CIP solution (0.3% w/v) with Dodecyl Maltoside as a penetration enhancer and carbopol/HPMC as viscosity enhancers. Two hours post-topical instillation (30 µL), AH and corneal CIP concentrations obtained with HPMC and carbopol formulation were 0.5 µg/mL and 4.2 µg/g, respectively (132). Taha et al prepared ciprofloxacin loaded liposomes (0.3% w/v) and evaluated AH concentration after 2 h following topical application (50 µL) in conscious rabbit model. The AH level was increased by ~0.3-fold when compared to marketed ophthalmic solution (133). In another study, 50 µL of CIP loaded pluronic micelles (0.3 % w/v) enhanced AH concentration of CIP by 10%, 2 h post topical application, when compared to commercial CIP eye drops (134). In the present study ocular bioavailability of CIP was enhanced in the anterior and posterior segment ocular tissues, ranging from ~3-5-fold increase with PEG-CIP-NLC formulation, in comparison to

control marketed formulation. This is significantly better than all earlier reports as well as the currently marketed ophthalmic formulation.

All ophthalmic products need to be sterilized. Autoclavable products are preferred, from a manufacturability point of view, over products that need aseptic processing or sterilization by filtration. Reports suggest that phospholipids undergo acidic / basic hydrolysis (pH < 5; pH > 9) and hence should be aseptically processed (135, 136). Our studies here demonstrate that selection of NLC formulation components can have a significant impact on the formulation stability during the sterilization process. Whereas long chain triglycerides components were stable, shorter chain length fatty acids and triglyceride containing NLCs could not withstand the autoclaving step. When a fraction of the phospholipids, in the heat unstable NLCs, were replaced with PEGylated phospholipids, the formulations are stabilized, suggesting that PEGs are able to preserve the supramolecular and molecular structure of colloids and protect the lipid environment. Addition of PEG externally or other known stabilizers to the NLCs did not impart thermal stability during the autoclave cycle. Additionally, it was observed that PEG-CIP-NLCs with PEG molecular weights of up to 10K stabilize the NLCs during the sterilization process, whereas PEG 20K fails to do so. Steric stabilization of liposomal formulations using PEG conjugated lipids is well documented in the literature (137-139). PEG has also been reported to be a surface modifying agent for improving permeability characteristics and decreasing phagocytic uptake of particulate drug carriers (52, 140). To the best of our knowledge, however, this is the first report that establishes the importance of the molecular weight and surface density of the PEG for preparing autoclave stable NLCs with enhanced transepithelial penetration and delivery characteristics, especially to the back-of-the eye tissues.

Interestingly, whereas chitosan chloride coated NLCs produced higher CIP concentrations in the cornea and sclera, the outer tunic of the eye, this did not translate into higher CIP penetration into the inner ocular layers. This, along with the observation that the CIP-NLCs (no surface modification) produced low CIP levels in all ocular tissues, suggests that PEGylation within the specified ranges improve transepithelial penetration of the CIP-NLCs into the deeper ocular tissues.

3.6. Conclusion

Surface functionalized NLCs appear to be a promising and effective platform for topical ocular delivery. Surface modification strategies could improve ocular retention and intraocular penetration of therapeutics agents; thus enhancing ocular bioavailability and distribution. In conclusion, PEG grafted phospholipids / amphiphilic di-block copolymers with molecular weights in the range of 2K - 5K lead to optimal ocular penetration and autoclave stability.

CHAPTER 4

MELT CAST NONINVASIVE OCULAR INSERTS FOR POSTERIOR SEGMENT DRUG DELIVERY

4. Introduction

Prolonged ocular inflammation/infection could precipitate several sight threatening disorders including, but not limited to, keratitis, conjunctivitis, iritis, uveitis, endophthalmitis, cystoid macular edema and choroidal neovascularization (141, 142). A host of different ocular tissues are involved in these complications, and the intricate barriers in the ocular milieu, which are essential and exclusive to the ocular anatomy and physiology, limit the penetration of therapeutic agents. Delivery of drugs to the posterior segment of the eye through oral/parenteral routes is highly challenging because of the expression of blood ocular barriers. Topical administration is promising in terms of safety and patient compliance but the delivery of therapeutic agents to the posterior ocular tissues through this route is also an extremely difficult task (143, 144). Although various technological advances enhanced drug delivery into the front-of-the eye, back-of-the eye delivery through the topical route needs innovative strategies to improve pre-corneal residence and trans-ocular permeation characteristics of drug molecules (85, 145). The complex interplay between static, dynamic, efflux barriers in the eye and their remarkable barrier functionalities, severely impedes the penetration and distribution of drug molecules into the inner ocular tissues. Delivering the drugs to the posterior segment of the eye, in effective concentrations, using conventional formulations like topical solutions, viscous solutions and gels, surfactant based systems, emulsions, suspensions has not been successful so far (83, 146). The topical solution based dosage form typically has the inherent drawback that most of the instilled volume is eliminated from the pre-corneal area, resulting in poor ocular bioavailability, ranging from 1-10%, of the total administered dose (147). Maurice et al calculated that bioavailability in vitreous cavity following topical instillation of solutions range from 0.0001 to 0.0004%. Viscous mucoadhesive solutions and ophthalmic ointments prolongs the ocular

residence time, forming drug depot on the ocular surface (148). Various colloidal nanoparticulate systems have been designed/developed to prolong the ocular residence of drugs for delivery to the back-of-the eye (149).

Topical formulation approaches targeting the retina through the trans-scleral pathway is still in its infancy. Effective strategies will require candidates with ideal physicochemical characteristics and novel strategies capable of increasing the retention and absorption on the ocular surface. Ointments, gels and conjunctival films are dosage forms that provide close proximity to the conjunctiva and sclera and high, localized, concentration gradient generated in the conjunctival cul-de-sac, which favors ocular penetration, probably via the trans-conjunctiva-scleral pathway. Solvent casting method is typically used in the preparation of ocular inserts/films. The dried solvent cast formulations prepared using this technique can contain trace amounts of residual solvents, which could present safety issues (147, 150). Melt-cast or melt-extrusion technique particularly overcomes this disadvantage of solvent cast method while maintaining all the advantages. Additionally, the technique can be easily transferred to the manufacturing floor employing melt-extruders. The ocular inserts/films offers an attractive approach to prolong the pre-ocular residence time as well as prolong the duration of the ocular absorption phase through the controlled release characteristics of the films - thus increasing drug exposure to the posterior ocular tissues.

The goal of the current research was to develop, characterize and evaluate the drug loaded topical inserts. Indomethacin (IN), prednisolone sodium phosphate (PSP) and ciprofloxacin hydrochloride (CIP) commonly employed in treatment of ocular inflammation and infections, and representing a wide range of physicochemical characteristics, were chosen for investigating ocular disposition from these topical, melt-cast films.

4.1. Materials and Methods

4.1.1. Chemicals

PEO [PolyOx® WSR N-10 (PEO N-10), MW: 100,000 Daltons] was kindly donated by Dow Chemical Company (Midland, MI). IN (Indomethacin), CIP (Ciprofloxacin hydrochloride) and PSP (Prednisolone sodium phosphate) were purchased from Sigma Aldrich (St. Louis, MO). All other chemicals were purchased from Fisher Scientific (St. Louis, MO).

4.1.2. Animal tissues

Whole eye globes of New Zealand albino rabbits were purchased from Pel-Freez Biologicals® (Rogers, AK), shipped overnight in Hanks Balanced Salt Solution (HBSS) over wet ice. Corneas and whole eye globes were used on the day of receipt.

4.1.3. Animals

Male New Zealand albino rabbits (2-2.5 kg) procured from Harlan laboratories® (Indianapolis, IN) were used for all the studies. All animal experiments conformed to the tenets of the Association for Research in Vision and Ophthalmology statement on the Use of Animals in Ophthalmic and Vision Research and followed the University of Mississippi Institutional Animal Care and Use Committee approved protocols (UM protocol no: 14-022).

4.1.4. Formulations

Preparation of ocular inserts / films

Melt-cast technique was utilized for the preparation of the polymeric ocular inserts. PEO N10, a thermoplastic polymer was selected as the matrix forming material because of its excellent pliability and thermogelation characteristics. Physical mixtures of IN or CIP or PSP and PEO N10 were prepared by geometric dilution. Drug load in all the inserts was maintained at 10% w/w. Polymeric films were cast using 13 mm die placed over a brass plate heated to 70°C using a hot

plate. The physical mixture of drug and polymer was introduced into the center of the die and compressed with the 13 mm punch to form a flat solid pre-mix. The mixture was further heated for 2-3 min. After cooling, 4 mm x 2 x 0.2 mm rectangular inserts weighing approximately 8 mg, providing a drug load of 0.8 mg, were cut and used for further studies.

IN control solution (IN-CS-SOL)

IN control formulation was prepared by dissolving IN in an aqueous solution containing 1% w/v Tween 80® and 29.3% w/v propylene glycol. Cationic polymer namely chitosan chloride (Mol wt < 200kDa) (0.25% w/v) was added into the formulation and pH was adjusted to 6.8.

PSP and CIP control solutions

Marketed PSP 1% w/v ophthalmic solution (Mfg. By: Bausch and Lomb®) and CIP 0.3% w/v ophthalmic solution (0.35 mg of CIP equivalent to 0.3 mg ciprofloxacin (base)) (Mfg. By: Hi-Tech Pharmacal) were used as control formulations to compare with PSP and CIP inserts. CIP control solution (0.2% w/v) prepared by dissolving CIP in phosphate buffer (pH 6.0) was used for *in vitro* studies. CIP marketed formulation (0.3% w/v) served as the control for the *in vivo* studies.

4.1.5. Analytical procedure for *in vitro* samples

Analysis of drug molecules was carried out using Waters HPLC system with 600 E pump controller, 717 plus auto sampler and 2487 UV detector. Data handling was carried out using an Agilent 3395 integrator. IN stock solution was prepared in methanol. A 71:29.5:0.5 mixture of methanol, water and o-phosphoric acid was used as mobile phase with Phenomenex *Luna*® 5 µm C_{18} 100 Å, *250* x 4.6 mm column at a flow rate of 1 mL/min and 270 nm (42).

Analysis of CIP was carried out using mobile phase mixture of Acetonitrile and water (50:50), pH was adjusted to 3.0 with o-phosphoric acid. Phenomenex *Luna*® 5 µm C_{18} 100 Å, *250* x 4.6 mm column used at a flow rate of 1 mL/min and 299 nm (151).

PSP was analyzed using a mixture of 18 mM phosphate buffer: methanol (38:62) and 0.1% w/v trimethylamine (pH 2.5) as the mobile phase. Phenomenex *Luna*® 5 µm C_8 100 Å, *250* x 4.6 mm column was used at a flow rate of 1 mL/min and detection wavelength 218 nm. The reported analytical method was modified and validated prior to sample analysis (152). The linearity regression correlation coefficient in the constructed calibration curves was within the limit (≥0.99). Percentage relative standard deviation (RSD) values for the precision were found to be less than 2%. The percentage RSD for peak area response and retention were found within the prescribed limits. The linearity, accuracy and precision were observed to be acceptable over the working standard ranges in the all of the analytical methods.

4.1.6. Assay and content uniformity

IN content in polymeric inserts was determined using methanol and dimethyl sulfoxide (DMSO) 50:50 mixture as an extraction solvent. CIP and PSP was extracted from the films using 50:50 water and methanol. Content uniformity was determined from four, randomly cut, units from a single 13 mm insert, and analyzed as described under analytical procedure using a high performance liquid chromatography – UV (HPLC-UV) method.

4.1.7. Differential scanning calorimetry (DSC) and Fourier transform infrared (FT-IR) Spectroscopy

DSC thermograms for pure IN or CIP or PSP, PEO N10 and the 10% w/w inserts were collected using a Diamond Differential Scanning Calorimeter (Perkin-Elmer Life and Analytical Sciences) (153).The samples were weighed and sealed in aluminum pans and were heated from 0°C to 270°C at a heating rate of 10°C/min under nitrogen purge (20 mL/min). Infrared spectra (IR) for PEO N10, drug/polymer physical mixture, IN or CIP or PSP, and melt cast inserts (10%

w/w) were obtained using a Cary 660 series FTIR (Agilent technologies) and MIRacle ATR (Attenuated Total reflectance).

4.1.8. *In vitro* release and transcorneal permeability studies

In vitro release of CIP, IN and PSP from the ocular inserts was tested across standard US 100 mesh sieve in 20 mL scintillation vials. The insert was placed in the vial and the sieve was placed over the films and 10 mL of 5% w/v RMβCD in IPBS (pH 7.4) was added as the release/dissolution media. A stir bar was placed on the sieve and the whole assembly was placed over a hot plate maintained at 34°C under stirring (spin bar) for 2 h. Aliquots (600 µL) were collected at specific intervals and replaced with fresh medium. Samples taken were analyzed using HPLC-UV.

Corneas excised from whole rabbit eyes were used for the determination of *in vitro* transcorneal flux of the compounds from the various formulations. Whole eyes were shipped overnight in HBSS, over wet ice, and were used immediately upon receipt. The corneas were excised with some scleral portion adhering to help secure the membrane between the donor and receptor compartments during the course of a transport study. The temperature was maintained at 34°C with the help of a circulating water bath. *In vitro* permeability of IN, PSP, CIP across the corneal membrane was investigated using the Valia-Chien cells (PermeGear, Inc., Hellertown, PA). The *in vitro* permeability studies were carried out for a period of 3 h. All the formulations were tested for transcorneal permeability at equivalent doses. Four hundred microliters of IN Control solution and IN Insert (5% w/w) (Dose: 400 µL (400 µg); 400 µg), PSP Control marketed solution (1% w/v) and PSP Insert (10% w/w) (Dose: 80 µL (800 µg); 800 µg), CIP Control (0.2% w/v) and CIP Insert (10% w/w) (Dose: 400 µL (800 µg); 800 µg) formulations were placed in the donor compartment. The inserts were slightly wetted, by adding 50 µL of IPBS in the donor

compartment, at the start of the experiment. Aliquots were withdrawn at specific time intervals and analyzed for CIP, PSP or IN content using HPLC-UV method.

4.1.9. Data Analysis

The transcorneal flux was obtained by dividing the rate of drug transport by the surface area exposed to permeant and rate of transport was obtained from slope of linear regression analysis plot between cumulative amounts of drug transported versus time. Transcorneal flux was calculated using the equation below.

$$\text{Flux (J)} = \frac{\frac{dM}{dt}}{A}$$

Where M is cumulative amount of drug and A is the surface area of the corneal membrane (0.636 cm^2) exposed to the permeant (drug).

4.1.10. *In vivo* bioavailability studies

In vivo ocular bioavailability of IN, PSP and CIP was determined in conscious Male New Zealand albino rabbits weighing between 2.0-2.5 kgs. In these studies, IN-CS-SOL, PSP and CIP solutions (control; 100 µL) were instilled as instilled as two doses (50 µL each dose) at two different time points, -30min and 0 min, to reduce pre-corneal loss. 10% w/w loaded IN insert (Dose: 0.8 mg) was placed in the cul-de-sac of the rabbit eyes. Ocular bioavailability of PSP and CIP was investigated following the instillation of 1% w/v PSP marketed topical ophthalmic formulation (control; 100 µL: 1 mg) (Bausch & Lomb), 0.3% w/v CIP marketed solution (Control; 100 µL: 300 µg) and administration of PSP insert (Dose: 0.8 mg), CIP insert (Dose: 0.8 mg) in conjunctival sacs of the rabbit eyes. At the end of 2 h, following topical application of the aforementioned formulations, the rabbits were euthanized with an overdose of pentobarbital injected through the marginal ear vein. The eyes were washed with ice cold IPBS and immediately

enucleated and washed again. Ocular tissues were separated, weighed and preserved at -80°C until further analysis. All experiments were carried out in triplicate.

4.1.11. Bio analytical method and samples preparation

The *in vitro* analytical HPLC-UV methods described above was employed for bio-sample analysis following method validation. Protein precipitation technique was used for determining drug concentrations in the ocular tissue homogenates. Briefly, tissues such as cornea, sclera, iris-ciliary (IC), retina-choroid (RC) were cut into very small pieces and added into Eppendorf® tubes. A mixture of ice-cold acetonitrile and 0.1% w/v formic acid (1 mL) was then added to precipitate proteins from each individual tissue. The supernatant was then collected after centrifugation for 1 h at 13,000 rpm prior to analysis. Aqueous humor (AH) (200 µL) and Vitreous humor (VH) (500 µL) were precipitated by adding an ice-cold mixture of 200 µL for AH and 500 µL for VH in the ratio (1:1). Quantification was carried out using calibration curves constructed from respective ocular tissues such as cornea (20-500 ng), sclera (20-500 ng), AH (10-200 ng), VH (10-200 ng), IC (10-200 ng), RPE (10-200 ng). All the standard curves had a coefficient of determination $r^2 \geq 0.96$. Recovery of the drugs was quantitated by spiking drug in blank AH, VH, and comparing the expected drug concentration with standard concentration. Recovery values were determined in AH (93.1-94.7) and VH (91.5-93.2). Interference was not observed from co-eluted protein residues with respect to drug peaks in all the tissues.

4.1.12. Statistical analysis

All the data presented in these experiments was reported as an average of triplicate for the same time points. One way ANOVA was carried out to test and compare treatment groups at different levels of significance and Student t-test was used to compare differences within two groups. A ‘p’ value less than 0.05 was considered to express statistically significant difference.

4.2. Results

4.2.1. Assay and content uniformity

IN / CIP / PSP content in all the inserts was approximately between 90% and 95% of the theoretical value. The compounds were observed to be uniformly distributed within the polymeric framework (RSD < 2.3%) and the films exhibited good pliability and tensile strength.

4.2.2. DSC and FT-IR studies

The polymeric inserts were studied for thermal characteristics and excipient compatibility using DSC. DSC thermograms of pure PEO N10, PEO N10 film, pure drug, physical mixture and polymeric insert are presented in Figures 4.1 and 4.2. IN (Fig. 4.1) and CIP (Fig. 4.2) exhibited an endothermic peak at 162°C and 153°C corresponding to their melting points. PEO N10 and PEO N10 film exhibited a melting point temperature of 68°C. The characteristic peaks of IN and CIP were absent in the polymeric inserts indicating that there was significant reduction in crystallinity.

FTIR spectra of pure IN exhibited characteristic bands of secondary carbonyl groups (C=O) at 1710 cm^{-1}, (C=O amide) at 1687 cm^{-1}, phenyl groups (C=C stretch vibration) at 1593 cm^{-1} and (O-H stretch vibration) at 2964 cm^{-1}. Pure PEO revealed –CH stretching at 2880 cm^{-1} (Fig. 4.3). FTIR spectra of PSP showed two carbonyl stretching peaks at 1708 cm^{-1} and 1654 cm^{-1} while peaks at 1596 cm^{-1} and 1100 cm^{-1} correspond to the NH and OH bending (Fig. 4.4). The FTIR spectra of CIP showed characteristic peak at 3500 and 3450 cm^{-1} corresponding to OH stretching vibration. The band at 1701 cm^{-1} indicated carbonyl C = O stretching, while the peak at 1617 cm^{-1} belongs to quinolone. The band at the 1445 cm^{-1} represented carbonyl group and the peak at 1250 cm^{-1} suggested bending vibration of O-H group which indicated the presence of carboxylic acid (Fig. 4.5). The FTIR spectra of physical mixtures were similar to those of respective drugs and PEON10 individual spectra, which suggest that there was no chemical

interaction between drug and PEON10 in physical mixtures. However, characteristic bands of the IN (carbonyl, amide and phenyl functional groups), CIP (quinolone group) and PSP (carbonyl group) displayed lesser degree of intensities / disappeared in the insert formulations indicating chemical interaction between drug and the carrier occurred during the formulation processing steps.

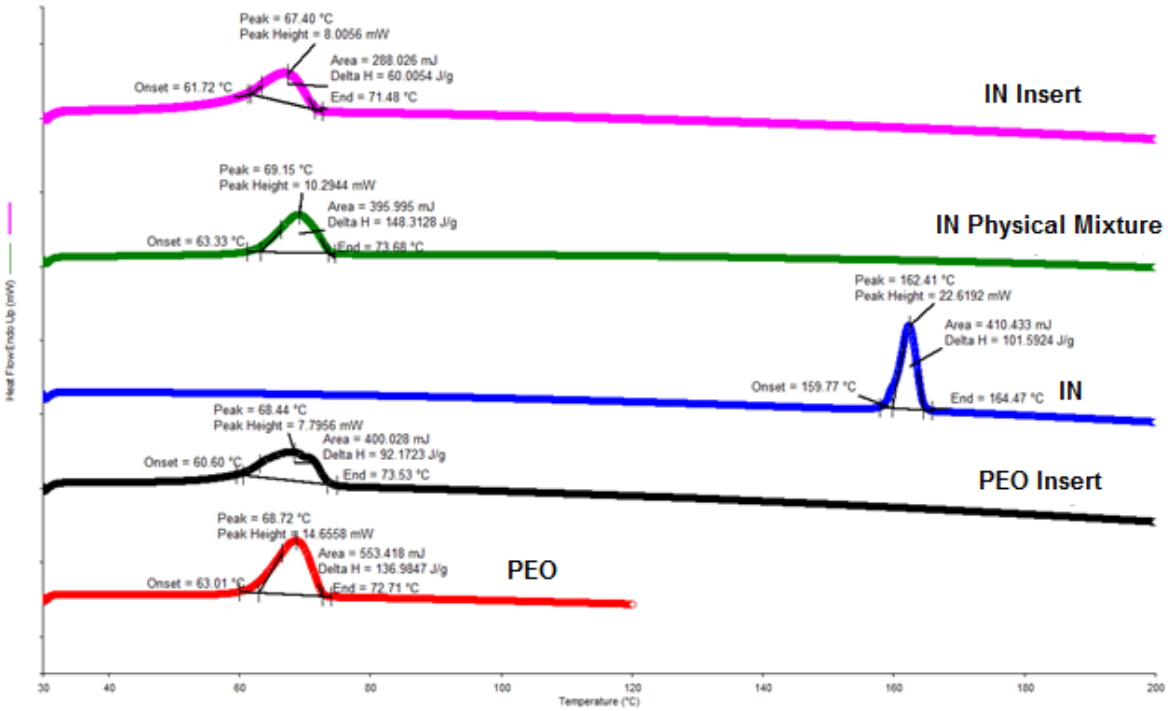

Figure 4.1: DSC thermograms of IN Insert, IN physical Mixture, pure IN, PEO Insert and pure PEO.

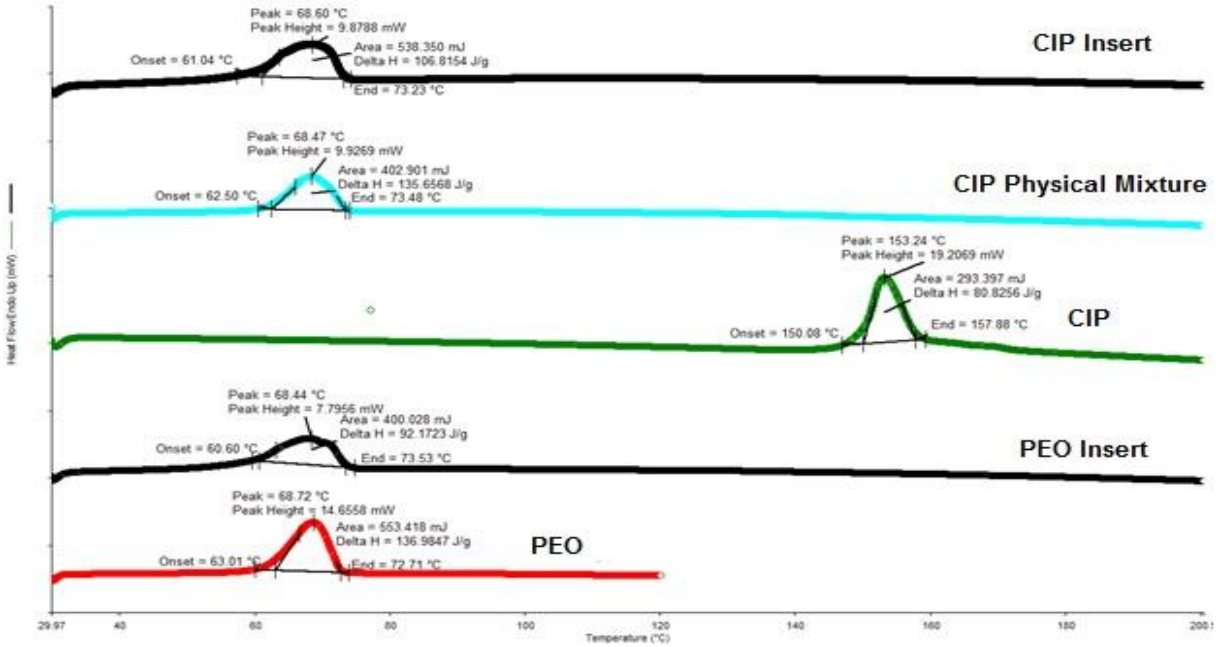

Figure 4.2: DSC thermograms of CIP Insert, CIP physical Mixture, pure CIP, PEO Insert and pure PEO.

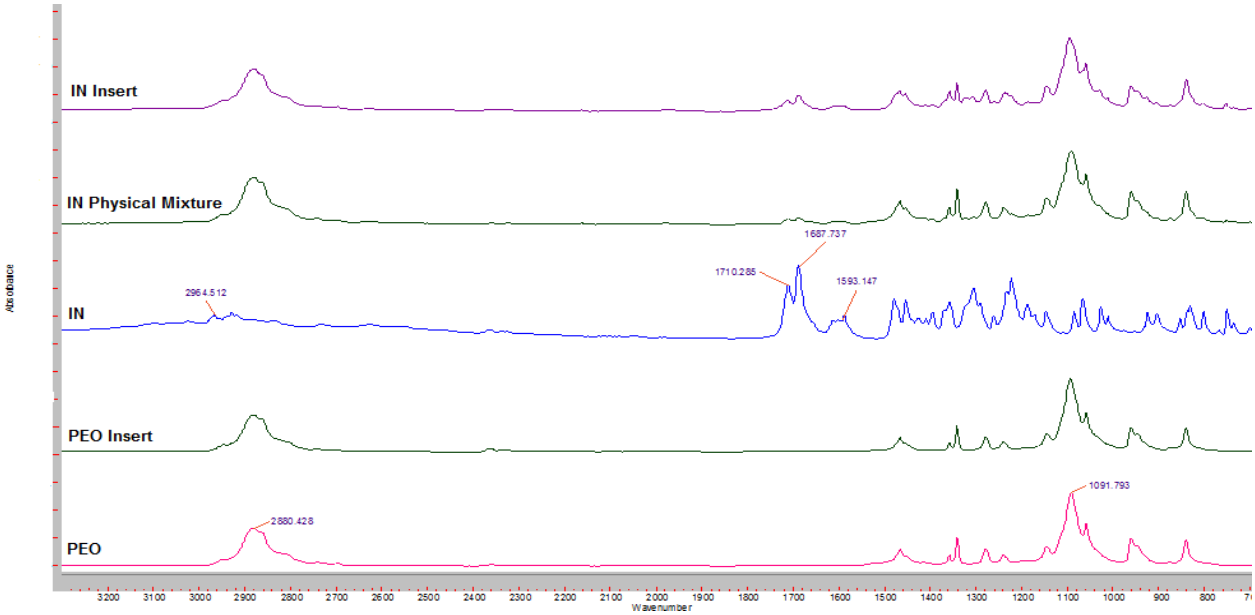

Figure 4.3: FT-IR spectra of IN Insert, IN Physical Mixture, pure IN, PEO Insert and pure PEO N10.

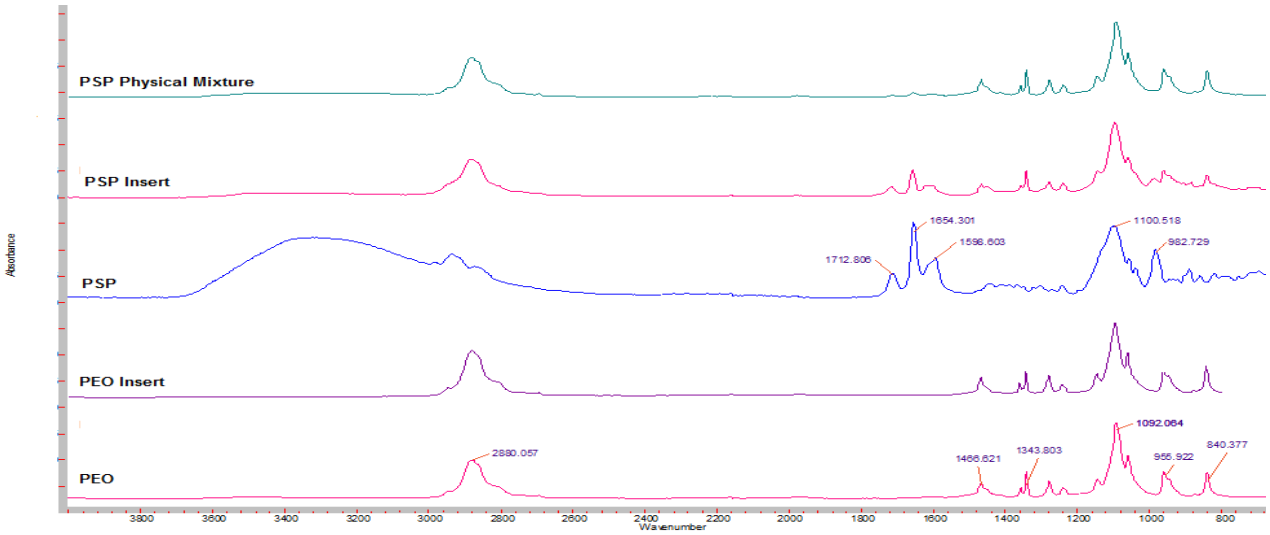

Figure 4.4: FT-IR spectra of PSP Physical Mixture, PSP Insert, pure PSP, PEO Insert and pure PEO N10.

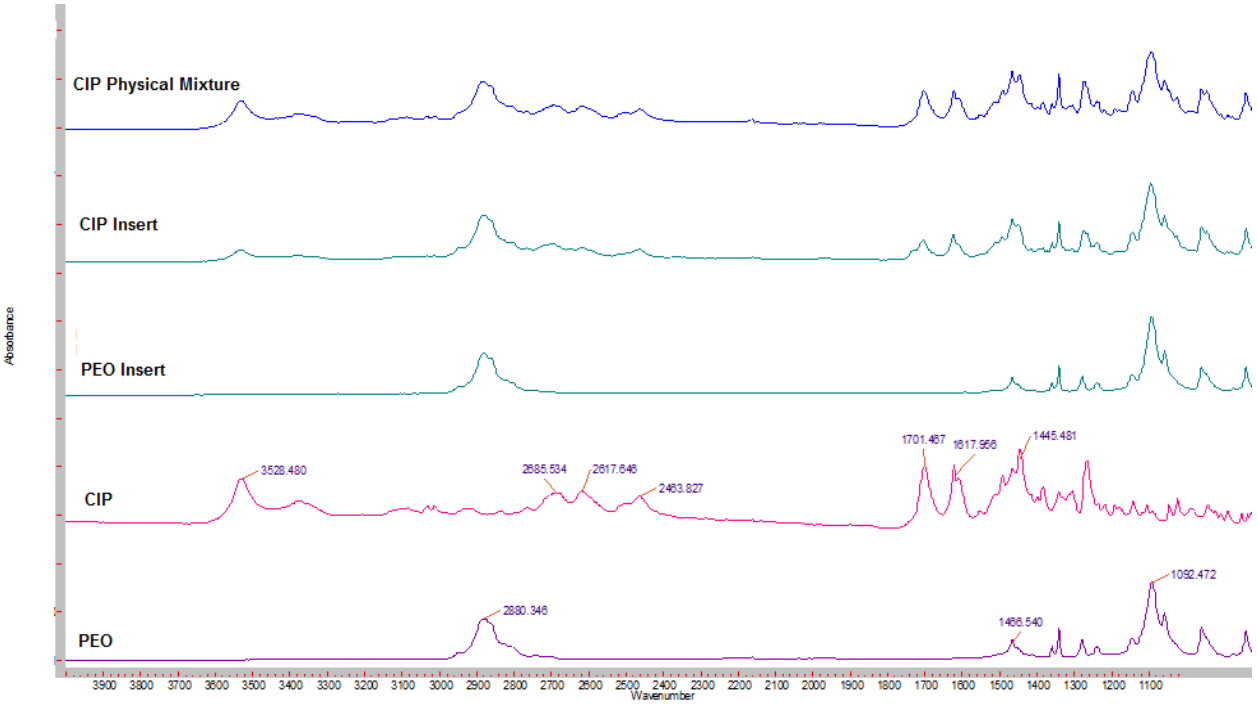

Figure 4.5: FT-IR spectra of CIP Physical Mixture, CIP Insert, PEO N10 Insert, pure CIP and PEO N10.

4.2.3. *In vitro* release

Percentage release of IN, PSP, CIP from the polymeric films was determined to be 100.2 ± 6.9, 92.7 ± 4.8 and 85.3 ± 9.4 %, respectively, at the end of 2 h (figure not presented).

4.2.4. Transcorneal permeability studies

In vitro transcorneal flux profiles obtained from different topical insert formulations, compared to their respective control solutions at an equivalent dose, is presented in Figure 4.6. Transcorneal flux of IN, PSP, CIP were enhanced by ~ 3.5, ~ 3.6 and ~ 2.9-folds, respectively, from the polymeric inserts when compared to their control formulations.

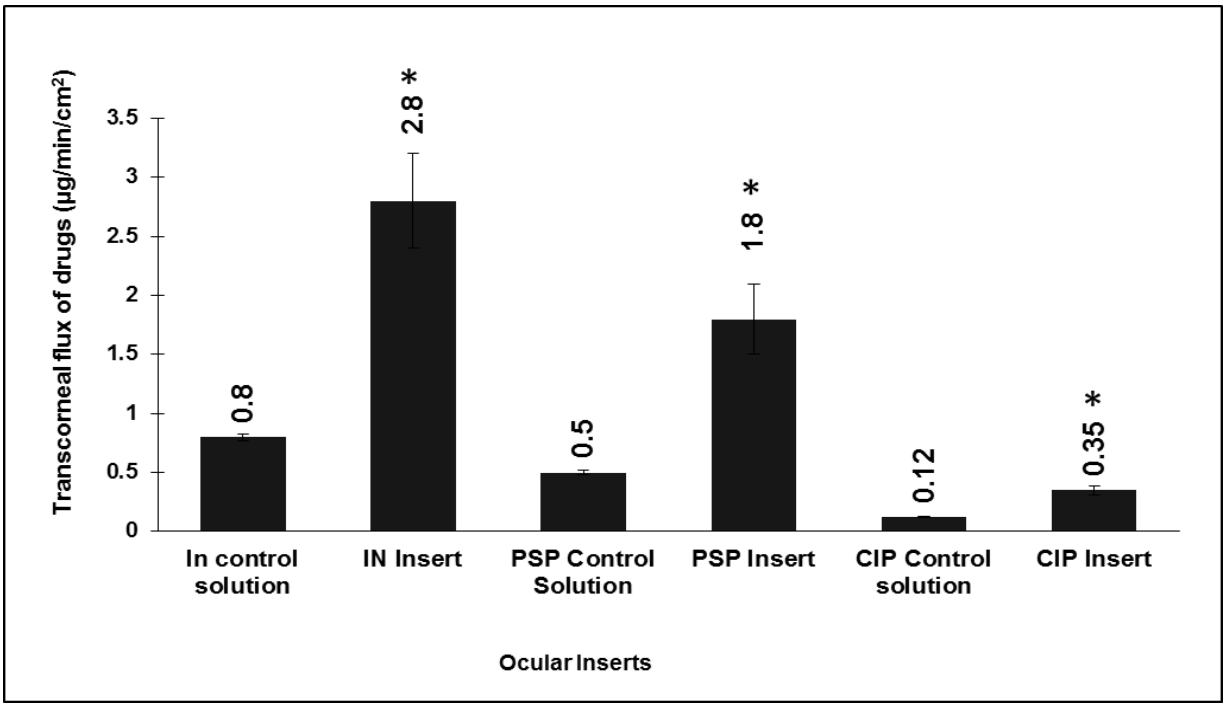

Figure 4.6: *In vitro* transcorneal flux obtained from different topical formulations at equivalent doses using valia-chien cells at 34°C. Formulation tested include IN Control (0.1% w/v), IN insert (5% w/w) (Dose: 400 µL (400 µg); 400 µg). PSP Control solution (1% w/v), PSP Insert (10% w/w) (Dose: 80 µL (800 µg); 800 µg). CIP Control (0.2% w/v), CIP Insert (10% w/w) (Dose: 400 µL (800 µg); 800 µg). Symbolic representation on the formulation indicate the statistically significant difference in flux compared to control.

4.2.5. *In vivo* bioavailability studies

Ocular tissue concentrations obtained with drug loaded polymeric inserts were evaluated in conscious rabbit model, 2 h post topical application. IN-CS-SOL did not deliver drug into RC but delivered into the cornea (0.9 ± 0.09 µg/g), sclera (0.4 ± 0.19 µg/g), IC (0.12 ± 0.04 µg/g) and AH (0.15 ± 0.03 µg/g) whereas IN insert delivered drug into RC (1.08 ± 0.26 µg/g). Furthermore, IN insert enhanced IN levels by ~10 folds (AH), ~27-folds (IC) and ~8.5-folds (cornea) when compared to IN-CS-SOL formulation (fig.4.7.).

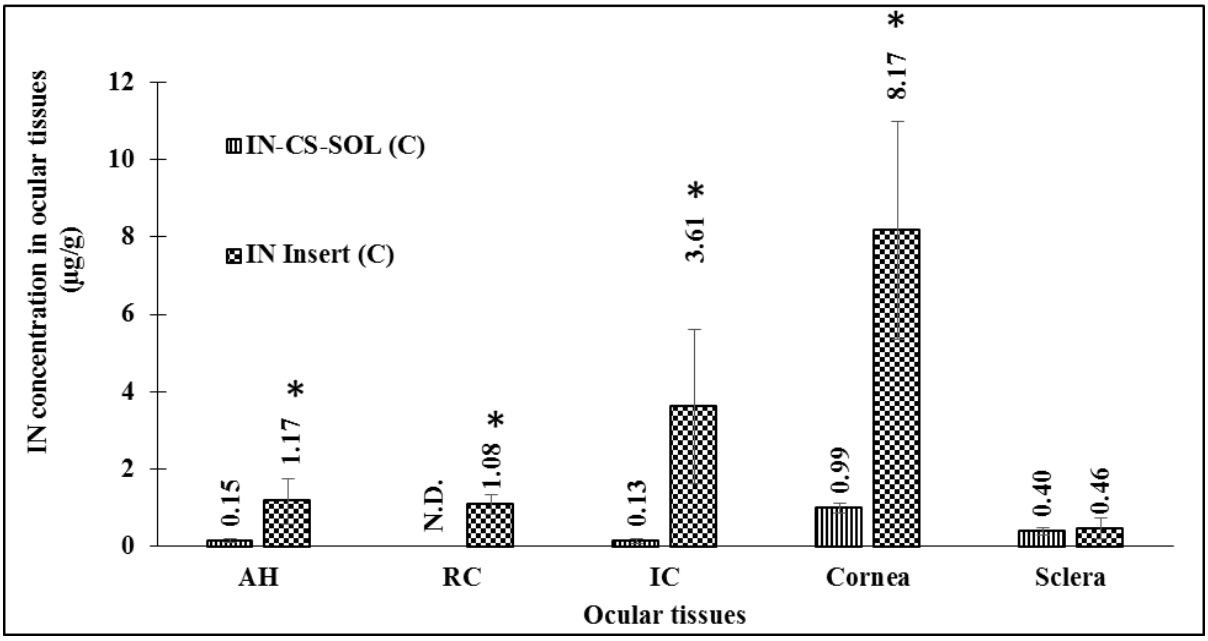

Figure 4.7: *In vivo* IN concentrations (µg/gm of tissue) obtained from 0.1% w/v IN-CS-SOL, and 10% w/w IN Insert (Dose: 0.1 mg, 0.8 mg & 0.8 mg respectively), 2 h post topical application in conscious rabbit model. All experiments were performed in triplicate. AH: Aqueous Humor; RC: Retina-Choroid; IC: Iris-Ciliary. No levels were detected in VH. ND-not detectable. * Symbol represented on ocular tissues indicate statistical significance of IN concentrations obtained from the IN insert in comparison to control ($p<0.05$).

PSP control solution delivered drug into ocular tissues namely AH (0.3 ± 0.04 µg/mL), IC (1.07 ± 0.5 µg/g), cornea (1.55 ± 0.85 µg/g) and sclera (0.77 ± 0.41 µg/g). While the PSP control solution couldn't deliver drug into the RC and VH, the insert - even at a lower dose compared to the PSP control - delivered PSP into the VH (0.09 ± 0.008 µg/mL) and RC (1.28 ± 0.52 µg/g). Moreover, the insert generated significantly greater PSP in all the other ocular tissues tested (fig.4.8.).

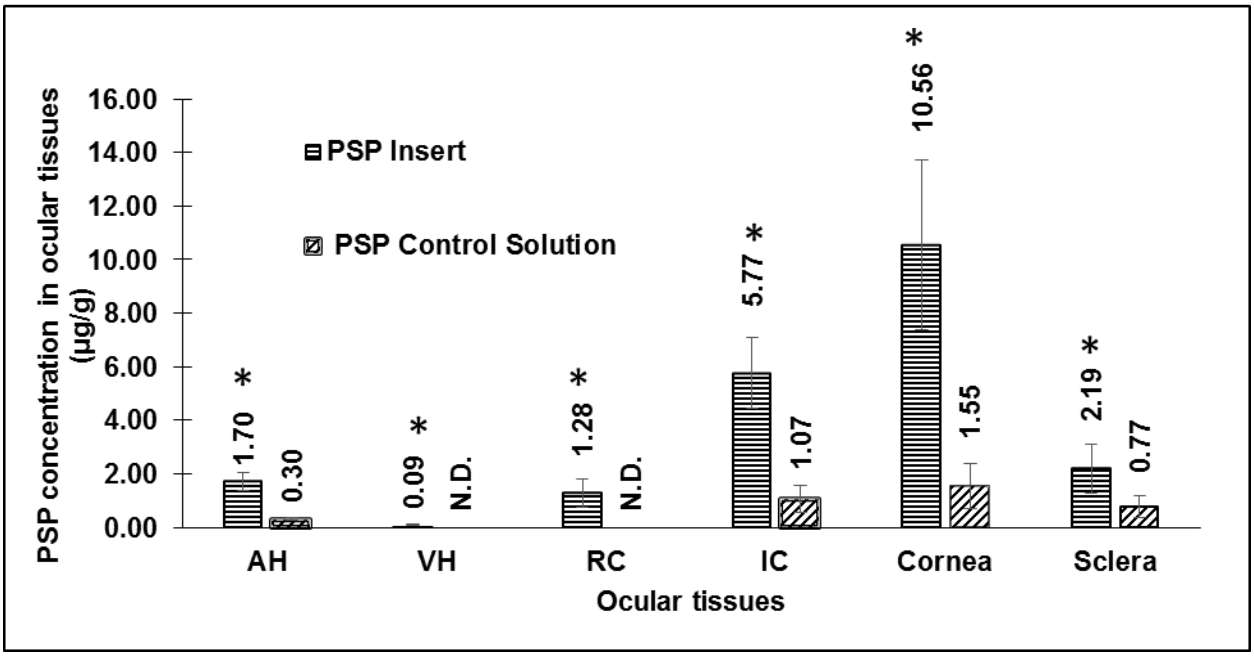

Figure 4.8: *In vivo* PSP concentrations (µg/gm of tissue) obtained from 10% w/w PSP Insert and PSP control solution (1% w/v) (Dose: 0.8 mg, 1 mg respectively), 2 h post application in conscious rabbit model. All experiments were in triplicates. AH: Aqueous Humor; RC: Retina-Choroid; IC: Iris-Ciliary; VH: Vitreous Humor. Low levels were detectable in VH. (N.D - Not detectable). Symbol representation on ocular tissues indicate the statistical significance of PSP concentrations obtained from the insert formulation in comparison to control ($p<0.05$).

Similarly, CIP concentrations obtained with the control solution in the AH (0.51± 0.2 µg/mL), IC (0.47 ± 0.17 µg/g), cornea (0.86 ± 0.16 µg/g) and sclera (0.15 ± 0.01 µg/g) were significantly lower than that obtained with the inserts. The control solution formulations did not deliver CIP to the VH and RC, whereas the insert successfully delivered CIP into the VH (0.13 ± 0.05 µg/mL) and RC (0.6 ± 0.17 µg/g) (fig.4.9.).

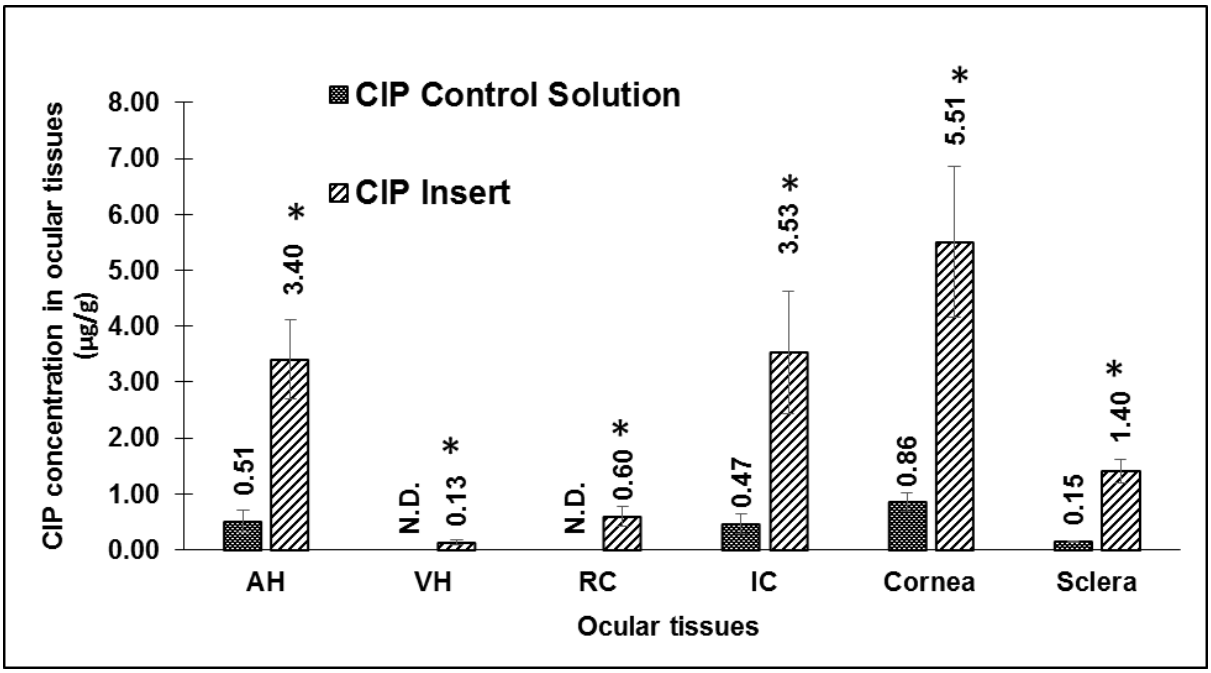

Figure 4.9: *In vivo* ocular tissue concentrations of CIP obtained from 0.3% w/v CIP control solution (Dose: 100 µL; 350 µg), 10% w/w CIP Insert (Dose: 0.8 mg) in conscious rabbit model following 2 h post topical application. AH: Aqueous Humor; RC: Retina-Choroid; IC: Iris-Ciliary; VH: Vitreous humor. ND: Not detectable. Symbolic representation on ocular tissues indicate the statistical significance of CIP concentrations obtained from the insert formulation in comparison to control ($p<0.05$).

4.3. Discussion

The overall objective of the current research is to develop a standard prototypical, noninvasive, ocular drug delivery platform, effective for molecules representing a wide spectrum of physico-chemical properties, for back-of-the eye drug delivery. The melt-cast / melt-extrusion technology is a simple, solvent free, continuous process, for preparing unit dosage forms, which undergo gelation upon contact with tear fluid, prolonging the release and retention on the ocular surface. The compound to be delivered can possess a range of hydrophilicity/lipophilicity, as demonstrated in the present project, and could be formulated at significantly higher loading. Compounds embedded in the carrier matrix will be transformed into an amorphous state or get entrapped as a molecular dispersion after fabrication using thermal technique. Moreover, preservatives and solubilizers are not required, eliminating unnecessary excipients and processing

steps. Furthermore, modified release platforms could be designed by varying the thermoplastic polymers or molecular weights and combinations.

The solubility of CIP, a zwitterion, is greatly reduced at the pH 7.4, which is close to its isoelectric point. This may cause CIP to crystalize when the ophthalmic solutions (formulated in the acidic pH range) come into contact with the tear fluid. In the melt-cast inserts, for all three drugs, absence of detectable crystalline domains in the DSC thermograms demonstrate that the drug was completely dispersed or solubilized in the carrier polymer, at this 10% w/w drug loading.

An interaction between drug and polymer could be reflected by a change in the position of C=O vibration and disappearance of O-H stretching in the FT-IR spectra depending on the extent of the interaction. The FT-IR spectra of the insert formulations exhibited lower peak intensities / were masked indicating slight interaction with the polymer PEO N10. The release studies, however, indicated that 100% of the drug was released within 2 hours. Moreover, *in vitro* transcorneal flux of the three actives from the inserts was increased by ~ 2.5 to 3.5-folds when compared to the respective control solutions. This could be due to enhanced drug retention and accumulation in the corneal and conjunctival epithelial layers from the transformed gel (*in vitro*).

Penetration of drugs through the conjunctival scleral pathway is reported in the literature (154, 155). Ocular tissue concentrations attained with the polymeric inserts in AH, IC and cornea was increased by ~6-8 folds in comparison to the control formulations. Cationic mucoadhesive polymer (CS) was used at a concentration of 0.1% w/v to improve corneal penetration characteristics and thereby intraocular bioavailability of IN from control solution. However, IC levels obtained with IN control solution was ~27-fold lower at 1/8th dose of insert formulation. IN control Retinal concentrations were obtained *in vivo* with the IN insert (1.08 ± 0.27 µg/g), PSP insert (1.28 ± 0.52 µg/g) and CIP insert (0.60 ± 0.17 µg/g) formulations, whereas control solutions,

couldn't deliver drug into RC. The inserts form localized drug depots, in close proximity to the conjunctival-scleral tissues, and thus helps drive the molecules to the retinal tissue, through the conjunctival-scleral route. Thus, advantage of inserts, as a platform providing access to the trans-scleral pathway, could be exploited to overcome the physico-chemical limitations of molecules. Additionally, feasibility of higher drug loading and use of penetration enhancers, if needed, provides even greater flexibility to the dosage form. The melt-cast technique can be easily translated or scaled up for manufacturing using melt-extrusion technology, which also minimizes the exposure time to higher temperatures (2-3 minutes) allowing processing of some thermolabile compounds also.

There have been a few reports attempting back-of-the eye delivery of therapeutic agents through the topical route. In an earlier study, IN was loaded into nanostructured lipid carrier (NLC) at 0.8% w/v and was evaluated in conscious rabbits, 2 h post-topical administration of 100 µL (Dose: 800 µg). Retinal levels (0.89 ± 0.31 µg/g) were also observed with the NLC formulation (156). In another report, an IN (0.1% w/v) ophthalmic solution made up of poloxamer® 407 (10% w/w) enhanced AH concentrations by ~2-fold when compared to Indocollyre® (marketed ophthalmic solution), 2 h post-topical administration of 150 µL formulation (Dose: 150 µg) (40). Schultz et al impregnated prednisolone into hydrogel contact lenses by placing them in diluted 5 mg/mL prednisolone suspension. These contact lenses were evaluated for posterior segment (retina, choroid, and macula) concentrations in anesthetized rabbits following 4 h treatments/application on days 1, 2, 5, 8 and 10. On day 11 retinal concentrations obtained were in range of 26-166 ng/g (157). Taha et al evaluated CIP loaded liposomes (0.3% w/v) in conscious rabbits following topical application of 50 µL formulation (Dose: 150 µg) (158). The authors report that AH concentrations was increased by ~0.3-folds when compared to CIP marketed

ophthalmic formulation. The polymeric noninvasive inserts developed in this study, delivered significantly higher drug levels to all the ocular tissues tested, in comparison to the control and other literature reports.

It is widely acknowledged that IN acts as an anti-inflammatory agent through the inhibition of COX-2 enzyme, abundantly present in ocular tissues namely cornea, iris, ciliary body and retina (159). Mitchell et al reported half-maximal inhibitory concentration (IC50) of IN required for COX-2 activity in endotoxin activated J774.2 macrophages to be 0.6 µg/mL (160). MIC90 of ciprofloxacin is reported to be 0.5 µg/mL (161). Therapeutic concentration of prednisolone required to inhibit inflammatory mediated processes in AH (humans) is reported to be 25 ng/mL (162). Drugs levels for optimal activity are reported in terms of solution concentrations, which reflects the therapeutic levels needed in AH and VH tissues. Ocular tissues namely IC and RC are in dynamic equilibrium with AH and VH, so the therapeutic levels required in AH and VH could be interpreted to be good therapeutic response indicators in the ocular tissues. Drug levels obtained in all the ocular tissues, post 2 h, with inserts were several folds higher than the reported minimal concentrations, demonstrating that inserts could maintain therapeutic drug levels for prolonged durations following topical application.

4.4. Conclusion

In conclusion, the results from these studies suggest that the development of solvent free, melt-cast or melt extruded ocular inserts is a highly feasible, noninvasive approach for the delivery of a wide range of drugs, with different physico-chemical properties, to the ocular tissues. The high localized drug loads, intimate contact with the conjunctiva, increased retention time and quick transformation into a gel form make this efficient for delivering to the back-of-the eye tissues also. These formulations would be marketed as unit dosage forms and do not need any preservatives or solubilizers. Penetration enhancers may be incorporated to further increase ocular bioavailability.

Thus, the melt-cast / melt-extruded films could shift the paradigm for drug delivery to the back-of-the eye.

CHAPTER 5

NON-INVASIVE CATIONIC COLLOIDAL NANOCARRIERS FOR OCULAR DELIVERY OF NATAMYCIN: PREPARATION AND EVALUATION

5. Introduction

Ocular drug delivery appears to be one of the most interesting and challenging fields for the pharmaceutical scientist. Topical application of drugs to the eye is the most favored, safest and popular route of administration for the treatment of various ocular disorders/complications. The ophthalmic bioavailability of topically instilled drugs is, however, very poor due to efficient protective mechanisms encountered in the ocular milieu (163-165). Ocular fungal infection, namely mycotic keratitis (MK), is characterized by feathery-edged infiltrates and satellite lesions across the cornea, which could lead to vision loss and blindness, if left untreated (166). Fungal keratitis may attack orbit, lids, lacrimal apparatus, conjunctiva, sclera, and other ocular structures during the progression (167). Natamycin (NT) is a macrolide polyene antifungal agent with a broad spectrum of activity against various infectious fungi such as Fusarium, Aspergillus, and Candida species. NT has been considered as the first line of therapy for filamentous MK *(168, 169)*. NT suffers from poor aqueous solubility but is effective at very low concentrations with MIC (minimum inhibitory concentration) of less than 10 ppm. NT elicits its activity by binding to ergosterol, a sterol unique to fungal cytoplasm (170, 171). Currently, Natacyn® (NT 5% w/v suspension) is the only commercially available US-FDA approved ophthalmic formulation for the treatment of MK. The frequency of administration of NT suspension is prescribed as one drop instilled in the conjunctival sac at hourly or two hourly intervals for several days. The shortcomings of the current therapy include high dosing frequency, long treatment duration (4–6 weeks), and low pre-ocular residence time. The current NT therapy may not attain optimal concentration at the site of infection, resulting in treatment failure and increased resistance (172, 173). Hence, there is a urgent clinical need to improve patient compliance and efficiency of therapy, with reduced frequency of administration, by designing a corneal targeted, prolonged release delivery system of

NT. There were a few reports in the literature on ocular delivery of NT using novel approaches (174, 175). To overcome the shortcomings associated with the marketed preparation, cationic lipid based nanoparticles (CLBN) were developed, which could prolong pre-ocular residence and improve mucoadhesion for efficient delivery of NT into the ocular tissues. Reports indicate that cationic nanoparticles exhibit greater corneal affinity and interaction compared to the negatively charged nanoparticles. The applicability of these nanoparticles as ocular delivery vehicles was investigated in this work. The goal of the present project is to prepare NT loaded CLBN, evaluate *in vitro* permeability and ocular tissue distribution *in vivo*, using Natacyn® 5% w/v Ophthalmic Suspension as the control.

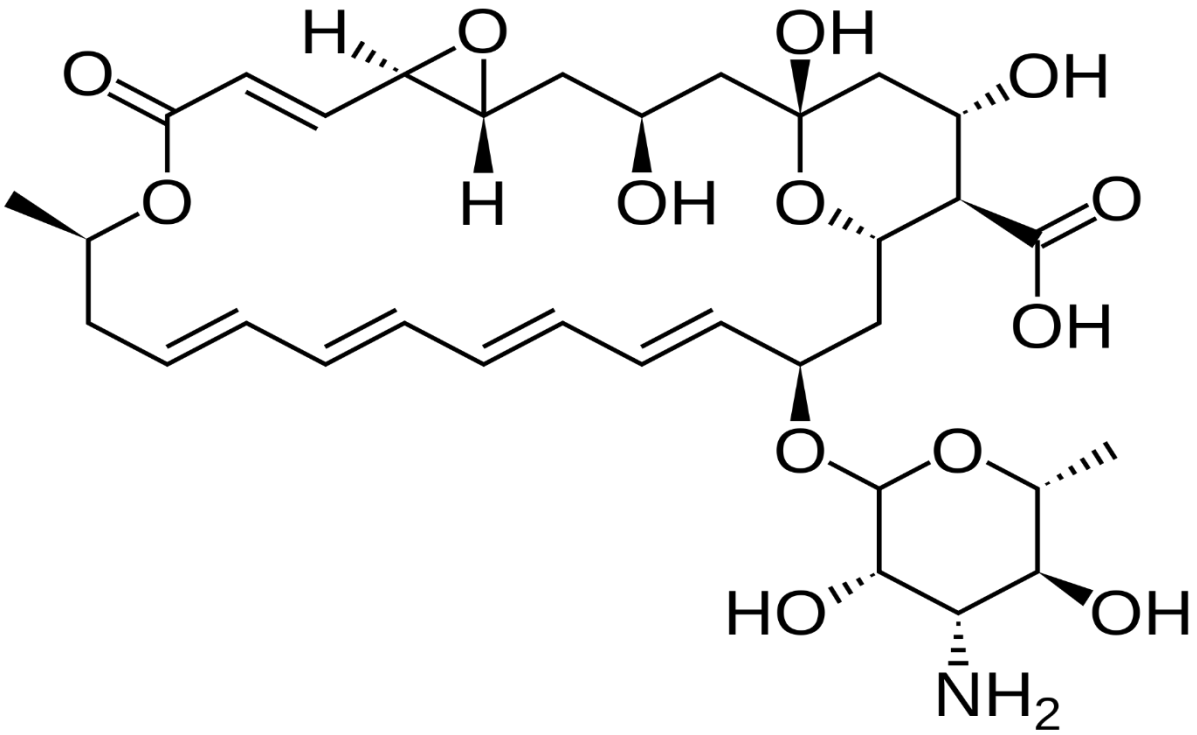

Figure 5.1: Chemical structure of Natamycin

5.1. Materials and Methods

5.1.1. Chemicals

Natamycin and di-dodecy dimethyl ammonium bromide was obtained from Sigma Aldrich (St. Louis, MO). Glyceryl Monostearate was obtained as a gift sample from Gattefossé (Paramus, NJ). Amicon® Ultra centrifugal filter devices with regenerated cellulose membrane (molecular weight cut off 100 kDa), Poloxamer 188, Tween®80, high performance liquid chromatography (HPLC) - grade solvents, and other chemicals (analytical grade) were obtained from Fisher Scientific (Hampton, NH). Whole eyes of male albino New Zealand rabbits were obtained from Pel-Freez Biologicals (Rogers, AR). Male albino New Zealand rabbits were procured from Harlan Labs (Indianapolis, IN).

5.1.2. Preparation of NT loaded CLBN

NT loaded CLBN were fabricated using ultra sonication method. Solid lipids, namely Glyceryl monostearate (GMS) and di-dodecyl dimethyl ammonium bromide (DDAB), were melted and NT was dissolved in it to obtain the lipid phase. An aqueous phase, prepared using surfactants such as Poloxamer 188 (0.25% w/v), Tween® 80 (0.75% w/v) and glycerin (2.25% w/v) in bidistilled water, was heated. The hot aqueous phase was then added to the melted lipid phase, under stirring, to form a premix (600 rpm, 1–2 min). The premix was then subjected to emulsification at 16,000 rpm for 6 min using T 25 digital Ultra-Turrax to form a hot pre-emulsion. The pre-emulsion obtained was subjected to ultrasonication resulting in the formation of hot emulsion dispersion. The temperature during the entire process was maintained at 80±2°C. The hot emulsion obtained was slowly cooled to room temperature to form NT-CLBN.

5.1.3. Analytical method for *in vitro* sample analysis

Samples were analyzed for NT content using an HPLC-UV method. The system comprised of Waters 717 plus Autosampler, Waters 2487 Dual λ Absorbance detector, Water 600 controller pump, and Agilent 3395 Integrator. A Phenomenex Luna® C_8 4.6 mm x 250 mm column was used under isocratic elution for chromatographic analysis. The mobile phase used was mixture (70:30) of phosphate buffer (pH 5.5) and acetonitrile. The flow rate was set at 1 mL/min with λ_{max} (detection wavelength) of 304 nm during the analysis (176).

5.1.4. Physico-chemical Characterization

The hydrodynamic radius and the PDI of the NT CLBN formulation was determined by photon correlation spectroscopy, using Zetasizer Nano ZS Zen3600 (Malvern Instruments, Inc.) at 25°C and 173° backscatter detection, in disposable clear cells. The measurements were obtained using a helium-neon laser of 633 nm, and the particle size analysis data was evaluated using volume distribution.

Zeta potential measurements were carried out at 25°C in disposable cells using the same instrument. For measurement of particle size distribution and zeta potential, CLBN samples were diluted (1:500) with water. Bi-distilled and 0.2 μM filtered water was used for these measurements, and were performed in triplicates.

5.1.5. Assay and Entrapment Efficiency

The lipid in the NT CLBN formulation was precipitated using methanol and, drug content in the supernatant after centrifugation (13,000 rpm for 20 min), was measured using an HPLC system following appropriate dilution.

The percentage of NT entrapped (% EE) in CLBN was determined by measuring the concentration of free drug in the aqueous phase of an undiluted formulation. The EE was evaluated by an ultrafiltration technique with a 100 kDa centrifugal filter device (Amicon Ultra). An aliquot

(500 μL) of the corresponding formulation was added to the sample reservoir and centrifuged at 5,000 rpm for 10 min. The filtrate was analyzed for drug content using HPLC. The %EE was calculated using Eq. (1) below. All the measurements were carried out in triplicates.

$$\%EE=[(Wi-Wf)/Wi]\times 100 \quad (1)$$

Where Wi =total drug content, and Wf =amount of free drug in aqueous phase.

5.1.6. *In vitro* release studies

In vitro release of NT from marketed ophthalmic formulation (Natacyn®) and CLBN was evaluated by dissolution method using scintillation vials. Randomly methylated beta-cyclodextrin (RMβCD) solution (2.5% w/v; 10 mL) prepared in isotonic phosphate buffer (pH 7.4) was used as receiver medium during the course of the study (30 min). Twenty microliters of the control formulation and 500 μL of CLBN was added into the medium. Aliquots (600 μL) were withdrawn from the receiver medium at predetermined time points and analyzed using HPLC-UV system.

5.1.7. Transcorneal permeability studies

Transmembrane permeability of NT from the formulations was evaluated across isolated rabbit cornea (Pel-Freez Biologicals®) using side-by-side diffusion cells. Three milliliters of 0.1% w/v NT-CLBN formulation, or, 1 mL of 5% w/v Natacyn® diluted with 2 mL of phosphate buffered saline (pH 7.4) were used as the donor formulations. Phosphate buffered saline containing 2.5% RMβCD was used as receiver medium (3.2 mL) during the experiment (3 h). Aliquots (0.6 mL) were withdrawn from the receiver side at predetermined time points and immediately replaced with an equal volume of fresh RMβCD solution. Steady state flux, rate and permeability of NT was calculated following sample analysis by HPLC-UV.

5.1.8. Biosample preparation and analysis

In vivo sample analysis was carried out using the HPLC-UV method mentioned above following method validation. Mixture of ice cold methanol and 0.1% formic acid (1 mL) was added to the sample to precipitate proteins and extract the drug from individual, tissues namely cornea, sclera, iris-ciliary (IC) and retina-choroid (RC), after cutting them into small pieces. The samples were centrifuged for 1 h at 13,000 rpm and the supernatant was then collected for further analysis. Aqueous humor (AH) (200 µL), vitreous humor (VH) (500 µL) tissues were precipitated by adding an ice cold mixture of acetonitrile & formic acid; 200 µL for AH and 500 µL for VH in the ratio (1:1). Standard calibration curves constructed from various ocular tissues such as cornea (20-500 ng/mL), sclera (20-500 ng/mL), AH (10-200 ng/mL), VH (10-200 ng/mL), IC (10-200 ng/mL), RPE (10-200 ng/mL) were used to determine the drug concentration in the samples. All the standard curves had a coefficient of determination $r^2 \geq 0.96$. Interference was not observed from the co-eluting proteins during analysis. System configuration was as described for the *in vitro* analysis.

5.1.9. *In vivo* bioavailability studies

In vivo bioavailability of NT was determined in conscious Male New Zealand albino rabbits weighing between (2-2.5 kg), procured from Harlan labs. All the animal studies conformed to University of Mississippi Institutional Animal Care and Use Committee (IACUC) approved protocols and Association for Research in Vision and Ophthalmology (ARVO) guidelines. NT formulations, namely marketed ophthalmic control suspension and CLBN formulation, were evaluated *in vivo* at doses of 5 mg and 100 µg, respectively. These topical formulations (100 µL) were instilled as two application (50 µL each application), at -30 min and 0 min, to reduce pre-corneal loss. At the end of 1 h post application of the second drop (0 min), rabbits were euthanized with an overdose of pentobarbital, injected through a marginal ear vein. The eyes were washed

thoroughly with ice cold DPBS and were immediately enucleated. The intraocular tissues were separated and stored at -80 °C until further analysis using an HPLC-UV system. Ocular disposition of NT from NT CLBN formulation was also evaluated at an additional time point - 2 h post dosing. All experiments were carried out in triplicate.

5.1.10 Statistical analysis

One way ANOVA with Post-hoc test was carried out to analyze the difference between the groups. Statistically significant difference was considered at a level of $p<0.05$.

5.2. Results

5.2.1. Physico-chemical characteristics and *in vitro* release

NT content in the formulations was observed to be in the range of 92-95% of the theoretical value. Mean hydrodynamic radius, zeta potential, polydispersity index & entrapment efficiency of the NT-CLBN were 159.6 ±12.5; 1.24 ± 0.07 mV; 0.28 ± 0.03 and 76.4 ± 2.1 %, respectively. Percentage release of NT from CLBN was observed to be 65 ± 1.14 in 30 minutes, whereas 94.1 ± 1.93 % NT dissolved within 5 minutes from the Natacyn® ophthalmic suspension.

5.2.2. *In vitro* corneal permeability

Transcorneal permeability of NT was enhanced ~ 3-folds from the CLBN formulation when compared to Natacyn® control suspension formulation. The results from these studies suggest that cationic lipid based NT loaded nanoparticles could enhance transmembrane delivery of the drug molecule.

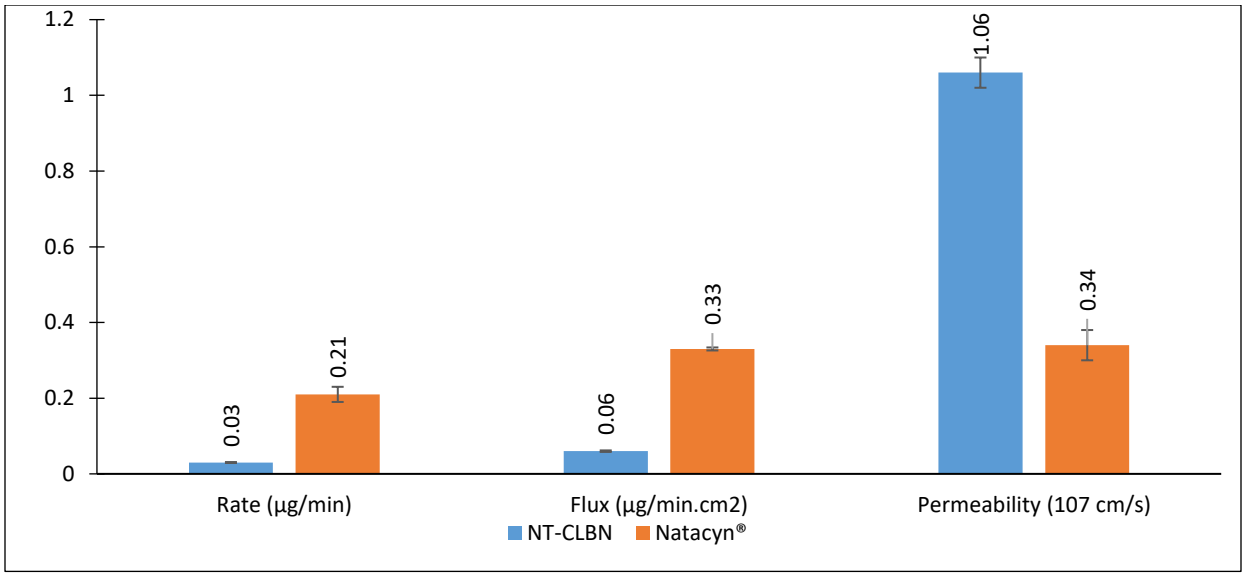

Figure 5.2: Transcorneal permeation characteristics of NT from CLBN (donor 1mg/mL) and Natacyn® (donor 17 mg/mL) suspension across isolated rabbit cornea at 34° C (n=3).

5.2.3. *In vivo* bioavailability studies

The NT suspension formulation produced significantly higher corneal concentrations than the NT CLBN. Interestingly, however, the AH NT concentration achieved with both formulations were similar, even though there was a 50-fold dose difference. Moreover, the NT CLBN was the only formulation that could deliver NT to the retina-choroid. Understandably, NT concentrations at the 2 h time point was significantly lower compared to that at the end of 1h.

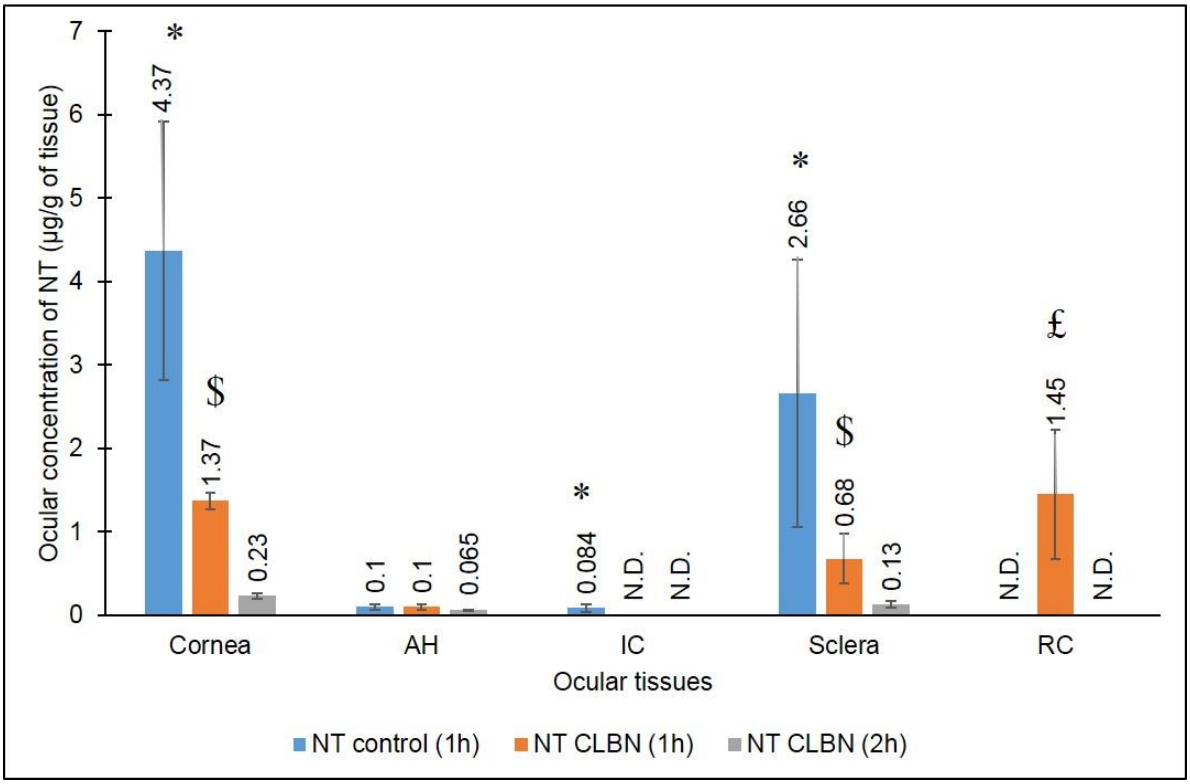

Figure 5.3: Ocular tissue concentrations of NT obtained from marketed control suspension (Dose: 100 µL; 5 mg) and NT CLBN (Dose: 100 µL; 100 µg) 1 & 2 h post topical application in a conscious rabbit model. * symbol represents statistically significant difference of NT control in comparison to all the formulations. $ symbol represents statistically significant difference of NT CLBN 1h compared to NT CLBN 2h. £ symbol represents statistically significant difference of NT CLBN 1h in comparison to all the formulations in RC.

5.3. Discussion

Nanotechnology revolutionized the field of ocular drug delivery by overcoming the limitations of rapid clearance and poor bioavailability into the deeper ocular tissues (177, 178). Nanoparticles owing to their smaller particle sizes may lessen ocular shear force during blinking elimination process, reduce discomfort and improve precorneal residence time thereby reducing the dose and dosing frequency, making them interesting candidates for ocular delivery (179-181). NT is amphipathic molecule with an isoelectric point of 6.5. Bulk of the NT molecule is hydrophobic, whereas carboxyl group and mycosamine moieties are hydrophilic. NT has a molecular weight of 665.73 g/mol and conjugated double bond structure with poor aqueous

solubility, therefore it is formulated as a conventional ophthalmic suspension formulation (181-183). Currently, NT is the only FDA-approved antifungal for the treatment of mycotic or fungal keratitis (MK/FK). The typical frequency of dosing is one drop at hourly or 2 hourly intervals for the first 48 hours depending on the severity of the infection and may be reduced subsequently. The therapy is generally continued for 6 weeks or until resolution of FK (184).

MK is an infection where the drug needs to localized and maintained at the target site for prolonged periods for management of disease condition. Polyene antibiotics with higher dose and dosing frequency may cause corneal irritation and systemic toxicity (due to naso-pharyngeal systemic absorption) with long term usage. Also, poor ocular bioavailability of NT from the marketed formulation could be attributed due to its low corneal permeability (185, 186). NT formulations with lower strength and higher penetrating ability across ocular mucosa would be more beneficial for the anti-fungal therapy. The objective of present study is to develop cationic lipid nanoparticulate delivery system of NT with a low payload and compare it with Natacyn in terms of *in vitro* transcorneal permeability and *in vivo* ocular disposition.

The physico-chemical characteristics of NP namely particle size, zeta potential and encapsulation efficiency play a crucial role in mucoadhesivity, penetration ability, and stability of the formulation (187, 188). The particle size obtained with NT loaded nanoparticles was below 200 nm, which could cross the corneal barrier, as per previously published reports in the literature (189-191). Also, zeta potential was slightly positive indicating that cationic lipid (DDABB) imparted surface charge onto the nanoparticles. Release studies conducted in aqueous media (10 mL) without use of artificial membrane indicate/simulate drug release into the ocular tear fluid. It was observed that lipid nanoparticles prolonged the NT released when compared to suspension in the dissolution medium.

Compared to Natacyn® control, transcorneal permeability of NT was enhanced ~3-folds from the CLBN formulation which could be due to transcytosis/endocytosis mechanisms across ocular epithelial layers. Also, due to the mucoadhesivity of the nanoparticles, lipid systems may prolong the pre-ocular residence of NT, when compared to suspension formulations. The MIC90 values were found to be 1.56 and 3.12 µg/mL for A. fumigatus and C. albicans strains respectively. Marketed suspension formulation was able to deliver ~3 and 4-fold higher concentrations to superficial tissues such as corneal and sclera when compared to NT nanoparticles at 50-fold higher dose 1 h post topical instillation. Lower concentrations were obtained in AH and IC tissues and NT was undetectable in RC with marketed formulation. However, NT lipid formulations delivered drug into RC 1 h post topical application. Cornea and sclera NT levels decreased by ~6 and 5-folds at the end of 2h when compared to 1hr from the lipid formulation. Also, retinal levels of NT were undetectable at the end of 2 h when compared to 1 h from the lipid formulation. NT lipid nanoparticles maintained MIC 90 levels (aspergillus) in the cornea and RC whereas marketed suspension formulation maintained 3, 1.7-folds over above the MIC90 levels in the cornea and sclera at 50-fold higher dose till 1hr time point.

5.4. Conclusion

Ultra-sonication method can be used to fabricate NT loaded cationic SLNs. The nanoparticles exhibited optimal physico-chemical characteristics with lower hydrodynamic radius and higher entrapment efficiency. Cationic lipid based nanoparticles of NT demonstrated better corneal permeability characteristics and higher ocular bioavailability at lower dose when compared to marketed suspension formulation. However, further studies are required to evaluate the clinical efficacy of NT nanoparticles. The results from the studies suggest that NT loaded nanoparticles

are feasible platforms for topical delivery with lower dose and dosing frequency of NT with improved patient compliance.

CHAPTER 6

OCULAR DELIVERY OF RESVERATROL FOR THE TREATMENT OF DIABETIC RETINOPATHY

6. Introduction

Diabetic retinopathy (DR) is the most common diabetic eye disease and a leading cause of blindness in American adults. From 2000 to 2010, the number of cases of DR increased 89%, from 4.06 million to 7.69 million, and is projected to increase to 14.6 million by 2050 (83, 84, 192). Oxidative stress and inflammation play a critical role in the initiation and progression of DR which could lead to progressive loss of vision and blindness if untreated (193, 194). Etiology of DR involves multiple pathological mechanisms. Current treatment strategies of DR involve surgical intervention, laser therapy and direct intravitreal drug administration. These extreme invasive therapies, may cause retinal detachment, conjunctival blebs, cataracts, endophthalmitis and increased intraocular pressure and many severe side effects (195-197). A major shortcoming of the current pharmacological approaches is that no one candidate appears to be capable of reversing/blocking the multifactorial pathology of DR. Multiple reports suggest that phytochemicals, with their antioxidant and anti-inflammatory properties, may have a potential role in the prevention and treatment of DR (198-200). Among the several other phytochemicals there is an increasing interest in the therapeutic effects of resveratrol (RES) on the eye, particularly in terms of intervention of DR (201-206). RES (3,5,41-trihydroxy-trans-stilbene) is a stilbenoid, a type of natural phenol, and a phytoalexin produced naturally by several plants in response to injury or when the plant is under attack by pathogens, such as bacteria or fungi (207). RES is present in abundant concentrations in grape juice, peanuts, mulberries and in other plant extracts (208, 209). The aqueous solubility of RES is reported as 300 µg/mL. RES acts as inverse agonist (cannabinoid ligand) with high nanomolar affinities to CB1 receptors (Ki=45 nM) and micromolar affinities towards CB2 receptors (210, 211). Inverse agonists antagonize the inflammatory properties of endocannabinoids, specifically 2-AG and also elicit neuroprotective action by downregulating

neurodegeneration associated processes (212). Moreover, Retina expresses CB1 and CB2 receptors, through which RES could elicit its activity (213, 214). Retinal protective effects of RES on conditions such as oxygen and antibody-induced retinopathy, retinal neovascularization, hyperglycemia-induced inflammation have recently been reported. Numerous reports demonstrated neuroprotective, anti-inflammatory, anti-oxidant, antiangiogenic, anti-apoptotic and anti-proliferative effects of RES in various pathological animal models and corresponding cell lines (215). RES is also reported to be well tolerated with no associated toxicity and adverse effects in humans following oral or systemic administration (216). Few reports indicated that RES did not exert toxicity on human corneal epithelial cell lines (ATCC-CRL-11515) and human retinal pigmented cell lines (ARPE- 19) even at higher concentrations (100 µM) (217). Furthermore, what makes RES particularly attractive is the fact that it acts on multiple pathways involved in DR.

Minimum Inhibitory (MIC50) and Minimum Effective concentrations (MEC50) of RES, 2.5-6.5 µM (0.72-3.25 µg/mL) are to be maintained in the retina for exertion of the relevant pharmacological activities, which is challenging in terms of delivery angle (218, 219). Lipid nanoparticles (NPs) can prolong pre-ocular residence, impart mucoadhesivity and improve corneal penetration when compared to conventional ocular drug delivery systems. The objective of present study is to formulate, characterize and evaluate the corneal permeability of the lipid nanoparticles loaded with RES.

6.1. Materials and Methods

RES was obtained from Cayman chemical (Ann Arbor, MI). Gelucire lipids (Gelucire® 44/14 and Gelucire® 50/13 was obtained as a gift sample from Gattefossé (Paramus, NJ). Amicon® Ultra centrifugal filter devices with regenerated cellulose membrane (100 kDa), Poloxamer 188, Cremophor® EL, Tween® 80, high performance liquid chromatography (HPLC) -

grade solvents, and other chemicals (analytical grade) were obtained from Fisher Scientific (Hampton, NH). Whole eyes of male albino New Zealand rabbits were obtained from Pel-Freez Biologicals (Rogers, AR).

6.1.1. Saturation solubility studies

Saturation solubility of RES was studied using the standard shake-flask method. An excess amount of RES was added to screw-capped glass vials containing different surfactants namely 1% w/v Tween® 20, Tween® 80, Cremophor® RH 40, Cremophor® EL and Brij® 97. To achieve uniform mixing, samples were stirred at 100 rpm for 24 h at 25°C in a reciprocating water bath (Fisher Scientific). After 24 h, the samples were centrifuged (AccuSpin 17R®), and the supernatant was analyzed for drug content.

6.1.2. *In vitro* chromatographic analysis

Chromatrographic analysis was carried out using HPLC-UV system. The system consists of Waters 717 plus Autosampler, Waters 2487 Dual λ Absorbance detector, Waters 600 controller pump, and Agilent 3395 Integrator. The desired chromatographic separation was achieved on a Pheneomenex C18 column under isocratic elution using UV detection wavelength at 306 nm. The mobile phase consisted of a mixture of methanol: 10 mM potassium dihydrogen phosphate buffer (pH 6.8): acetonitrile (63 : 30 : 7, v/v/v) at a flow rate of 1 mL/min (220).

6.1.3. Preparation of RES loaded SLN

RES (0.7% w/v) was dissolved under stirring in melted lipid phase (Gelucire® 44/14 F-1 or Gelucire® 50/13 F-2 4% w/v). Simultaneously, an aqueous phase consisting of surfactants namely Tween 80 (0.75% w/v), Cremophor EL (1% w/v) and glycerin (2.25% w/v) was heated to 80° C. Then, aqueous phase was added into the lipid phase, dropwise, under heat to form a coarse emulsion. The emulsion was subjected to ultra-turrax at 16000 rpm to form pre-mix. The pre-

emulsion was then ultra-sonicated (40% amplitude; 6 min) to form hot final emulsion. Then the formulation was allowed to cool down to room temperature to form RES SLNs.

6.1.4. RES control formulation

RES control solution was formulated by dissolving RES (0.7% w/v) in the mixture of 2.5% w/v Randomly methylated β-Cyclodextrin (RMβCD), 5% v/v poly (ethylene) glycol 400 and 1% w/v Brij® 97 solution. This RES control solution was used for further studies.

6.1.5. Physico-chemical Characterization

The particle size and the PDI of the RES formulation was determined by using Zetasizer Nano ZS Zen3600 (Malvern Instruments, Inc.) in disposable clear cells. The measurements were obtained using a helium-neon laser of 633 nm, and the particle size analysis data was evaluated using volume distribution. Zeta potential measurements were carried out at 25°C in disposable cells using the same instrument. For measurement of particle size distribution and zeta potential, RES samples were diluted (1:500) with water. Bi-distilled and 0.2 μM filtered water was used for these measurements, and were performed in triplicates.

6.1.6. Assay and Entrapment Efficiency

The lipid in the RES formulation was precipitated using methanol and, RES content in the supernatant after centrifugation (13,000 rpm for 20 min), was measured using an HPLC system following appropriate dilution.

The percentage of RES entrapped (% EE) in nanoparticles was determined by measuring the concentration of free drug in the aqueous phase of an undiluted formulation. The EE was evaluated by an ultrafiltration technique with a 100 kDa centrifugal filter device (Amicon Ultra). An aliquot (500 μL) of the corresponding formulation was added to the sample reservoir and

centrifuged at 5,000 rpm for 10 min. The filtrate was and analyzed for drug content using HPLC. The %EE was calculated using Eq. (1) below. All the measurements were carried out in triplicates.

$$\%EE=[(Wi-Wf)/Wi]\times 100$$

Where Wi =total drug content, and Wf =amount of free drug in aqueous phase.

6.1.7. *In vitro* release and transcorneal permeability studies

RES release kinetics was studied through Spectra/Por® dialysis membrane (MWCO: 3.5 kDa) at 34°C using Valia-Chien cells. Formulations, RES loaded SLNs (F-1 and F-2) and RES control solution, were evaluated for *in vitro* release upto 6 h. Spectra/por® membrane is mounted onto diffusion cells and fastened with airtight clamps. 500 µL (0.7%w/v) of formulation was added into the donor chamber. Five milliliters of 2.5% w/v RMβCD in IPBS pH 7.4 was used as media in the receiver chamber. Samples were taken at predetermined time points and analyzed using HPLC-UV system.

Transcorneal permeability of RES formulations was determined across isolated rabbit cornea using valia-chien cells (3 h). Ocular globes were shipped overnight and used for isolating cornea. The corneal membrane was excised with some scleral portion to help secure the membrane onto the diffusion cells and fastened between donor/receiver compartments with air tight clamps. Five hundred microliters of 0.7% w/v RES SLNs and control solution were added into donor chamber. Receiver chamber consisted of 2.5% w/v RMβCD in IPBS (5 mL). The samples were taken at predetermined time points and analyzed using HPLC-UV system.

6.2. Results

6.2.1. Physico-chemical characterization

RES SLNs exhibited lower hydrodynamic radius and higher entrapment efficiencies at a drug load of 0.7% w/v. Particle size and PDI of two RES formulations did not show any significant

difference. However, zeta potential and entrapment efficiency of F-2 formulation was marginally higher when compared to F-1 formulation. The physico-chemical characteristics of SLN formulations are presented below.

Table 6.1: Physico-chemical characteristics of RES loaded SLN formulations

Characteristics	RES-SLN F-1	RES-SLN F-2
Particle size (nm)	120 ± 12.3	131 ± 9.6
PDI	0.23 ± 0.02	0.26 ± 0.04
Zeta potential (mV)	-0.6 ± 0.01	-6.5 ± 0.05
EE (%)	87.4 ± 1.6	90.2 ± 3.8
Assay (%)	91-95	92-96

6.2.2. Saturation solubility studies

RES exhibited lower solubility in Tween 80® and predominantly higher solubility in Cremophor EL® and Brij 97® compared to other solvents. Solubility profile of RES is presented in figure 1.

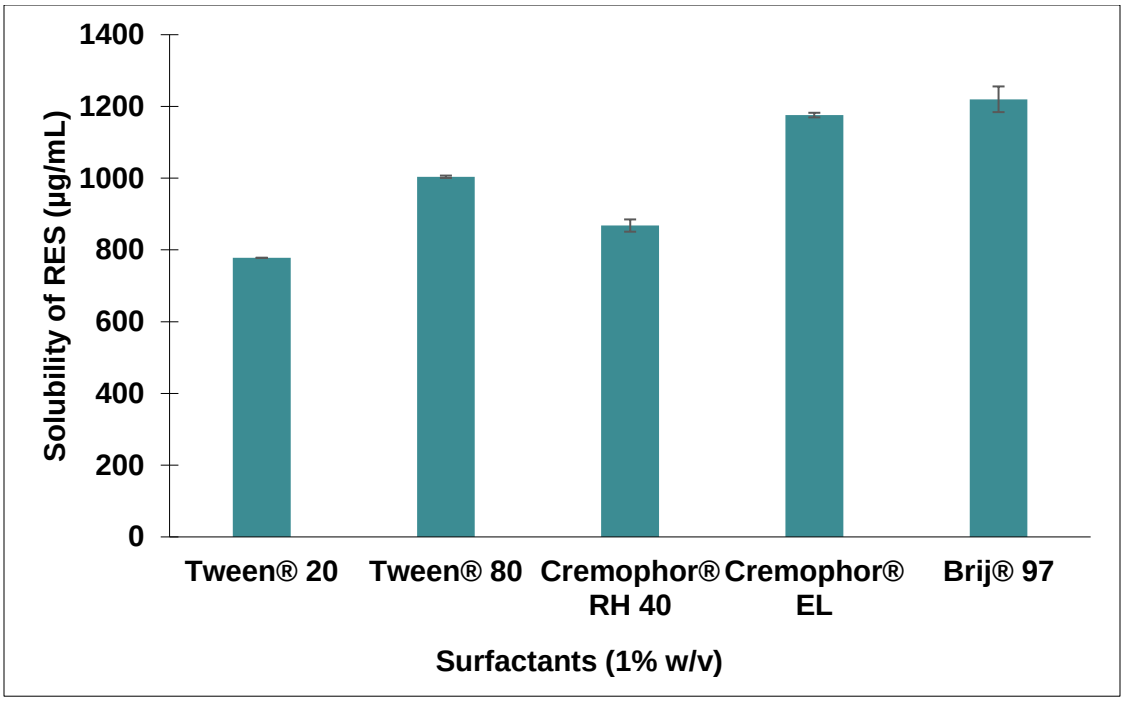

Figure 6.1: Saturation solubility of RES (µg/mL) obtained from various surfactants (1% w/v).

6.2.3. *In vitro* release and transcorneal permeability studies

Percentage release of RES SLNs was lower when compared to control formulation, due to the slow degradation of carrier matrix. Transcorneal flux of RES, however, was increased to ~ 1.5-folds with SLN formulation, when compared to control formulation. Transcorneal permeability of the two RES loaded SLN formulations was not significantly different from each other under comparison. *In vitro* release and transcorneal permeability of RES from the formulations is presented in figures 6.2 and 6.3 respectively.

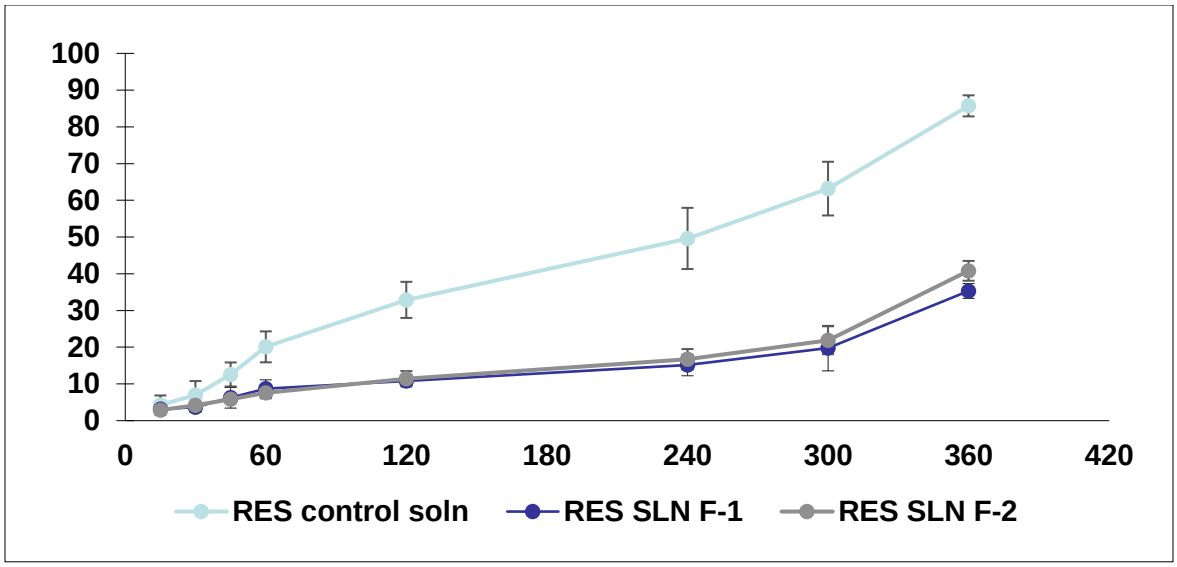

Figure 6.2: *In vitro* release of RES from the topical ocular formulations and diffusion across Spectra/Por® membrane (MWCO 3.5kDa) at 34°C obtained using Valia-chien cells.

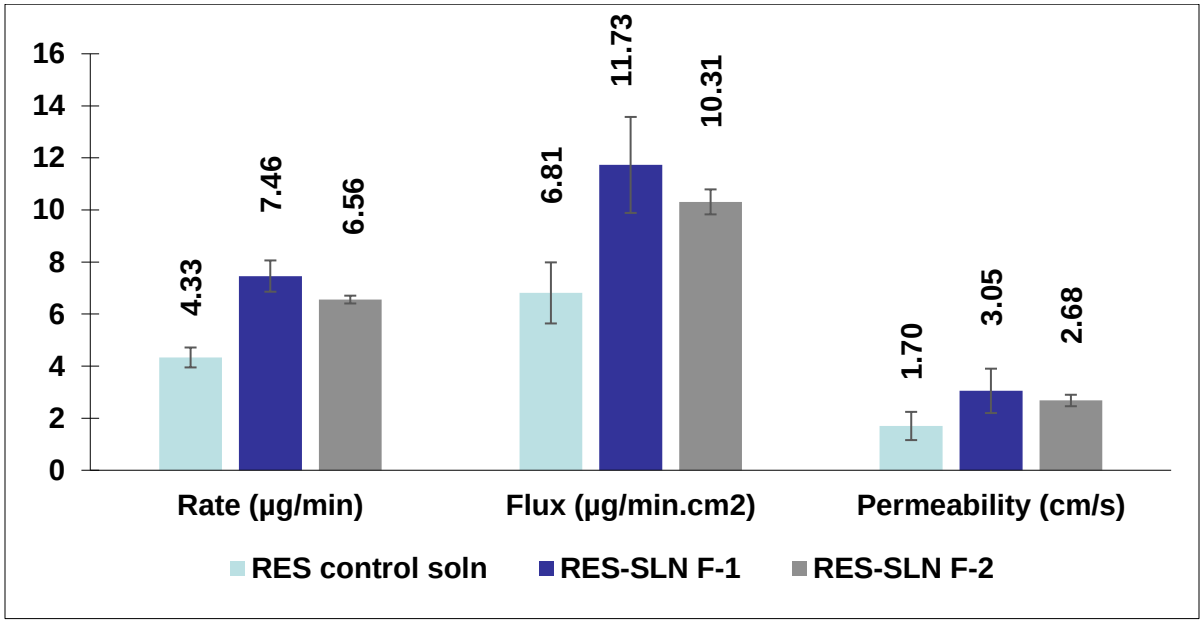

Figure 6.3: *In vitro* transcorneal permeability of RES from the topical ocular formulations obtained using Valia-chien cells at 34°C.

6.3. Discussion

The objective of the present study was to formulate and characterize the RES loaded lipid nanoparticulate formulations. Topical, non-invasive colloidal carriers are designed to act as a drug reservoir to modulate/tailor the drug release from the lipid core, and are endocytosed by the corneal

epithelial cells. These carriers change the tear dynamics by decreasing tear washout/drainage and sustain the release of drugs on the ocular surface into inner barriers (221). Lipid based nanoparticle systems are particulates in the size range of 50-1000 nm whose matrix is made of biocompatible solid lipids or their appropriate mixtures which are generally recognized as safe (GRAS) excipients (222). Solid lipid nanoparticles (SLN) are considered to be among the most effective lipid-based colloidal vehicles. They are constituted of a solid lipid matrix surrounded by a layer of surfactants in an aqueous dispersion. Hot high-pressure homogenization, melt-emulsification, and ultrasonication methods are generally used to fabricate the lipid nanoparticle formulations

SLNs are reported to increase the mucoadhesion and prolong pre-ocular residence when compared to solution/suspension formulations. The particle size of nanoparticles play an important role in the penetration across ocular mucosa (223, 224). Nanoparticles with size ranging between 50-400 nm are better tolerated than larger ones, because of their ability to penetrate across the corneal and conjunctival barriers (225). Nanoparticles with particle size (<20 nm) are cleared by blood and lymphatic system without achieving any ocular effect (226). The polymeric NP system showed slow and prolonged *in vitro* release of the RES when compared to control formulation. The release was slow because of the lower degradation and corrosion rate of Gelucire lipids. The release of RES from the control formulation was higher indicating that solution formulation could overcome the barrier resistance. Better corneal permeation characteristics for targeting intraocular diseases such as DR is highly desirable (227). Cornea is a major and formidable barrier to the penetration of small molecules into the inner/deeper ocular tissues. SLNs are made up of bio-compatible and bio-degradable lipids which are generally recognized as safe (GRAS). In the corneal permeation study, higher amount of RES penetrated across the excised rabbit cornea from the Gelucire® lipid nanoparticulate formulations compared to control formulation. Transmembrane

flux of RES was enhanced ~1.5 folds from the lipid formulations when compared to control solution. Reports suggest that lipid nanoparticles can cross the ocular barriers by endocytosis/transcytosis mechanisms. The higher order of permeation was observed due to permeation enhancement characteristics of lipid nanoparticles with their inherent mucoadhesive properties.

6.4. Conclusion

RES loaded SLNs are successfully prepared by ultra-sonication method. The physico-chemical characteristics such as lower hydrodynamic radius and higher entrapment efficiencies are achieved for lipid formulations at a higher drug load 0.7% w/v. From the in vitro study, RES was released from the lipid nanoparticles in a slow and sustained manner than the RES control formulation possibly due to the slow degradation of carrier matrix. Ex vivo corneal permeation study demonstrated that the RES-loaded nanoparticles are more permeable than the control formulation. These results suggest that RES loaded lipid systems are viable carriers for topical ocular delivery.

BIBLIOGRAPHY

1. Gaudana R, Ananthula HK, Parenky A, Mitra AK. Ocular drug delivery. AAPS J. 2010;12(3):348-60.
2. Urtti A. Challenges and obstacles of ocular pharmacokinetics and drug delivery. Advanced drug delivery reviews. 2006;58(11):1131-5.
3. Maurice DM. The dynamics and drainage of tears. International ophthalmology clinics. 1973;13(1):103-18.
4. Mishima S, Gasset A, Klyce S, Baum J. Determination of tear volume and tear flow. Investigative Ophthalmology & Visual Science. 1966;5(3):264-76.
5. Ralph RA. Tetracyclines and the treatment of corneal stromal ulceration: a review. Cornea. 2000;19(3):274-7.
6. Ayaki M, Yaguchi S, Iwasawa A, Koide R. Cytotoxicity of ophthalmic solutions with and without preservatives to human corneal endothelial cells, epithelial cells and conjunctival epithelial cells. Clinical & experimental ophthalmology. 2008;36(6):553-9.
7. Hämäläinen KM, Kontturi K, Auriola S, Murtomäki L, Urtti A. Estimation of pore size and pore density of biomembranes from permeability measurements of polyethylene glycols using an effusion-like approach. Journal of controlled release. 1997;49(2):97-104.
8. Freddo TF. Shifting the paradigm of the blood–aqueous barrier. Experimental eye research. 2001;73(5):581-92.
9. Sasaki H, Yamamura K, Nishida K, Nakamura J, Ichikawa M. Delivery of drugs to the eye by topical application. Progress in Retinal and Eye Research. 1996;15(2):583-620.
10. Bansil R, Turner BS. Mucin structure, aggregation, physiological functions and biomedical applications. Current Opinion in Colloid & Interface Science. 2006;11(2):164-70.
11. Ambati J, Adamis AP. Transscleral drug delivery to the retina and choroid. Progress in retinal and eye research. 2002;21(2):145-51.
12. Cenedella RJ, Fleschner CR. Kinetics of corneal epithelium turnover in vivo. Studies of lovastatin. Investigative ophthalmology & visual science. 1990;31(10):1957-62.
13. Lee VH-L, Robinson JR. Preliminary examination of rabbit conjunctival mucins. Journal of pharmaceutical sciences. 1980;69(4):430-8.
14. Hosoya K-i, Lee VH, Kim K-J. Roles of the conjunctiva in ocular drug delivery: a review of conjunctival transport mechanisms and their regulation. European journal of pharmaceutics and biopharmaceutics. 2005;60(2):227-40.
15. Ashton P, Podder SK, Lee VH. Formulation influence on conjunctival penetration of four beta blockers in the pigmented rabbit: a comparison with corneal penetration. Pharmaceutical research. 1991;8(9):1166-74.
16. Occhiutto ML, Freitas FR, Maranhao RC, Costa VP. Breakdown of the Blood-Ocular Barrier as a Strategy for the Systemic Use of Nanosystems. Pharmaceutics. 2012;4(2):252-75.
17. Chen M-S, Hou P-K, Tai T-Y, Lin BJ. Blood-ocular barriers. Tzu Chi Medical Journal. 2008;20(1):25-34.
18. Smith R, Rudt L. Ocular vascular and epithelial barriers to microperoxidase. Investigative Ophthalmology & Visual Science. 1975;14(7):556-60.
19. Cunha-Vaz JG. The blood-ocular barriers: past, present, and future. Documenta ophthalmologica. 1997;93(1-2):149-57.
20. Raghava S, Hammond M, Kompella UB. Periocular routes for retinal drug delivery. Expert opinion on drug delivery. 2004;1(1):99-114.
21. Bishop PN. Structural macromolecules and supramolecular organisation of the vitreous gel. Progress in retinal and eye research. 2000;19(3):323-44.

22. De Smet PA, Denneboom W, Kramers C, Grol R. A composite screening tool for medication reviews of outpatients. Drugs & aging. 2007;24(9):733-60.
23. Hughes PM, Olejnik O, Chang-Lin J-E, Wilson CG. Topical and systemic drug delivery to the posterior segments. Advanced Drug Delivery Reviews. 2005;57(14):2010-32.
24. Wilkinson-Berka JL. Vasoactive factors and diabetic retinopathy: vascular endothelial growth factor, cycoloxygenase-2 and nitric oxide. Curr Pharm Des. 2004;10(27):3331-48.
25. Ryan CM, Klein BE, Lee KE, Cruickshanks KJ, Klein R. Associations between recent severe hypoglycemia, retinal vessel diameters, and cognition in adults with type 1 diabetes. J Diabetes Complications. 2016.
26. Wilkinson-Berka JL. Vasoactive factors and diabetic retinopathy: vascular endothelial growth factor, cycoloxygenase-2 and nitric oxide. Current pharmaceutical design. 2004;10(27):3331-48.
27. Gardner TW, Antonetti DA, Barber AJ, Lanoue KF, Nakamura M. Review Paper: New Insights into the Pathophysiology of Diabetic Retinopathy: Potential Cell-Specific Therapeutic Targets. Diabetes technology & therapeutics. 2000;2(4):601-8.
28. Kempen JH, O'colmain B, Leske M, Haffner S, Klein R, Moss S, et al. The prevalence of diabetic retinopathy among adults in the United States. Archives of ophthalmology (Chicago, Ill: 1960). 2004;122(4):552-63.
29. Buschini E, Piras A, Nuzzi R, Vercelli A. Age related macular degeneration and drusen: neuroinflammation in the retina. Progress in neurobiology. 2011;95(1):14-25.
30. Khandhadia S, Lotery A. Oxidation and age-related macular degeneration: insights from molecular biology. Expert reviews in molecular medicine. 2010;12:e34.
31. Ding X, Patel M, Chan C-C. Molecular pathology of age-related macular degeneration. Progress in retinal and eye research. 2009;28(1):1-18.
32. Olofsson EM, Marklund SL, Behndig A. Enhanced diabetes-induced cataract in copper-zinc superoxide dismutase–null mice. Investigative ophthalmology & visual science. 2009;50(6):2913-8.
33. Ali M, Byrne ME. Challenges and solutions in topical ocular drug-delivery systems. Expert Rev Clin Pharmacol. 2008;1(1):145-61.
34. Toker MI, Erdem H, Erdogan H, Arici MK, Topalkara A, Arslan OS, et al. The effects of topical ketorolac and indomethacin on measles conjunctivitis: randomized controlled trial. Am J Ophthalmol. 2006;141(5):902-5.
35. Allegri P, Murialdo U, Peri S, Carniglia R, Crivelli MG, Compiano S, et al. Randomized, double-blind, placebo-controlled clinical trial on the efficacy of 0.5% indomethacin eye drops in uveitic macular edema. Invest Ophthalmol Vis Sci. 2014;55(3):1463-70.
36. Weber M, Kodjikian L, Kruse FE, Zagorski Z, Allaire CM. Efficacy and safety of indomethacin 0.1% eye drops compared with ketorolac 0.5% eye drops in the management of ocular inflammation after cataract surgery. Acta Ophthalmol. 2013;91(1):e15-21.
37. Botting RM. Inhibitors of cyclooxygenases: mechanisms, selectivity and uses. J Physiol Pharmacol. 2006;57 Suppl 5:113-24.
38. Russo A, Costagliola C, Delcassi L, Parmeggiani F, Romano MR, Dell'Omo R, et al. Topical nonsteroidal anti-inflammatory drugs for macular edema. Mediators Inflamm. 2013;2013:476525.
39. Kern TS, Miller CM, Du Y, Zheng L, Mohr S, Ball SL, et al. Topical administration of nepafenac inhibits diabetes-induced retinal microvascular disease and underlying abnormalities of retinal metabolism and physiology. Diabetes. 2007;56(2):373-9.
40. Chetoni P, Panichi L, Burgalassi S, Benelli U, Saettone MF. Pharmacokinetics and anti-inflammatory activity in rabbits of a novel indomethacin ophthalmic solution. J Ocul Pharmacol Ther. 2000;16(4):363-72.
41. Kahanne LI, Bogi J, Farkas A, Tudos FH, Imre G. [Indosol--a nonsteroidal anti-inflammatory drug with therapeutic efficacy]. Acta Pharm Hung. 1994;64(4):125-9.

42. Hippalgaonkar K, Adelli GR, Hippalgaonkar K, Repka MA, Majumdar S. Indomethacin-loaded solid lipid nanoparticles for ocular delivery: development, characterization, and in vitro evaluation. J Ocul Pharmacol Ther. 2013;29(2):216-28.
43. Morrison PW, Khutoryanskiy VV. Advances in ophthalmic drug delivery. Ther Deliv. 2014;5(12):1297-315.
44. Sultana Y, Jain R, Aqil M, Ali A. Review of ocular drug delivery. Curr Drug Deliv. 2006;3(2):207-17.
45. Murugan K, Choonara YE, Kumar P, Bijukumar D, du Toit LC, Pillay V. Parameters and characteristics governing cellular internalization and trans-barrier trafficking of nanostructures. Int J Nanomedicine. 2015;10:2191-206.
46. Liu D, Li J, Pan H, He F, Liu Z, Wu Q, et al. Potential advantages of a novel chitosan-N-acetylcysteine surface modified nanostructured lipid carrier on the performance of ophthalmic delivery of curcumin. Sci Rep. 2016;6:28796.
47. Mainardes RM, Urban MC, Cinto PO, Khalil NM, Chaud MV, Evangelista RC, et al. Colloidal carriers for ophthalmic drug delivery. Curr Drug Targets. 2005;6(3):363-71.
48. Khare A, Grover K, Pawar P, Singh I. Mucoadhesive Polymers for Enhancing Retention in Ocular Drug Delivery. Progress in Adhesion and Adhesives: John Wiley & Sons, Inc.; 2015. p. 451-84.
49. Ranaldi G, Marigliano I, Vespignani I, Perozzi G, Sambuy Y. The effect of chitosan and other polycations on tight junction permeability in the human intestinal Caco-2 cell line(1). J Nutr Biochem. 2002;13(3):157-67.
50. Caramella C, Ferrari F, Bonferoni MC, Rossi S, Sandri G. Chitosan and its derivatives as drug penetration enhancers. Journal of Drug Delivery Science and Technology. 2010;20(1):5-13.
51. Bonferoni MC, Sandri G, Rossi S, Ferrari F, Caramella C. Chitosan and its salts for mucosal and transmucosal delivery. Expert Opin Drug Deliv. 2009;6(9):923-39.
52. Uner M, Yener G. Importance of solid lipid nanoparticles (SLN) in various administration routes and future perspectives. Int J Nanomedicine. 2007;2(3):289-300.
53. Liu R, Liu Z, Zhang C, Zhang B. Nanostructured lipid carriers as novel ophthalmic delivery system for mangiferin: improving in vivo ocular bioavailability. J Pharm Sci. 2012;101(10):3833-44.
54. Ahuja M, Dhake AS, Majumdar DK. Effect of formulation factors on in-vitro permeation of diclofenac from experimental and marketed aqueous eye drops through excised goat cornea. Yakugaku Zasshi. 2006;126(12):1369-75.
55. Ahuja M, Dhake AS, Sharma SK, Majumdar DK. Topical ocular delivery of NSAIDs. AAPS J. 2008;10(2):229-41.
56. Kim SJ, Schoenberger SD, Thorne JE, Ehlers JP, Yeh S, Bakri SJ. Topical Nonsteroidal Anti-inflammatory Drugs and Cataract Surgery: A Report by the American Academy of Ophthalmology. Ophthalmology. 2015;122(11):2159-68.
57. Tres F, Treacher K, Booth J, Hughes LP, Wren SA, Aylott JW, et al. Indomethacin-Kollidon VA64 Extrudates: A Mechanistic Study of pH-Dependent Controlled Release. Mol Pharm. 2016;13(3):1166-75.
58. Bahl D, Bogner RH. Amorphization alone does not account for the enhancement of solubility of drug co-ground with silicate: the case of indomethacin. AAPS PharmSciTech. 2008;9(1):146-53.
59. McMillan J, Batrakova E, Gendelman HE. Cell delivery of therapeutic nanoparticles. Prog Mol Biol Transl Sci. 2011;104:563-601.
60. Almeida H, Amaral MH, Lobao P, Frigerio C, Sousa Lobo JM. Nanoparticles in Ocular Drug Delivery Systems for Topical Administration: Promises and Challenges. Curr Pharm Des. 2015;21(36):5212-24.
61. Battaglia L, Serpe L, Foglietta F, Muntoni E, Gallarate M, Del Pozo Rodriguez A, et al. Application of lipid nanoparticles to ocular drug delivery. Expert Opin Drug Deliv. 2016:1-15.
62. Chime SA, Onyishi IV. Lipid-based drug delivery systems (LDDS): Recent advances and applications of lipids in drug delivery. African Journal of Pharmacy and Pharmacology. 2013;7(48):3034-59.

63. Uner M. Preparation, characterization and physico-chemical properties of solid lipid nanoparticles (SLN) and nanostructured lipid carriers (NLC): their benefits as colloidal drug carrier systems. Pharmazie. 2006;61(5):375-86.
64. De Campos AM, Sanchez A, Gref R, Calvo P, Alonso MJ. The effect of a PEG versus a chitosan coating on the interaction of drug colloidal carriers with the ocular mucosa. Eur J Pharm Sci. 2003;20(1):73-81.
65. de la Fuente M, Seijo B, Alonso MJ. Novel hyaluronic acid-chitosan nanoparticles for ocular gene therapy. Invest Ophthalmol Vis Sci. 2008;49(5):2016-24.
66. Vllasaliu D, Exposito-Harris R, Heras A, Casettari L, Garnett M, Illum L, et al. Tight junction modulation by chitosan nanoparticles: comparison with chitosan solution. Int J Pharm. 2010;400(1-2):183-93.
67. de Campos AM, Diebold Y, Carvalho EL, Sanchez A, Alonso MJ. Chitosan nanoparticles as new ocular drug delivery systems: in vitro stability, in vivo fate, and cellular toxicity. Pharm Res. 2004;21(5):803-10.
68. Gukasyan JH, Kim K-J, Lee HLV. The Conjunctival Barrier in Ocular Drug Delivery. In: Ehrhardt C, Kim K-J, editors. Drug Absorption Studies: In Situ, In Vitro and In Silico Models. Boston, MA: Springer US; 2008. p. 307-20.
69. He J, Hou S, Lu W, Zhu L, Feng J. Preparation, Pharmacokinetics and Body Distribution of Silymarin-Loaded Solid Lipid Nanoparticles After Oral Administration. Journal of Biomedical Nanotechnology. 2007;3(2):195-202.
70. Manjunath K, Venkateswarlu V. Pharmacokinetics, tissue distribution and bioavailability of nitrendipine solid lipid nanoparticles after intravenous and intraduodenal administration. J Drug Target. 2006;14(9):632-45.
71. Mei D, Mao S, Sun W, Wang Y, Kissel T. Effect of chitosan structure properties and molecular weight on the intranasal absorption of tetramethylpyrazine phosphate in rats. Eur J Pharm Biopharm. 2008;70(3):874-81.
72. Verheul RJ, Amidi M, van Steenbergen MJ, van Riet E, Jiskoot W, Hennink WE. Influence of the degree of acetylation on the enzymatic degradation and in vitro biological properties of trimethylated chitosans. Biomaterials. 2009;30(18):3129-35.
73. Dale O, Nilsen T, Olaussen G, Tvedt KE, Skorpen F, Smidsrod O, et al. Transepithelial transport of morphine and mannitol in Caco-2 cells: the influence of chitosans of different molecular weights and degrees of acetylation. J Pharm Pharmacol. 2006;58(7):909-15.
74. Al-Halafi AM. Nanocarriers of nanotechnology in retinal diseases. Saudi J Ophthalmol. 2014;28(4):304-9.
75. Barar J, Asadi M, Mortazavi-Tabatabaei SA, Omidi Y. Ocular Drug Delivery; Impact of in vitro Cell Culture Models. J Ophthalmic Vis Res. 2009;4(4):238-52.
76. Thassu D, Chader GJ. Ocular drug delivery systems: barriers and application of nanoparticulate systems: CRC Press; 2012.
77. Liu CH, Chiu HC, Wu WC, Sahoo SL, Hsu CY. Novel lutein loaded lipid nanoparticles on porcine corneal distribution. J Ophthalmol. 2014;2014:304694.
78. Castelli F, Puglia C, Sarpietro MG, Rizza L, Bonina F. Characterization of indomethacin-loaded lipid nanoparticles by differential scanning calorimetry. International Journal of Pharmaceutics. 2005;304(1–2):231-8.
79. Bucolo C, Melilli B, Piazza C, Zurria M, Drago F. Ocular pharmacokinetics profile of different indomethacin topical formulations. J Ocul Pharmacol Ther. 2011;27(6):571-6.
80. Klang S, Abdulrazik M, Benita S. Influence of emulsion droplet surface charge on indomethacin ocular tissue distribution. Pharm Dev Technol. 2000;5(4):521-32.

81. Yamaguchi M, Ueda K, Isowaki A, Ohtori A, Takeuchi H, Ohguro N, et al. Mucoadhesive properties of chitosan-coated ophthalmic lipid emulsion containing indomethacin in tear fluid. Biol Pharm Bull. 2009;32(7):1266-71.
82. Adelli GR, Balguri SP, Majumdar S. Effect of Cyclodextrins on Morphology and Barrier Characteristics of Isolated Rabbit Corneas. AAPS PharmSciTech. 2015;16(5):1220-6.
83. Cholkar K, Patel SP, Vadlapudi AD, Mitra AK. Novel strategies for anterior segment ocular drug delivery. J Ocul Pharmacol Ther. 2013;29(2):106-23.
84. Chen P, Chen H, Zang X, Chen M, Jiang H, Han S, et al. Expression of efflux transporters in human ocular tissues. Drug Metab Dispos. 2013;41(11):1934-48.
85. Patel A, Cholkar K, Agrahari V, Mitra AK. Ocular drug delivery systems: An overview. World J Pharmacol. 2013;2(2):47-64.
86. Yellepeddi VK, Palakurthi S. Recent Advances in Topical Ocular Drug Delivery. J Ocul Pharmacol Ther. 2016;32(2):67-82.
87. Geroski DH, Edelhauser HF. Drug Delivery for Posterior Segment Eye Disease. Invest Ophthalmol Vis Sci. 2000;41(5):961-4.
88. Adelli GR, Balguri SP, Bhagav P, Raman V, Majumdar S. Diclofenac sodium ion exchange resin complex loaded melt cast films for sustained release ocular delivery. Drug Deliv. 2017;24(1):370-9.
89. Sharma PK SP, Jaswanth A, Chalamaiah M, Tekade KR and Balasubramaniam A. Novel Encapsulation of Lycopene in Niosomes and Assessment of its Anticancer Activity. Journal of Bioequivalence & Bioavailability. 2016;8(5):224-32.
90. Singh VK, Singh PK, Sharma PK, Srivastava PK, Mishra A. Formulation and evaluation of topical gel of acelofenac containing piparine. Indo-American Journal of Pharmaceutical Research. 2013;3(7):5268.
91. Rowe-Rendleman CL, Durazo SA, Kompella UB, Rittenhouse KD, Di Polo A, Weiner AL, et al. Drug and gene delivery to the back of the eye: from bench to bedside. Invest Ophthalmol Vis Sci. 2014;55(4):2714-30.
92. Barar J, Aghanejad A, Fathi M, Omidi Y. Advanced drug delivery and targeting technologies for the ocular diseases. Bioimpacts. 2016;6(1):49-67.
93. Adelli GR, Balguri SP, Punyamurthula N, Bhagav P, Majumdar S. Development and evaluation of prolonged release topical indomethacin formulations for ocular inflammation. Invest Ophthalmol Vis Sci. 2014;55(13):463-.
94. Maeda H, Bharate GY, Daruwalla J. Polymeric drugs for efficient tumor-targeted drug delivery based on EPR-effect. Eur J Pharm Biopharm. 2009;71(3):409-19.
95. Barenholz Y. Doxil® — The first FDA-approved nano-drug: Lessons learned. J Control Release. 2012;160(2):117-34.
96. Kompella UB, Amrite AC, Pacha Ravi R, Durazo SA. Nanomedicines for back of the eye drug delivery, gene delivery, and imaging. Prog Retin Eye Res. 2013;36:172-98.
97. Yoon G, Park JW, Yoon I-S. Solid lipid nanoparticles (SLNs) and nanostructured lipid carriers (NLCs): recent advances in drug delivery. Journal of Pharmaceutical Investigation. 2013;43(5):353-62.
98. Müller RH, Radtke M, Wissing SA. Solid lipid nanoparticles (SLN) and nanostructured lipid carriers (NLC) in cosmetic and dermatological preparations. Adv Drug Deliv Rev. 2002;54, Supplement:S131-S55.
99. Tiwari R, Pathak K. Nanostructured lipid carrier versus solid lipid nanoparticles of simvastatin: comparative analysis of characteristics, pharmacokinetics and tissue uptake. Int J Pharm. 2011;415(1-2):232-43.
100. Chen Y, Ma P, Gui S. Cubic and hexagonal liquid crystals as drug delivery systems. Biomed Res Int. 2014;2014:815981.
101. Balguri SP, Adelli G, Bhagav P, Repka MA, Majumdar S. Development of nano structured lipid carriers of ciprofloxacin for ocular delivery: Characterization, in vivo distribution and effect of PEGylation. Invest Ophthalmol Vis Sci. 2015;56(7):2269-.

102. Zheng J, Wan Y, Elhissi A, Zhang Z, Sun X. Targeted paclitaxel delivery to tumors using cleavable PEG-conjugated solid lipid nanoparticles. Pharm Res. 2014;31(8):2220-33.
103. Schilt Y, Berman T, Wei X, Barenholz Y, Raviv U. Using solution X-ray scattering to determine the high-resolution structure and morphology of PEGylated liposomal doxorubicin nanodrugs. Biochim Biophys Acta. 2016;1860(1 Pt A):108-19.
104. Kakkar S, Karuppayil SM, Raut JS, Giansanti F, Papucci L, Schiavone N, et al. Lipid-polyethylene glycol based nano-ocular formulation of ketoconazole. Int J Pharm. 2015;495(1):276-89.
105. Balguri SP, Adelli GR, Majumdar S. Topical ophthalmic lipid nanoparticle formulations (SLN, NLC) of indomethacin for delivery to the posterior segment ocular tissues. Eur J Pharm Biopharm. 2016;109:224-35.
106. Hosny KM. Ciprofloxacin as ocular liposomal hydrogel. AAPS PharmSciTech. 2010;11(1):241-6.
107. Hussain AH, Muhammad; Shoaib, Muhammad Harris; Yousuf, Rabia Ismail; Shafi, Nigha. Bioanalytical method development and validation of ciprofloxacin by RP-HPLC method. Asian Journal of Pharmaceutical & Biological Research October 2012;Vol. 2 (Issue 4):p219.
108. Guidance for Industry: Bioanalytical Method Validation 2013 [Available from: https://www.fda.gov/downloads/Drugs/Guidances/ucm368107.pdf.
109. Lizunova A, Loshkarev A, Tokunov YM, Ivanov V. Comparison of the Results of Measurements of the Sizes of Nanoparticles in Stable Colloidal Solutions by the Methods of Acoustic Spectroscopy, Dynamic Light Scattering, and Transmission Electron Microscopy. Measurement Techniques. 2017:1-5.
110. Anderson W, Kozak D, Coleman VA, Jämting ÅK, Trau M. A comparative study of submicron particle sizing platforms: accuracy, precision and resolution analysis of polydisperse particle size distributions. Journal of colloid and interface science. 2013;405:322-30.
111. Tuoriniemi J, Johnsson A-CJ, Holmberg JP, Gustafsson S, Gallego-Urrea JA, Olsson E, et al. Intermethod comparison of the particle size distributions of colloidal silica nanoparticles. Science and Technology of Advanced Materials. 2014;15(3):035009.
112. Morlet N, Graham GG, Gatus B, McLachlan AJ, Salonikas C, Naidoo D, et al. Pharmacokinetics of ciprofloxacin in the human eye: a clinical study and population pharmacokinetic analysis. Antimicrobial agents and chemotherapy. 2000;44(6):1674-9.
113. Lim SB, Banerjee A, Onyuksel H. Improvement of drug safety by the use of lipid-based nanocarriers. J Control Release. 2012;163(1):34-45.
114. Martins S, Sarmento B, Ferreira DC, Souto EB. Lipid-based colloidal carriers for peptide and protein delivery--liposomes versus lipid nanoparticles. Int J Nanomedicine. 2007;2(4):595-607.
115. Kulkarni SA, Feng SS. Effects of particle size and surface modification on cellular uptake and biodistribution of polymeric nanoparticles for drug delivery. Pharm Res. 2013;30(10):2512-22.
116. He C, Hu Y, Yin L, Tang C, Yin C. Effects of particle size and surface charge on cellular uptake and biodistribution of polymeric nanoparticles. Biomaterials. 2010;31(13):3657-66.
117. Kou L, Sun J, Zhai Y, He Z. The endocytosis and intracellular fate of nanomedicines: Implication for rational design. Asian Journal of Pharmaceutical Sciences. 2013;8(1):1-10.
118. Qaddoumi MG, Ueda H, Yang J, Davda J, Labhasetwar V, Lee VHL. The Characteristics and Mechanisms of Uptake of PLGA Nanoparticles in Rabbit Conjunctival Epithelial Cell Layers. Pharm Res. 2004;21(4):641-8.
119. Contreras-Ruiz L, de la Fuente M, Parraga JE, Lopez-Garcia A, Fernandez I, Seijo B, et al. Intracellular trafficking of hyaluronic acid-chitosan oligomer-based nanoparticles in cultured human ocular surface cells. Mol Vis. 2011;17:279-90.
120. Tosi G, Vergoni AV, Ruozi B, Bondioli L, Badiali L, Rivasi F, et al. Sialic acid and glycopeptides conjugated PLGA nanoparticles for central nervous system targeting: In vivo pharmacological evidence and biodistribution. J Control Release. 2010;145(1):49-57.

121. Vergoni AV, Tosi G, Tacchi R, Vandelli MA, Bertolini A, Costantino L. Nanoparticles as drug delivery agents specific for CNS: in vivo biodistribution. Nanomedicine. 2009;5(4):369-77.
122. De Campos AM, Sánchez A, Gref R, Calvo P, Alonso M, amp, et al. The effect of a PEG versus a chitosan coating on the interaction of drug colloidal carriers with the ocular mucosa. Eur J Pharm Sci. 2003;20(1):73-81.
123. Giannavola C, Bucolo C, Maltese A, Paolino D, Vandelli MA, Puglisi G, et al. Influence of Preparation Conditions on Acyclovir-Loaded Poly-d,l-Lactic Acid Nanospheres and Effect of PEG Coating on Ocular Drug Bioavailability. Pharm Res. 2003;20(4):584-90.
124. Fresta M, Fontana G, Bucolo C, Cavallaro G, Giammona G, Puglisi G. Ocular tolerability and in vivo bioavailability of poly(ethylene glycol) (PEG)-coated polyethyl-2-cyanoacrylate nanosphere-encapsulated acyclovir. J Pharm Sci. 2001;90(3):288-97.
125. Zeng N, Hu Q, Liu Z, Gao X, Hu R, Song Q, et al. Preparation and characterization of paclitaxel-loaded DSPE-PEG-liquid crystalline nanoparticles (LCNPs) for improved bioavailability. Int J Pharm. 2012;424(1-2):58-66.
126. Adelli GR, Hingorani T, Punyamurthula N, Balguri SP, Majumdar S. Evaluation of topical hesperetin matrix film for back-of-the-eye delivery. Eur J Pharm Biopharm. 2015;92:74-82.
127. Pozzi D, Colapicchioni V, Caracciolo G, Piovesana S, Capriotti AL, Palchetti S, et al. Effect of polyethyleneglycol (PEG) chain length on the bio-nano-interactions between PEGylated lipid nanoparticles and biological fluids: from nanostructure to uptake in cancer cells. Nanoscale. 2014;6(5):2782-92.
128. Veronese FM, Pasut G. PEGylation, successful approach to drug delivery. Drug Discov Today. 2005;10(21):1451-8.
129. Veronese FM, Mero A. The impact of PEGylation on biological therapies. BioDrugs. 2008;22(5):315-29.
130. Vij N, Min T, Marasigan R, Belcher CN, Mazur S, Ding H, et al. Development of PEGylated PLGA nanoparticle for controlled and sustained drug delivery in cystic fibrosis. J Nanobiotechnology. 2010;8(1):22.
131. Li W, Zhan P, De Clercq E, Lou H, Liu X. Current drug research on PEGylation with small molecular agents. Prog Polym Sci. 2013;38(3–4):421-44.
132. Ke TL, Cagle G, Schlech B, Lorenzetti OJ, Mattern J. Ocular bioavailability of ciprofloxacin in sustained release formulations. J Ocul Pharmacol Ther. 2001;17(6):555-63.
133. Taha EI, El-Anazi MH, El-Bagory IM, Bayomi MA. Design of liposomal colloidal systems for ocular delivery of ciprofloxacin. Saudi Pharmaceutical Journal. 2014;22(3):231-9.
134. Taha EI, Badran MM, El-Anazi MH, Bayomi MA, El-Bagory IM. Role of Pluronic F127 micelles in enhancing ocular delivery of ciprofloxacin. J Mol Liq. 2014;199:251-6.
135. Hui PK, Diluzio WR. Stabilization and terminal sterilization of phospholipid formulations. Google Patents; 2002.
136. Mishra AK. Thermoprotected compositions and process for terminal steam sterilization of microparticle preparations. Google Patents; 2013.
137. Allen TM, Hansen C, Martin F, Redemann C, Yau-Young A. Liposomes containing synthetic lipid derivatives of poly(ethylene glycol) show prolonged circulation half-lives in vivo. Biochim Biophys Acta. 1991;1066(1):29-36.
138. Woodle MC, Newman MS, Cohen JA. Sterically stabilized liposomes: physical and biological properties. J Drug Target. 1994;2(5):397-403.
139. Woodle MC. Sterically stabilized liposome therapeutics. Advanced Drug Delivery Reviews. 1995;16(2):249-65.
140. Verhoef JJF, Anchordoquy TJ. Questioning the use of PEGylation for drug delivery. Drug Deliv Transl Res. 2013;3(6):499-503.

141. Bodh SA, Kumar V, Raina UK, Ghosh B, Thakar M. Inflammatory glaucoma. Oman J Ophthalmol. 2011;4(1):3-9.
142. Pan J, Kapur M, McCallum R. Noninfectious Immune-Mediated Uveitis and Ocular Inflammation. Current Allergy and Asthma Reports. 2013;14(1):409.
143. Schopf LR, Popov AM, Enlow EM, Bourassa JL, Ong WZ, Nowak P, et al. Topical Ocular Drug Delivery to the Back of the Eye by Mucus-Penetrating Particles. Transl Vis Sci Technol. 2015;4(3):11.
144. Boddu SH, Gupta H, Patel S. Drug delivery to the back of the eye following topical administration: an update on research and patenting activity. Recent Pat Drug Deliv Formul. 2014;8(1):27-36.
145. Shah SS, Denham LV, Elison JR, Bhattacharjee PS, Clement C, Huq T, et al. Drug delivery to the posterior segment of the eye for pharmacologic therapy. Expert Rev Ophthalmol. 2010;5(1):75-93.
146. Shafaie S, Hutter V, Cook MT, Brown MB, Chau DY. In Vitro Cell Models for Ophthalmic Drug Development Applications. Biores Open Access. 2016;5(1):94-108.
147. Kumari A, Sharma PK, Garg VK, Garg G. Ocular inserts - Advancement in therapy of eye diseases. J Adv Pharm Technol Res. 2010;1(3):291-6.
148. M G. Ophthalmic Dosage Forms Gibson M, editor2009.
149. Zhou HY, Hao JL, Wang S, Zheng Y, Zhang WS. Nanoparticles in the ocular drug delivery. Int J Ophthalmol. 2013;6(3):390-6.
150. Yamashita T, Ozaki S, Kushida I. Solvent shift method for anti-precipitant screening of poorly soluble drugs using biorelevant medium and dimethyl sulfoxide. Int J Pharm. 2011;419(1-2):170-4.
151. Hussain AH, Muhammad; Shoaib, Muhammad Harris; Yousuf, Rabia Ismail; Shafi, Nighat. Bioanalytical method development and validation of ciprofloxacin by RP-HPLC method. Asian Journal of Pharmaceutical & Biological Research (AJPBR);Oct2012, Vol 2 Issue 4, p219. 2012.
152. Razzaq SN, Khan IU, Mariam I, Razzaq SS. Stability indicating HPLC method for the simultaneous determination of moxifloxacin and prednisolone in pharmaceutical formulations. Chem Cent J. 2012;6(1):94.
153. Fathi. M, Varshosaz. J, Mohebbi. M, Shahidi. F. Hesperetin-Loaded Solid Lipid Nanoparticles and Nanostructure Lipid Carriers for Food Fortification: Preparation, Characterization, and Modeling. Food Bioprocess Technol. 2012.
154. Pescina S, Santi P, Ferrari G, Nicoli S. Trans-scleral delivery of macromolecules. Ther Deliv. 2011;2(10):1331-49.
155. Ranta V-P, Urtti A. Transscleral drug delivery to the posterior eye: Prospects of pharmacokinetic modeling. Advanced Drug Delivery Reviews. 2006;58(11):1164-81.
156. Sai Prachetan Balguri GRA, Soumyajit Majumdar. Topical ophthalmic lipid nanoparticle formulations (SLN, NLC) of indomethacin for
delivery to the posterior segment ocular tissues. European Journal of Pharmaceutics and Biopharmaceutics. 2016.
157. Schultz C, Breaux J, Schentag J, Morck D. Drug delivery to the posterior segment of the eye through hydrogel contact lenses. Clin Exp Optom. 2011;94(2):212-8.
158. Taha EI, El-Anazi MH, El-Bagory IM, Bayomi MA. Design of liposomal colloidal systems for ocular delivery of ciprofloxacin. Saudi Pharm J. 2014;22(3):231-9.
159. Wang J, Wu Y, Heegaard S, Kolko M. Cyclooxygenase-2 expression in the normal human eye and its expression pattern in selected eye tumours. Acta Ophthalmol. 2011;89(7):681-5.
160. Mitchell JA, Akarasereenont P, Thiemermann C, Flower RJ, Vane JR. Selectivity of nonsteroidal antiinflammatory drugs as inhibitors of constitutive and inducible cyclooxygenase. Proc Natl Acad Sci U S A. 1993;90(24):11693-7.
161. Kowalski RP, Karenchak LM, Eller AW. The role of ciprofloxacin in endophthalmitis therapy. Am J Ophthalmol. 1993;116(6):695-9.

162. Del Sole MJ, Schaiquevich P, Aba MA, Lanusse CE, Moreno L. Plasma and ocular prednisolone disposition after oral treatment in cats. Biomed Res Int. 2013;2013:209439.
163. Alhalafi AM. Applications of polymers in intraocular drug delivery systems. Oman Journal of Ophthalmology. 2017;10(1):3.
164. Kalam MA. Development of chitosan nanoparticles coated with hyaluronic acid for topical ocular delivery of dexamethasone. International Journal of Biological Macromolecules. 2016;89:127-36.
165. Tan G, Yu S, Pan H, Li J, Liu D, Yuan K, et al. Bioadhesive chitosan-loaded liposomes: A more efficient and higher permeable ocular delivery platform for timolol maleate. International Journal of Biological Macromolecules. 2017;94, Part A:355-63.
166. Chang H-YP, Chodosh J. Diagnostic and therapeutic considerations in fungal keratitis. International ophthalmology clinics. 2011;51(4):33-42.
167. Kalkanci A, Ozdek S. Ocular Fungal Infections. Current Eye Research. 2011;36(3):179-89.
168. Tanure MAG, Cohen EJ, Sudesh S, Rapuano CJ, Laibson PR. Spectrum of fungal keratitis at Wills eye hospital, Philadelphia, Pennsylvania. Cornea. 2000;19(3):307-12.
169. Phan C-M, Subbaraman LN, Jones L. In vitro drug release of natamycin from β-cyclodextrin and 2-hydroxypropyl-β-cyclodextrin-functionalized contact lens materials. Journal of Biomaterials Science, Polymer Edition. 2014;25(17):1907-19.
170. NAGESWARA RAO. G RKA. FORMULATION DESIGN AND IN-VITRO EVALUATION OF NATAMYCIN OCULAR
INSERT. INTERNATIONAL JOURNAL OF
PHARMACEUTICAL RESEARCH AND BIO-SCIENCE. 2014;Volume 3(2).
171. Bhatta R, Chandasana H, Rathi C, Kumar D, Chhonker Y, Jain G. Bioanalytical method development and validation of natamycin in rabbit tears and its application to ocular pharmacokinetic studies. Journal of pharmaceutical and biomedical analysis. 2011;54(5):1096-100.
172. Thomas PA. Current Perspectives on Ophthalmic Mycoses. Clinical Microbiology Reviews. 2003;16(4):730-97.
173. Xie L, Zhong W, Shi W, Sun S. Spectrum of fungal keratitis in north China. Ophthalmology. 2006;113(11):1943-8.
174. Bhatta R, Chandasana H, Chhonker Y, Rathi C, Kumar D, Mitra K, et al. Mucoadhesive nanoparticles for prolonged ocular delivery of natamycin: in vitro and pharmacokinetics studies. International journal of pharmaceutics. 2012;432(1):105-12.
175. Kaur IP, Rana C, Singh H. Development of effective ocular preparations of antifungal agents. Journal of Ocular Pharmacology and Therapeutics. 2008;24(5):481-94.
176. Thangabalan B, Kumar PV. Analytical method development and validation of Natamycin in eye drop by RP-HPLC. Asian Journal of Pharmaceutical and Clinical Research. 2013;6(1):134-5.
177. Campos EJ, Campos A, Martins J, Ambrósio AF. Opening eyes to nanomedicine: Where we are, challenges and expectations on nanotherapy for diabetic retinopathy. Nanomedicine: Nanotechnology, Biology and Medicine.
178. Farid RM, El-Salamouni NS, El-Kamel AH, El-Gamal SS. Chapter 16 - Lipid-based nanocarriers for ocular drug delivery A2 - Andronescu, Ecaterina. In: Grumezescu AM, editor. Nanostructures for Drug Delivery: Elsevier; 2017. p. 495-522.
179. Gratieri T, Gelfuso GM, Lopez RFV, Souto EB. Current efforts and the potential of nanomedicine in treating fungal keratitis. Expert Review of Ophthalmology. 2010;5(3):365-84.
180. Kambhampati SP, Kannan RM. Dendrimer nanoparticles for ocular drug delivery. Journal of Ocular Pharmacology and Therapeutics. 2013;29(2):151-65.
181. Ogunjimi AT, Melo SMG, Vargas-Rechia CG, Emery FS, Lopez RFV. Hydrophilic polymeric nanoparticles prepared from Delonix galactomannan with low cytotoxicity for ocular drug delivery. Carbohydrate Polymers. 2017;157:1065-75.

182. Raab W. Natamycin (Pimaricin): its properties and possibilities in medicine: Geor Thieme; 1972.
183. Thomas A. Analysis and assay of polyene antifungal antibiotics. A review. Analyst. 1976;101(1202):321-40.
184. Müller GG, Kara-José N, Castro RSd. Antifungals in eye infections: drugs and routes of administration. Revista Brasileira de Oftalmologia. 2013;72(2):132-41.
185. Thomas PA, Kaliamurthy J. Mycotic keratitis: epidemiology, diagnosis and management. Clinical Microbiology and Infection. 2013;19(3):210-20.
186. Kalavathy CM, Parmar P, Kaliamurthy J, Philip VR, Ramalingam MDK, Jesudasan CAN, et al. Comparison of Topical Itraconazole 1% With Topical Natamycin 5% for the Treatment of Filamentous Fungal Keratitis. Cornea. 2005;24(4):449-52.
187. Souto EB, Doktorovova S, Gonzalez-Mira E, Egea MA, Garcia ML. Feasibility of Lipid Nanoparticles for Ocular Delivery of Anti-Inflammatory Drugs. Current Eye Research. 2010;35(7):537-52.
188. Kumar R, Sinha VR. Solid lipid nanoparticle: an efficient carrier for improved ocular permeation of voriconazole. Drug Development and Industrial Pharmacy. 2016;42(12):1956-67.
189. Joseph RR, Venkatraman SS. Drug delivery to the eye: what benefits do nanocarriers offer? Nanomedicine. 2017;12(6):683-702.
190. Calvo P, Vila-Jato JL, Alonso MJ. Comparative in vitro evaluation of several colloidal systems, nanoparticles, nanocapsules, and nanoemulsions, as ocular drug carriers. Journal of Pharmaceutical Sciences. 1996;85(5):530-6.
191. Kaye GI, Pappas GD. STUDIES ON THE CORNEA : I. The Fine Structure of the Rabbit Cornea and the Uptake and Transport of Colloidal Particles by the Cornea in Vivo. The Journal of Cell Biology. 1962;12(3):457-79.
192. Sivaprasad S, Gupta B, Crosby-Nwaobi R, Evans J. Prevalence of diabetic retinopathy in various ethnic groups: a worldwide perspective. Survey of ophthalmology. 2012;57(4):347-70.
193. Levkovitch-Verbin H. Retinal ganglion cell apoptotic pathway in glaucoma: Initiating and downstream mechanisms. Progress in brain research. 2015;220:37-57.
194. Kowluru RA, Mishra M. Oxidative stress, mitochondrial damage and diabetic retinopathy. Biochimica et Biophysica Acta (BBA)-Molecular Basis of Disease. 2015;1852(11):2474-83.
195. Short BG. Safety evaluation of ocular drug delivery formulations: techniques and practical considerations. Toxicologic pathology. 2008;36(1):49-62.
196. Sampat KM, Garg SJ. Complications of intravitreal injections. Current opinion in ophthalmology. 2010;21(3):178-83.
197. Jager RD, Aiello LP, Patel SC, Cunningham Jr ET. Risks of intravitreous injection: a comprehensive review. Retina. 2004;24(5):676-98.
198. Rhone M, Basu A. Phytochemicals and age-related eye diseases. Nutrition reviews. 2008;66(8):465-72.
199. Jeong SJ, Koh W, Lee EO, Lee HJ, Lee HJ, Bae H, et al. Antiangiogenic phytochemicals and medicinal herbs. Phytotherapy Research. 2011;25(1):1-10.
200. Gaikwad SB, Mohan GK, Rani MS. Phytochemicals for diabetes management. Pharmaceutical Crops. 2014;31(2):261-6.
201. Soufi FG, Mohammad-nejad D, Ahmadieh H. Resveratrol improves diabetic retinopathy possibly through oxidative stress – nuclear factor κB – apoptosis pathway. Pharmacological Reports. 2012;64(6):1505-14.
202. Kim YH, Kim YS, Roh GS, Choi WS, Cho GJ. Resveratrol blocks diabetes-induced early vascular lesions and vascular endothelial growth factor induction in mouse retinas. Acta Ophthalmologica. 2012;90(1):e31-e7.

203. Kim Y-H, Kim Y-S, Kang S-S, Cho G-J, Choi W-S. Resveratrol Inhibits Neuronal Apoptosis and Elevated Ca²⁺/Calmodulin-Dependent Protein Kinase II Activity in Diabetic Mouse Retina. Diabetes. 2010;59(7):1825-35.
204. Guo R, Liu B, Wang K, Zhou S, Li W, Xu Y. Resveratrol ameliorates diabetic vascular inflammation and macrophage infiltration in db/db mice by inhibiting the NF-κB pathway. Diabetes and Vascular Disease Research. 2014;11(2):92-102.
205. Kumar A, Kaundal RK, Iyer S, Sharma SS. Effects of resveratrol on nerve functions, oxidative stress and DNA fragmentation in experimental diabetic neuropathy. Life Sciences. 2007;80(13):1236-44.
206. Kumar A, Negi G, Sharma SS. Neuroprotection by Resveratrol in Diabetic Neuropathy: Concepts & Mechanisms. Current Medicinal Chemistry. 2013;20(36):4640-5.
207. Langcake P, Pryce R. A new class of phytoalexins from grapevines. Cellular and Molecular Life Sciences. 1977;33(2):151-2.
208. Lamuela-Raventos RM, Romero-Perez AI, Waterhouse AL, De La Torre-Boronat MC. Direct HPLC analysis of cis-and trans-resveratrol and piceid isomers in Spanish red Vitis vinifera wines. Journal of Agricultural and Food Chemistry. 1995;43(2):281-3.
209. Romero-Pérez AI, Ibern-Gómez M, Lamuela-Raventós RM, de la Torre-Boronat MC. Piceid, the major resveratrol derivative in grape juices. Journal of agricultural and food chemistry. 1999;47(4):1533-6.
210. Atanacković MT, Gojković-Bukarica LC, Cvejić JM, editors. Improving the low solubility of resveratrol. BMC Pharmacology and Toxicology; 2012: Springer.
211. Seely KA, Levi MS, Prather PL. Retraction: the dietary polyphenols trans-resveratrol and curcumin selectively bind human CB1 cannabinoid receptors with nanomolar affinities and function as antagonists/inverse agonists. Journal of Pharmacology and Experimental Therapeutics. 2009;330(1):31-9.
212. Seely KA. Cannabinoid Receptor Inverse Agonists as Novel Therapeutic Agents: ProQuest; 2009.
213. Cécyre B, Zabouri N, Huppé-Gourgues F, Bouchard J-F, Casanova C. Roles of Cannabinoid Receptors Type 1 and 2 on the Retinal Function of Adult MiceRoles of CB1R and CB2R in the Retina. Investigative ophthalmology & visual science. 2013;54(13):8079-90.
214. Bouskila J, Javadi P, Casanova C, Ptito M, Bouchard JF. Müller cells express the cannabinoid CB2 receptor in the vervet monkey retina. Journal of Comparative Neurology. 2013;521(11):2399-415.
215. Abu-Amero KK, Kondkar AA, Chalam KV. Resveratrol and Ophthalmic Diseases. Nutrients. 2016;8(4):200.
216. Cottart CH, Nivet-Antoine V, Laguillier-Morizot C, Beaudeux JL. Resveratrol bioavailability and toxicity in humans. Molecular nutrition & food research. 2010;54(1):7-16.
217. Tsai T-Y, Chen T-C, Wang I-J, Yeh C-Y, Su M-J, Chen R-H, et al. The Effect of Resveratrol on Protecting Corneal Epithelial Cells from Cytotoxicity Caused by Moxifloxacin and Benzalkonium ChlorideResveratrol Protects Cytotoxicity From Moxifloxacin. Investigative ophthalmology & visual science. 2015;56(3):1575-84.
218. van Ginkel PR, Darjatmoko SR, Sareen D, Subramanian L, Bhattacharya S, Lindstrom MJ, et al. Resveratrol inhibits uveal melanoma tumor growth via early mitochondrial dysfunction. Investigative ophthalmology & visual science. 2008;49(4):1299-306.
219. Pezzuto JM, Moon RC, Jang M-S, Ouali A, Lin S, Barillas KS. Pharmaceutical formulations of resveratrol and methods of use thereof. Google Patents; 2002.
220. Singh G, Pai RS. A Rapid Reversed-Phase HPLC Method for Analysis of Trans-Resveratrol in PLGA Nanoparticulate Formulation. ISRN Chromatography. 2014;2014.
221. Sahoo SK, Dilnawaz F, Krishnakumar S. Nanotechnology in ocular drug delivery. Drug discovery today. 2008;13(3):144-51.
222. Okur NÜ, Gökçe EH. Lipid nanoparticles for ocular drug delivery. International Journal of Ophthalmic Research. 2015;1(3):77-82.

223. Seyfoddin A, Shaw J, Al-Kassas R. Solid lipid nanoparticles for ocular drug delivery. Drug delivery. 2010;17(7):467-89.
224. Uner M, Yener G. Importance of solid lipid nanoparticles (SLN) in various administration routes and future perspectives. International Journal of Nanomedicine. 2007;2(3):289.
225. Almeida H, Amaral MH, Lobão P, Silva AC, Loboa JMS. Applications of polymeric and lipid nanoparticles in ophthalmic pharmaceutical formulations: present and future considerations. Journal of Pharmacy & Pharmaceutical Sciences. 2014;17(3):278-93.
226. Amrite AC, Edelhauser HF, Singh SR, Kompella UB. Effect of circulation on the disposition and ocular tissue distribution of 20 nm nanoparticles after periocular administration. 2008.
227. Xu Q, Kambhampati SP, Kannan RM. Nanotechnology approaches for ocular drug delivery. Middle East African journal of ophthalmology. 2013;20(1):26.

APPENDIX

APPENDIX A

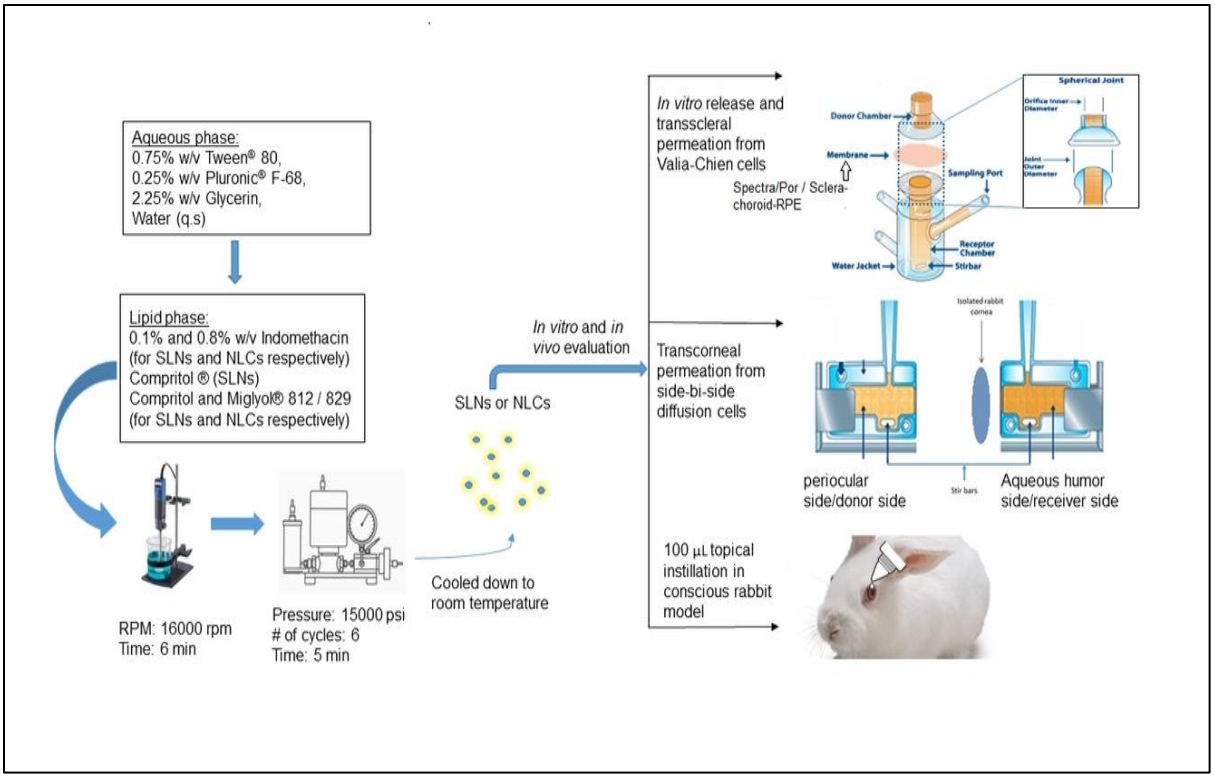

8. Graphical abstract: IN SLN/NLCs preparation and in vitro/ in vivo evaluation

APPENDIX B

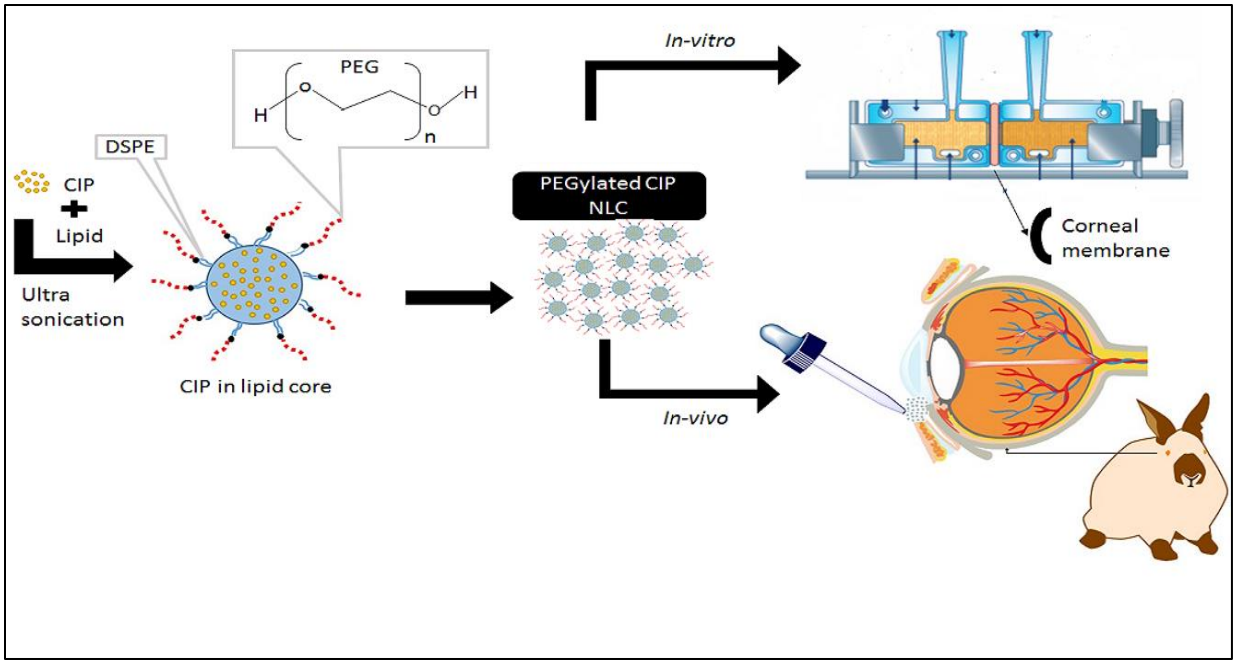

9. Graphical abstract : CIP NLCs preparation and in vitro/in vivo evaluation

VITA

- **Oct 26 1989** Born- Karimnagar, Telangana, India

- **June 2011** B. Pharmacy, Kakatiya University

- **August, 2011** Joined Ph.D. Program,
  Department of Pharmaceutics and Drug Delivery,
  The University of Mississippi

- **Peer-Reviewed Publication** Five

- **Achievements/Awards**

  COBRE fellowship: Center of Research Excellence in Natural Products Neuroscience (CORE-NPN) –2016, University of Mississippi, Mississippi

- **Professional Activities**

  Member of ARVO and AAPS

  Teaching assistant: Formulation and compound lab

  Instructor/assistant: Hands-on tablet course

  Reviewer for AAPS Pharm SciTech and JDDST Journals